Neurogenic Determinants of Left-Right Brain Asymmetry: Developmental Investigations of the Zebrafish Habenular Nuclei

By

Benjamin Jurrien Dean

Dissertation

Submitted to the Faculty of the

Graduate School of Vanderbilt University

in partial fulfillment of the requirements

for the degree of

DOCTOR IN PHILOSOPHY

In

Neuroscience

December, 2014

Nashville, Tennessee

Approved:

David M. Miller, III, Ph.D.

Douglas G. McMahon, Ph.D.

Charles C. Hong, M.D., Ph.D.

Joshua T. Gamse, Ph.D.

The following work is gratefully dedicated to my parents for feeding an inquisitive mind, to my siblings for the joy that they take in the world, to my friends for their time and patience and to Ms. Sarah Jean Edmonds for her light.

ACKNOWLEDGEMENTS

TABLE OF CONTENTS

LIST OF TABLES & FIGURES

LIST OF ABBREVIATIONS

A/P	anteroposterior
bHLH	basic helix-loop-helix
CNS	central nervous system
DD	dorsal diencephalon
DDCS	dorsal diencephalic conduction system
D/V	dorsoventral
HbN	habenular nuclei
HD	homeodomain
Hpf	hours post-fertilization
IPN	interpeduncular nucleus
L/R	left-right
M/L	mediolateral
NE	neuroepithelium
NP	neural progenitor
pP	parapineal
RT	room temperature
S/T	spatiotemporal
Tg	transgenic
VTA	ventral tegmental area

CHAPTER I

INTRODUCTION

Neuronal Diversity in the Vertebrate Central Nervous System

The central nervous systems (CNS) of vertebrates are compelling examples of cell fate diversity yielding extraordinary evolutionary adaptation. Excitatory, inhibitory and neuromodulatory neurons interact in feed forward, feedback and recursive motifs that yield intricate neural circuits and highly complex behaviors. From Ramon y Cajal's early monographs of neuronal morphology, to rapidly expanding molecular characterization, the diversity of neurons and neuronal subtypes in the vertebrate brain continues to astound. Variations in neurotransmitter release, receptor diversity, axon and dendritic projection patterns form the foundation for the remarkable interconnected network of brain pathways and circuits that yield vertebrate behavior (Anderson & Vanderhaeghen 2014; Klausberger & Somogyi 2008; Markram et al. 2004; Smidt & van Hooft 2013; Roeper 2013; Ramon Y Cajal 1909).

Primary Neural Patterning

From a developmental point of view, the diversity of neuronal subtypes raises a deep question: How do organisms generate neuronal diversity during development? All neurons arise from a population of progenitors (multipotent stem cells) that are set aside early in embryogenesis. By the early stages of gastrulation, secreted morphogens and inhibitors of the BMP, Wnt, FGF and Shh protein families act along the anteroposterior (A/P) and mediolateral (M/L) axes to specify a subsection of the ectoderm as the neural plate (Kiecker & Lumsden 2012; De Robertis & Kuroda 2004; Muñoz-Sanjuán & Brivanlou 2002; Stern 2006). As these morphogens diffuse from their points of secretion, different regions of the newly formed neuroepithelium (NE) ex-

perience different levels of these developmental signals. This combinatorial code imbues the NE with a basic, but highly conserved, three-dimensional pattern (Kiecker & Lumsden 2012). After neurulation, where the medial NE invaginates and the two lateral edges close over, the M/L axis becomes a dorsoventral (D/V) axis. The lumen formed by the invagination will become the ventricles and central canal of the CNS. The NE that surround this lumen is composed of multipotent neural progenitors (NPs) that take on a pseudostratified morphology shortly before neurulation (Vieira et al. 2010). Beginning after neurulation, NPs in all regions increase their number through successive cell divisions wherein both daughters retain progenitor status. These 'proliferative' divisions continue until, in a tightly controlled manner, NPs begin to divide asymmetrically maintaining the NP population, but also generating daughters which exit the cell cycle and begin to differentiate in 'neurogenic' divisions (Noctor et al. 2004; Doe 2008). The neuronal subtype, or fate, of the neuronal daughters depends, in part, on the patterning signature from primary neural induction (Kohwi & Doe 2013).

Secondary Neural Patterning

As mentioned, early A/P and D/V patterning is broad and crude. Subsequent to primary patterning, more regionalized secondary (local) organizers arise and refine and elaborate primary neural patterning (Kiecker & Lumsden 2012; Vieira et al. 2010). Secondary organizers redeploy the same families of morphogens and inhibitors used during primary patterning, but from a larger number of small organizing centers. This secondary patterning results in further subdivision of the NE. While the primary A/P and D/V patterning components are deeply conserved – some features are even found in pre-tunicates like hydra (Technau & Steele 2012) – the evolutionary deployment of secondary organizers is much more scattered across the evolutionary tree (Kiecker & Lumsden 2012). This suggests that secondary organizers remain an active unit of selection and a source of evolutionary diversity in the complex and highly specialized CNS's of the vertebrate lineage. Developmentally, the effect of secondary organizers is to create a much more nuanced

3D patterning milieu, further specifying select groups of NPs and preparing them to give rise to particular neuronal subtypes.

Secondary organizers in vertebrates include more intricate D/V patterning centers in the floor plate, roof plate and zona limitans interthalamica as well as discretely spaced A/P patterning centers including the anterior neural ridge, dorsal diencephalon, midbrain-hindbrain boundary and more (Kiecker & Lumsden 2004; Kiecker & Lumsden 2012; Vieira et al. 2010). These centers secrete BMPs, Wnts, Shh, FGFs and their antagonists which diffuse as gradients, often acting in a mutually inhibitory fashion to set up more refined domains with perpetually regulated boundaries (Achim et al. 2014; Vieira et al. 2010; Sunmonu et al. 2011; Cholfin & Rubenstein 2007; Garel et al. 2003; Kiecker & Lumsden 2004). This results in a precise regionalization of the CNS into the telencephalon, diencephalon, midbrain, hindbrain and spinal column along the A/P axis as well as further subdivisions along the D/V axis within each region (Kiecker & Lumsden 2012).

With an understanding of the broad features of primary and secondary organizer activity in defining NP niches, we can now turn to how signaling events downstream of morphogen activity specify regional ensembles of NPs to generate an array of neuronal subtypes. Essentially, how are these early patterning events interpreted by NPs to generate specific neuronal subtypes at particular times over the course of neural development?

Spatiotemporal Patterning of the Neuroepithelium

I will begin from a more conceptual framework and proceed to a more mechanistic description of the transition from NE patterning to NP specification. There are 2 general, non-mutually exclusive, models to explain how progenitors generate diverse cell types:

      (1)   Spatial patterning

      (2)   Temporal patterning

As discussed, in the earliest stages of neurogenesis, the NE in which the NPs reside is

exposed to a variety of extrinsic cues that work combinatorially to pattern the NE into discrete regions, as zip codes on a map (Achim et al. 2014; Kohwi & Doe 2013). NPs in a particular domain will generate neurons of a particular subtype (e.g. primary motor neurons in the motor cortex and dopaminergic neurons in the dorsal raphe). This is the spatial component of neural patterning.

Along the temporal axis of development, the extrinsic milieu of patterning molecules is not static, but changes as organizers form, actively secrete patterning molecules and experience feedback that can alter their secretory dynamics. Indeed this is evident in the ability of NPs in the same spatial location to produce different neuronal subtypes in a time-dependent manner. This is the temporal component of neural patterning.

In addition to a changing extrinsic environment, intrinsic cues play a role in temporal patterning. Work in *Drosophila* has demonstrated the ability of NPs to generate certain neuronal subtypes based on the number of divisions they have undergone. More recent work has strongly suggested that such roles are also present in vertebrate brain development; for example, in the retina (Kohwi & Doe 2013). In some contexts, NPs are thought to maintain an internal clock. As the clock unwinds distinct populations of neurons are generated at predetermined times. Some mechanisms appear to be linked to cell-cycle length and changes in DNA methylation status (Decembrini et al. 2009; Takizawa et al. 2001). While detailed mechanisms have yet to be determined, intrinsic cues are thought to function as timekeepers or counters restricting the fate of neuronal daughters based on developmental time or birth order.

Ultimately, the division of patterning mechanisms into spatial and temporal components is artificial as both function simultaneously during development. There may be conceptual pitfalls in the false dilemma of spatial versus temporal patterning that could obscure deeper insights, as with the separation of space and time before the Einsteinian advent of spacetime. Nevertheless, it is clear that spatiotemporal (S/T) patterning by primary and secondary organizers generates permissive and instructive microenvironments throughout the NE (defined by extrinsic cues) as well as intrinsic mechanisms that drive NPs to generate diverse neuronal populations.

Though it is beyond the scope of this introduction, it is important to point out that we have only discussed the generation of neuronal diversity, a new and exciting field has opened up defining gene networks that maintain neuronal identity (Deneris & Hobert 2014).

Molecular Mechanisms of Neuronal Diversity

Molecularly, two broad families of genes drive the progressive restriction of NPs to generate specific neuronal subtypes, homeodomain-containing (HD) and basic helix-loop-helix (bHLH) transcription factors (Achim et al. 2014; Guillemot 2007). As discussed, local and long-distance secreted factors pattern the NE resulting in the differential activation of one or more of several developmental signal transduction pathways (e.g. FGF, Wnt, etc.,). In a still largely elusive combinatorial manner, signal transduction of one or more pathways results in the activation of combinations of HD-containing TFs, including but not limited to *otx*, *sox*, *lhx*, *pax*, *dbx* and *dlx* gene families. Thus each S/T microdomain contains a set of NPs that express a particular combination of HD-containing TFs (Guillemot 2007).

Patterned expression of HD-containing TFs, in turn, activates the expression of pro-neural bHLH TFs. These TFs act in the neuronal progeny of S/T patterned NPs to drive the particular differentiation program of that neuronal subtype, often by utilizing the lateral inhibition of the Notch pathway, chromatin remodeling pathways or cell-cycle-exit pathways (Zhou & Huang 2011; Ronan et al. 2013). The ultimate effect of the bHLH genes is to drive the suites of genes – encoding biosynthetic enzymes, receptor molecules, axonal and dendritic determinants – that direct specific differentiation for distinct neuronal behavior. These waves of gene transcription are the molecular signature of NE S/T patterning and are the foundation for progenitor diversity.

Uncovering the combinatorial code of HD TFs, and their coordination with bHLH TFs in driving neuronal diversity, has been central to understanding the origins of neuronal diversity (Achim et al. 2014; Guillemot 2007). And while great strides have been made, there is a rich reservoir of complexity and nuance to the interplay between these two gene families. The charting

of how HD TFs and bHLH proteins work together to drive neuronal diversity is slowing revealing its elegance and importance for brain development and function.

Left-Right CNS Asymmetry is Functionally Conserved Across Vertebrates

As has been discussed, S/T patterning along the A/P axis and D/V axes has been a subject of investigation for over two decades. Strikingly, all of the examples mentioned above are symmetric with respect to the left-right (L/R) body axis. However, all known branches of the vertebrate lineage contain CNS asymmetries with respect to the L/R axis (Table I). Once thought to only exist in the human CNS, and in language centers specifically, L/R functional brain asymmetries have been identified in other human brain circuits including memory and executive control (Corballis 2009; Corballis 2014). In addition to humans, evidence is robust for functional lateralization across vertebrate classes and across a wide variety of behaviors (Table I). Despite the large and growing body of examples of asymmetry, the developmental and molecular signature of CNS asymmetry remains ill defined. The pervasiveness of CNS asymmetry strongly suggests that NPs on the left and right, in certain brain regions, must experience different patterning cues. More to the point, the neurogenic mechanisms that allow neurons on one side of the L/R axis to be different than those on the other are unknown. This in turn raises the question: how is S/T neuronal patterning deployed asymmetrically across the L/R axis to drive CNS asymmetry?

Evolutionary and Developmental Considerations in CNS Asymmetry

To better frame this question, I will now review the developmental origins of the L/R axis. The L/R axis – the third spatial axis to be patterned - is defined by embryogenic events concomitant with the development of the neural plate during gastrulation; interestingly this axis has an inflection point along the midline and is not continuous. Neural plate induction begins with the secretion of BMP antagonists from 'the node' (in zebrafish, Spemann's organizer; in

FUNCTION	LATERALIZATION	SPECIES	CITATION
Vocalization	Left	Human	*Bradshaw & Nettleton, 1981; Lindell, 2013*
		Primate	*Peterson et al., 1978; Peterson et al., 1984*
		Rodent	*Ehret, 1987; Fitch et al., 1993*
		Bird	*Nottebohm, 1971; Nottebohm, 1977; Nottenohm, 1980*
Facial Expression	Right	Human	*Sackeim et al., 1978*
		Monkey	*Hauser, 1993; Hook-Costigan & Rogers, 1997*
Handedness	Left	Human	*Corballis, 2014*
Emotional Processing	Right	Human	*Bradshaw, 1989; Lindell, 2013*
		Primate	*Ifune et al., 1984; Lindell 2013*
		Rodent	*Denenberg et al., 1981*
		Bird	*Andrew & Brennan, 1983; Regolin & Vallortigara, 1996; Rogers, 1991*
Spatial Processing	Right	Human	*De Renzi, 1982*
		Rodent	*Crowne et al., 1992; King & Corwin, 1992*
		Bird	*Clayton & Krebs, 1994*
Recognition of Novel Objects or Predators	Left	Bird	*Dharmarstnam & Andrew, 1994*
		Fish	*Miklosi & Andrew, 1999*
Recognition of Familiar Objects or Conspecifics	Right	Human	*Bradshaw & Nettleton, 1981*
		Primate	*Hamilton & Vermeire, 1988; Morris & Hopkins, 1993*
		Bird	*Vallortiagara, 1992; Vallortigara, 1991*
		Fish	*Miklosi & Andrew, 1999*
Escape Behavior	Left	Fish	*Cantalupo et al., 1995*

Table I: Lateralized brain function is highly conserved across vertebrate classes. Lateralized brain function was once thought to only be found in human. Now brain lateralization is known to be widespread through the vertebrate kingdom. This table relates several brain functions with high degree of laterality and lists in which species these lateralizations have been found.

chick, Henson's node; in mammals, the node). The mammalian node contains a small cluster of cells whose primary cilia form an array, with each cilium angled slightly toward the tissue surface (in other organisms ciliated arrays are formed in nearby, but non-nodal structures, e.g. Kupffer's vesicle in zebrafish (Essner et al. 2005) dorsal forerunner cells (DFCs). The coordinated beating of these cilia generates a leftward flow in the extracellular compartment (Nonaka et al. 1998; Nonaka et al. 2002). Through still contentious mechanisms, the morphogen Nodal is locally secreted and driven leftward, caught in 'the Nodal flow' Essner et al. 2005). This extraordinary process sets

off a wave of Nodal signaling that proceeds anteriorly through the lateral plate mesoderm, and in some species, into the anterior neural plate (Essner et al. 2005). This single patterning event is thought to dictate the majority of L/R asymmetry in the viscera of vertebrates. The case for Nodal-driven CNS asymmetry is less clear as Nodal signaling components have only been identified in the CNS of zebrafish and no other vertebrate to date. It is also important to appreciate that left-sided Nodal signaling dictates only the direction of asymmetry. In various models where the L/R aspect of Nodal signaling has been compromised, viscera and CNS structures are still asymmetric, but their lateralization is randomized. This is the distinction between breaking symmetry (or anti-symmetry) and consistent lateralization.

Whether Nodal-dependent or not, the pervasiveness of CNS asymmetry in the vertebrate lineage begs the question: What are the evolutionary advantages of a L/R body axis? While no causative data have been generated, the advantage is consistent with the following explanation: The L/R axis generates two mediolateral sides. A bilateral body plan is thought to have evolved as a significant adaptation for directional movement propelled by symmetric limbs (Corballis 2009). As directional movement evolved this likely drove formation of anterior mouth and eye structures for feeding and sensory feedback respectively, but the L/R axis remained largely symmetric. One explanation for the high selective pressure for L/R symmetry is that any deviation from symmetric sensory capacity would leave an animal vulnerable to predation (Corballis 2009). Of course, this sort of pressure only limits asymmetry in the peripheral nervous system. As with the visceral organs, because the CNS is 'inside' the animal, its asymmetry does not directly leave the organism open to predation. Essentially, as the central and peripheral nervous systems separated, bilateral representation of computational units in the central nervous system (higher order sensory processing, emotional processing, perception, decision making, memory) was less crucial. This relaxes the previously hypothesized selection against L/R asymmetry. This of course only creates a permissive environment for CNS asymmetry. Either drift or a selective advantage is required to drive the evolution of CNS L/R asymmetry as a pervasive feature of vertebrate brains. The broad conservation of lateralizations suggests a selective advantage for CNS

asymmetry (Table I).

To date, insight into the adaptiveness of CNS L/R asymmetry is almost entirely speculative. From a computational point of view, lateralization leads to more efficient use of neuronal space by reducing redundancy, which in turn prevents conflicts between hemispheres and allows for increased parallel processing (Lindell 2013). Not only is reduced redundancy a more efficient use of neuronal space, lateral specialization eliminates conflicts inherent in redundant processing. A tantalizing illustration of this is suggested by the association of reductions in asymmetry in human brains with increased susceptibility to sensory illusions, dyslexia, schizophrenia and strong belief in the paranormal (Niebauer et al. 2002; Claridge et al. 1998; Pizzagalli et al. 2000; Upadhyay et al. 2004). The common thread in these diverse diseases is their foundation on impaired reality testing; essentially, they consist in cognitive mistakes that are convincing as much as they are misleading. It is fascinating to think that the mild mistakes of dyslexia or the disturbing delusions of schizophrenia may both be downstream of left and right CNS outputs that simply do not match up, hemispheric inconsistencies of otherwise rational computation (Corballis 2009). Another interesting feature of these human data is their correlation not with reversed lateralization, but with reduced asymmetry, suggesting again that antisymmetry may be more crucial than the direction of lateralization. One final consideration is the progressive expansion of interhemispheric relays, from the tectal and posterior commissures of fish, reptiles and birds to the corpus callosum of mammals. Increased interhemispheric communication would also allow for lateralization of CNS function as the output would be accessible to both sides (Bisazza et al. 1998). It is clear at this point that there are more questions than answers when it comes to lateralization in the CNS. A rich and growing array of observations of L/R asymmetry across vertebrate classes makes these questions all the more compelling. As evolutionary dissection of CNS laterality proceeds, there is an opportunity for molecular biology to address cellular and developmental questions on this topic, namely:

(1)   How are left and right brain regions instructed to develop different

computational properties?

(2)   What are the neural correlates of functional CNS asymmetry?

(3)   How are L/R patterning programs integrated into neuronal cell fate decisions?

Functional Asymmetry in the Habenular Nuclei

The habenular nuclei (HbN) are the central relay of the evolutionarily conserved dorsal diencephalic conduction system (DDCS) connecting forebrain limbic regions with midbrain and hindbrain monoaminergic centers. The mammalian medial habenula is more conserved than the lateral and will be the focus of our discussion going forward. Found in all vertebrates, the HbN nuclei sit on the dorsal aspect of the third ventricle. Most afferents arrive via the stria medullaris from the septum and indirectly from the hippocampus and subiculum (a main output for hippocampal processing). As well, a small group of ascending afferents arrive from the ventral tegmental area (VTA) and locus coeruleus. Cholinergic and substance P efferent projections travel as the fasciculus retroflexus and innervate the VTA and raphe nuclei via the interpeduncular nucleus (IPN, Bianco & Wilson 2009).

Functionally, the HbN regulate dopaminergic tone in relation to learning, memory and reward, as well as attention (Lecourtier & Kelly 2007). They are also important for learning conditional avoidance and stress-dependent regulation of monoaminergic systems (Heldt & Ressler 2006), and they are broadly linked to regulation of sleep and reproductive behavior (Bianco & Wilson 2009). Pathologically in humans, habenular dysfunction has been correlated with depression, schizophrenia and nicotine withdrawal (Morris et al. 1999; Lecourtier et al. 2004; Shepard et al. 2006; De Biasi & Salas 2008).

Interestingly, asymmetries in the habenular nuclei have been found in virtually every class of vertebrates (Concha & Wilson 2001, Figure 1). These asymmetries involve size, cytoarchitecture and neurochemistry of the HbN themselves as well as axonal morphology, myelination

10
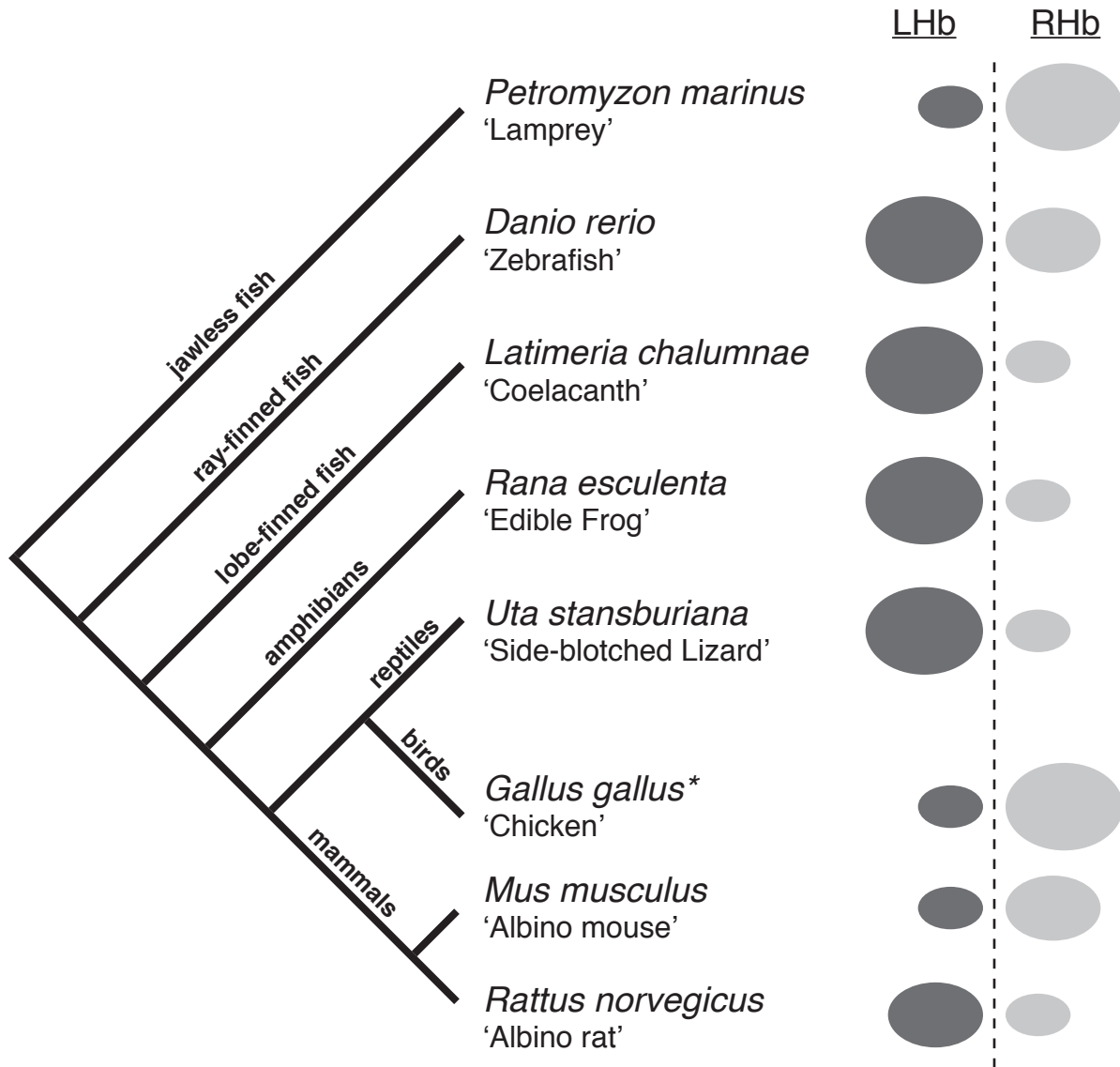
Figure 1: The habenular nuclei are a highly conserved feature of the vertebrate brain and show a wide variety of anatomical asymmetry across classes. Most classes of vertebrates have examples of habenular asymmetry. Thus, there is great likelyhood that these asymmetries are functionally important for survival. However, the developmental underpinning of habenular asymmetry are only just beginning to be explored in a handful a species. This figure depicts various exemplars of vertebrate classes and a cartoon of the left and right habenulae of specific species. It is very interesting to note that while asymmetry is highly conserved, the direction of the asymemtry is not. LHb: left habenula, RHb: right habenula. *In the chicken, male habenulae are as depicted, while female habenulae are asymmetric, but the direction of lateralization is random.

and targeting (Bianco & Wilson 2009). Very recently, the behavioral implications of habenular

asymmetry have started to be investigated. As in tetrapods, fish use their right eye to exam-

ine novel objects and environments while they use their left eye to investigate familiar objects

such as conspecifics (Andrew et al. 1998; Miklosi & Andrew 1999). Zebrafish with mutations that randomize CNS laterality show a concordant randomization of eye preference (Barth et al. 2009). This is the first experimental evidence of a causal link between asymmetry in the CNS and lateralized behavior. It remains to be seen if such causal relations are more widely held in the vertebrate clade. Importantly, the presence of habenular asymmetry in the zebrafish – as well as its functional significance – means we have an example of CNS asymmetry in an experimentally tractable organism. While research continues to catalog and investigate CNS asymmetries, and habenular asymmetries in particular, zebrafish present an amazing opportunity to delve into the developmental and molecular underpinning of CNS asymmetry at the genetic, cellular, circuit and behavior levels.

The Zebrafish Dorsal Diencephalon: A Model of Left-Right Brain Development

A powerful entry point into the evolution of CNS asymmetry is a deep understanding of the development of CNS asymmetry during embryogenesis. By far the most productive model for probing the molecular and mechanistic origins of vertebrate CNS asymmetry is the zebrafish dorsal diencephalon (epithalamus). The zebrafish dorsal diencephalon (DD) is anatomically, molecularly and functionally asymmetric. The rapid development, transparent nature of embryos, amenability to genetic manipulation and behavioral testing are key features that have allowed great progress toward understanding how vertebrate CNSs break symmetry in a directionally consistent manner, as well as ascertaining the implications of brain circuitry and animal behavior downstream of CNS asymmetry. The power of a system where researchers can move from genes to behavior cannot be overstated.

The zebrafish DD has 2 main functional units, the pineal complex and the habenular nuclei (ure 2). The pineal complex (PC) contains the highly conserved pineal gland along the midline and left-lateralized small nucleus of 12 or so neurons called the parapineal (pP). Flanking the PC are the bilateral habenular nuclei (HbN), which, as previously discussed, are part of
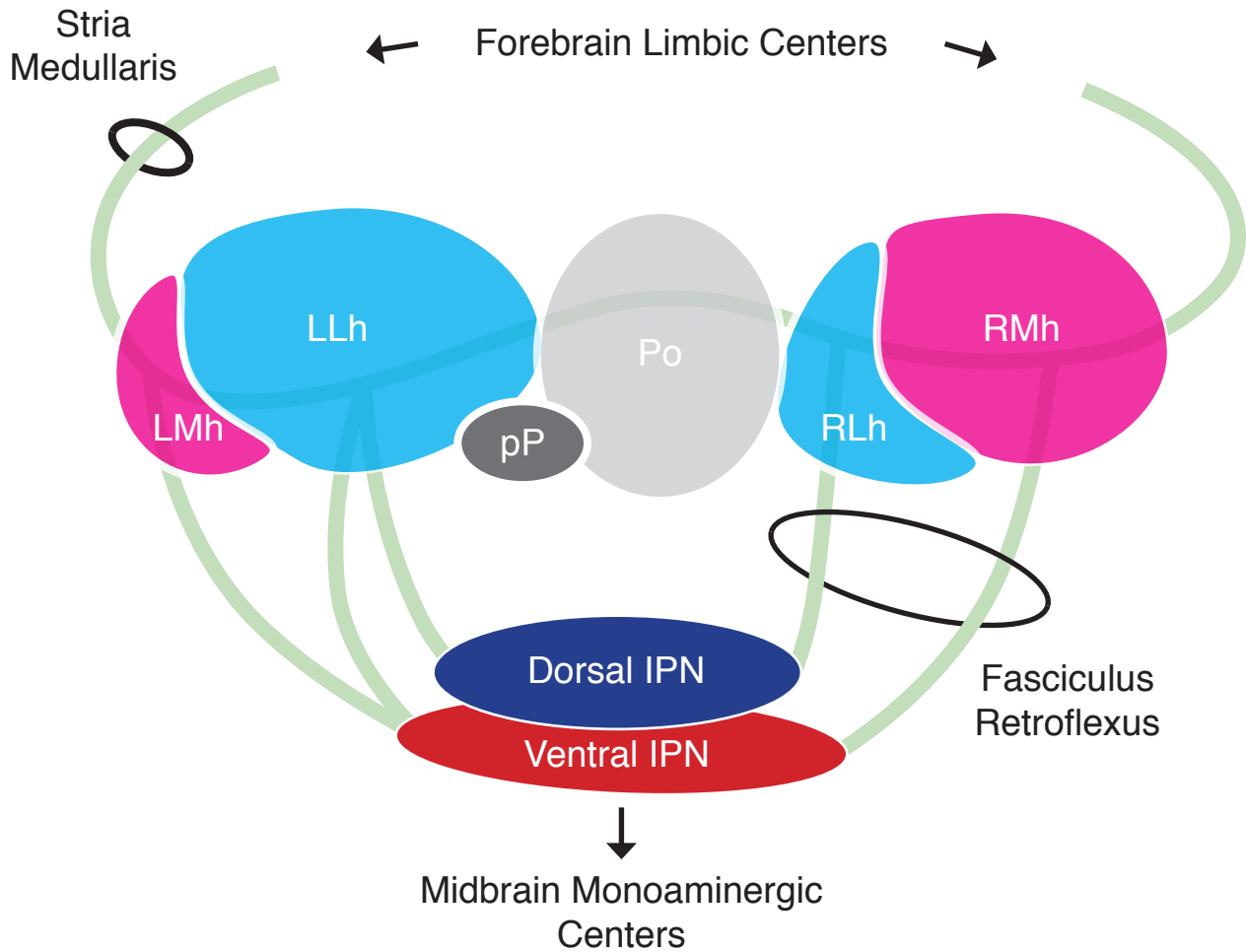
Figure 2: The habenular nuclei are located in the epithalamus and serve as a crucial relay between limbic forbrain regions and monoamineric centers in the midbrain and are robustly asymmetric in the zebrafish. The bilaterally paired habenular nuclei of the zebrafish flank the centrally located pineal organ and left-sided parapineal. In the zebrafish each nucleus is divided into lateral and medial subnuclei (named for their location in the adult, and in the embryos are reversed with the lateral subnucleus nearer the midline). Each pair of subnuclei are asymmetrically sized across the left-right axis. This asymmetry correlates to number of neurons and neuronal subtype (as marked by expression of Kctd12.1 in the lateral subnucleus and Kctd12.2+ in the medial subnucleus). Forebrain limbic structures send projections to the habenulae via the stria medullaris and the habenulae in turn project to the interpeduncular nucleus and on to the dorsal raphe and ventral tegmental area via the fasciculus retroflexus. LLh: left-lateral habenula, LMh: left-medial habenula, RLh: right-lateral habenula, RMh: right-medial habenula, Po: pineal organ, pP: parapineal.

the DDCS, linking limbic forebrain regions with dopaminergic, serotonergic and cholinergic output regions in the midbrain and brainstem. Additionally, the left habenula receives innervation from the pP. In the zebrafish, each habenular nucleus is subdivided into lateral and medial

subnuclei that show asymmetries in anatomy, gene expression, axonal projection and behavioral function. In zebrafish, the left lateral subnucleus is larger than its counterpart on the right while the medial subnucleus is larger on the right. Lateral subnucleus neurons are marked by expression of Kctd12.1 while Kctd12.2 marks medial subnucleus neurons. Thus, in expression patterns, Kctd12.1 has a large expression domain on the left while Kctd12.2's expression domain is large on the right. Both subnuclei project to the interpeduncular nucleus (IPN), but while medial subnuclei predominantly innervate the ventral IPN, lateral subnuclei send the majority of their projections to the dorsal IPN. Thus the left habenula predominantly projects to the dorsal IPN while the right projects mostly to the ventral. From genes, to circuits, to behavior, the zebrafish DD provides a powerful platform for investigating the development of CNS asymmetries and the neurogenic programs at its foundation.

Molecular Development of the Dorsal Diencephalon

Zebrafish development is measured in hours post-fertilization (hpf). All key developmental stages of epithalamic development – including patterning, specification and differentiation – take place from 12 hpf-96 hpf. The pineal complex is initially patterned by A/P Wnt and D/V BMP signals which activate expression of the HD-containing TF *floating head* (*flh*) (Barth et al. 2009; Masai et al. 1997). Between 12 hpf and 24 hpf, the *flh*-positive domain organizes into a coherent array containing cells fated to pineal as well as pP fates. The pP contains mostly projection neurons while the pineal is a mix of laterally located projection neurons flanking rod and cone photoreceptors. The generation of these various cell fates depends on BMP, Notch and FGF signaling pathways (Quillien et al. 2011; Clanton et al. 2013). BMP and Notch fundamentally regulate cell fate decisions between pineal projection neuron and photoreceptor fate. Specifically, BMP is necessary and sufficient to drive photoreceptor fate while inhibition of Notch laterally allows for projection neuron specification. Furthermore, Clanton et al. (2009) suggest that pP projection neurons are specified from cone precursors by FGF signaling present in the anterior

region of the pineal anlage. Subsequent to pP specification between 12 hpf and 18 hpf, pP cell migrate leftward beginning at 28 hpf; FGF signaling is also required for their leftward migration. In the absence of FGF there are fewer pP cells and an proportional increase in cone cells (Clanton et al. 2013). In an apparently parallel process, the HD-containing TF, *tbx2b*, acts to specify pP fate. In its absence very few pP cells are specified and these fail to migrate, also implicating *tbx2b* in pP migration (Snelson et al. 2008).

Comparatively little is known about early habenular development. Presumably, the HbN develop more like other brain nuclei and cortical regions, arising from a patterned group of NPs. Habenulogenesis (specification of NPs and eventual differentiation of neuronal daughters in the HbN) is thought to begin shortly before 24 hpf, as measured by BrdU incorporation (Aizawa et al. 2007). Indeed, recently a marker of habenular neural progenitors, *dbx1b*, been identified (Dean et al., Submitted). *Dbx1b*, a HD-containing TF, marks a set of proliferative cells along the ventricle of the dorsal diencephalon by 24 hpf. Lineage labeling experiments demonstrate that these *dbx1b+* progenitors give rise to all cells of the habenula. As NP daughters move away from the ventricle they are marked by expression first of the chemokine receptor, *cxcr4b*, and then HuC (a post-mitotic neuronal marker) as they exit the cell cycle. Finally, habenular neurons undergo a binary fate decision, differentiating and expressing either Kctd12.1 or Kctd12.2. Expression of one of these proteins correlates precisely with the localization of a habenular neuron in the lateral or medial habenular subnucleus respectively.

The birth order of habenular neurons correlates roughly with habenular cell fate with most early-born neurons taking on the Kctd12.1 fate and most late-born neurons taking on the Kctd12.2 fate. Thus, NPs appear to be biased toward generating lateral subnucleus neurons early and that later in development this bias shifts to favor medial subnucleus neurons. Clearly, S/T cell fate decisions occur in the habenular NE. However, a mechanistic accounting of these observations is lacking.

Aizawa et al., (2007) demonstrated clearly that Notch signaling is crucial to habenular neurogenesis. Sustained activation of Notch signaling led to delays in neurogenesis and loss of

lateral subnuclear (Kctd12.1+) cell fates and a gain of medial (Kctd12.2+) cell fates. Conversely, premature termination of Notch signaling and concomitant early neurogenesis produced more lateral and fewer medial habenular neurons. It seems clear that Notch signaling drives habenular neurogenesis, but the mechanism that drives asymmetry in neuronal cell fate and its connection with the Notch pathway is unclear.

From an experimental point of view, the HbN are an ideal system to explore how L/R patterning integrates with cell fate decisions during neurogenesis. Habenular neurons arise from a neuroepithelium, and undergo a binary cell fate decision that is apportioned asymmetrically. Furthermore, as discussed, this decision has important implications for circuit formation and behavior.

Parapineal-Dependent Habenular Asymmetry

Much of what we understand about habenular development comes from detailed study of the pP. The pP plays a vital role in the elaboration of habenular asymmetries (Gamse 2003; Snelson & Gamse 2009). Investigation of *tbx2b* mutants alongside laser ablation of the pP demonstrated that the loss of the pP greatly reduces asymmetry of Kctd12 expression leaving the left habenular more 'right-like;' simultaneously the anatomical asymmetries of the subnuclei also become more 'right-like' and ultimately the projection pattern shifts 'rightward' with both HbN predominantly projecting to the ventral IPN and few projections to the dorsal IPN remaining (Snelson et al. 2008; Roussigne et al. 2012; Bianco et al. 2008).

A fascinating, and unanswered, question in the field is how the pP influences habenular development. Not only does the pP migrate to the left, but it also innervates the lateral subnucleus of the left Hb (Roussigne et al. 2012). These two features suggest mechanisms by which the pP may influence habenular development. First, it is hard to not be struck by the positioning of the pP relative to the fates of the surrounding habenular neurons (Figure 2). Spatially, the habenular cells in closest proximity take on a lateral subnucleus fate, while those at a distance take on a

medial subnucleus fate. The correlation of distance from pP and fate strongly suggests a secreted factor as a mechanism for determining fate. However, such a pP-secreted factor remains elusive; though, Wnt signaling components are promising candidates (Carl et al. 2007). It is also evident that the pP innervates the left habenula and innervation is known to correlate with differentiation (Concha et al. 2003). So it may also be the case that the pP acts instructively at a later stage via neuronal contacts.

Parapineal-Independent Habenular Asymmetry

Despite the clear role the pP plays in habenular asymmetry in the zebrafish, many species both more ancestral and more recently evolved possess asymmetric HbN but either a midline pP or no pP at all. This suggests that other mechanisms for habenular asymmetry are preserved in the evolutionary record. A natural question is, do pP-independent asymmetries exist in the HbN of zebrafish? Asymmetries in Kctd gene expression, neuropil organization, the asymmetric timing of neurogenesis and the morphology of axonal innervations to the IPN all persist after pP ablation (Roussigné et al. 2009; Bianco et al. 2008; Concha et al. 2003). Thus factors in addition to the pP must drive the full elaboration of habenular asymmetry. However, the sources of ha-benular asymmetry that are pP-independent are unknown at this point.

After almost 15 years of revealing the mechanisms of asymmetry derived from the pP, the zebrafish DD is poised to reveal yet another secret of asymmetric development. Indeed, given the lack of conservation of a left-sided pP, pP-independent mechanisms may be more generaliz-able than pP-directed CNS asymmetry. Of particular interest in this work are the pP-independent mechanisms regulating the timing of neurogenesis. Roussigne et al. (2009) demonstrate that Nodal signaling is responsible for the asymmetric timing of habenular neurogenesis. It is un-known at this point if other pP-independent asymmetries are Nodal-dependent (Roussigne et al. 2012). Thus, to uncover the pP-independent sources of habenular asymmetry, a close investiga-tion of the mechanisms that underpin the timing of habenular neurogenesis is important. Indeed,

habenular neurogenesis raises questions about how the convergence of L/R and S/T patterning cues is achieved. Specifically, in the context of habenulogenesis, what regulates the timing of neurogenesis of the habenular neurons downstream of the fundamental L/R patterning events of Nodal signaling? Furthermore, what are the implications for asymmetric timing of neurogenesis in the developing habenulae with regards to cell fate? And more broadly, are pP-independent mechanisms of asymmetric HbN formation conserved in other species?

Mechanisms for Asymmetric Timing of Habenular Neurogenesis

Presently, I will focus on the central question of the regulatory mechanisms for asymmetric habenular neurogenesis. We can pull the central question of this work apart into two questions:

(1)   Which genes and pathways regulate the timing of neurogenesis?

(2)   How are L/R and S/T patterning cues integrated?

The following three chapters will describe some novel tools and insights into the mechanisms that regulate the timing of neurogenesis in the HbN. Chapter IV will also begin to address the integration of L/R and S/T patterning in habenular development. These chapters will be followed by a final section where implications for the work herein, future direction and evolutionary speculation will be featured.

CHAPTER II

LIGHT AND MELATONIN SCHEDULE NEURONAL DIFFERENTIATION IN THE HABENULAR NUCLEI

INTRODUCTION

The light-dark cycle synchronizes the circadian clock of organisms with the environment (Vallone et al., 2007). In zebrafish, light can be perceived not only by the eyes and pineal gland (photoreceptive organs) but, uniquely among model vertebrates, also by other organs and cultured cells (Kaneko et al., 2006; Tamai et al., 2004; Tamai et al., 2007; Whitmore et al., 2000; Whitmore et al., 1998). Light has been shown to initiate molecular oscillations in the zebrafish embryo (Dekens and Whitmore, 2008; Kazimi and Cahill, 1999; Vatine et al., 2009; Vuilleumier et al., 2006) and affect the timing of the cell cycle (Dekens et al., 2003), as well as modulate predator avoidance behavior in zebrafish larvae (Budaev and Andrew, 2009). However, the consequences of light on neurogenesis have only recently begun to be characterized (D'Autilia et al., 2010; Dulcis and Spitzer, 2008; Toyama et al., 2009).

Melatonin acts as a marker of photoperiod in vertebrates, regulating both daily and seasonal behavior in adults via receptors found in specific brain regions (Pandi-Perumal et al., 2008). In the zebrafish pineal organ, melatonin is synthesized from serotonin by a series of enzymes including arylalkylamine-N-acetyltransferase (*aanat2*). Transcription of *aanat2* is cyclic, with peaks during the night and troughs during the day. Under conditions of alternating light:dark

(L:D) periods, *aanat2* is expressed by 22 hours post fertilization (hpf) in zebrafish embryos (Gothilf et al., 1999; Zilberman-Peled et al., 2007) and robust, circadian rhythmic melatonin production can be detected by 37 hpf (Kazimi and Cahill, 1999). This circadian rhythmic expression depends on the synchronization of circadian oscillations so that *aanat2* expression is in phase in all pineal cells. The oscillators are synchronized by Period-2 (Per2), a transcriptional repressor induced by light in cells of the zebrafish pineal organ. In the absence of Per2 activity due to constant darkness, *aanat2* expression and melatonin production reach a constant, intermediate level of expression (Kazimi and Cahill, 1999; Ziv et al., 2005). Melatonin receptors are present at high levels in the embryonic brain (Rivkees and Reppert, 1991; Seron-Ferre et al., 2007), and in mammals, melatonin can be transferred to the developing fetus via the placenta (Klein, 1972) and to the newborn via milk (Reppert and Klein, 1978). Low melatonin synthesis due to mutation of the biosynthetic enzyme acetylserotonin O-methyltransferase (ASMT) has been linked to autism spectrum disorders (Melke et al., 2008). Melatonin treatment of mammalian neural stem cells induces their differentiation (Bellon et al., 2007; Kong et al., 2008; Moriya et al., 2007). Finally, in zebrafish embryos, melatonin stimulates increased cell division (Danilova et al., 2004). Therefore, a link between light stimulation, gene expression and melatonin exists during early development, but its influence on neurogenesis is not well understood.

In order to investigate the effects of light and melatonin on neurogenesis, we examined the development of the habenular nuclei. These are a pair of brain nuclei that are adjacent to the pineal organ and make up part of the highly conserved dorsal diencephalic conduction system (DDCS) implicated in modulation of the dopamine and serotonin systems (Hikosaka, 2010; Sutherland, 1982). The habenular nuclei express opsin proteins in fish and amphibians (Bertolucci and Foa, 2004) and receive projections from pinealocytes in the Djungarian hamster (Korf et al., 1986). In addition, neurons of the habenular nuclei express melatonin receptors in mice (Weaver et al., 1989) and undergo seasonal changes in morphology in frogs (Kemali et al., 1990). We examined neuronal differentiation and gene expression in the zebrafish habenular nuclei and find that light and melatonin control the timing of neuronal differentiation. In particular, reduc-

tion of light and melatonin produce a delay in differentiation, which ultimately alters the DDCS by reducing the extension of neuronal processes in the habenular nuclei. Our results demonstrate that light and melatonin have significant effects on vertebrate brain formation.

MATERIALS & METHODS

Zebrafish

Zebrafish were raised at 28.5°C on a 14/10 hour light/dark cycle or constant darkness beginning at 5 minutes post fertilization. Embryos and larvae were staged according to hours (h) or days (d) post fertilization. The wild-type AB strain (Walker, 1999) was used. To prevent melanosome darkening, embryos were raised in water containing 0.003% phenylthiourea.

Drug treatments

Embryos were treated by placing them in egg water containing melatonin (1 or 23.2 μmolar, Sigma), U0126 (100 μmolar, Sigma), or luzindole (5, 7.5 or 10 μmolar, Sigma) for the duration of the treatment. For controls, embryos were placed in egg water with vehicle alone (ethanol for melatonin or DMSO for luzindole and U0126).

Melatonin receptor cloning

For cloning of melatonin receptor *mtnr1aa* by RT-PCR, total RNA was isolated from 24 hpf zebrafish embryos using Trizol (Invitrogen), and cDNA prepared using Superscript II reverse transcriptase (Invitrogen). cDNA was amplified using primers within the ORF of *mtnr1aa* and cloned into the pCRII-Topo vector (Invitrogen). For cloning of melatonin receptors *mtnr1a-like* and *mtnr1ba*, total genomic DNA was isolated from zebrafish caudal fin samples using NaOH

(Roche) digestion, followed by buffering (Tris pH8.0). The largest exon of each gene was amplified using primers within the exon and cloned into the pCRII-Topo vector. An EST for *mtnr1bb* was purchased from Open Biosystems.

RNA in situ hybridization

Whole-mount RNA *in situ* hybridization was performed as described previously (Snelson et al., 2008), using reagents from Roche Applied Bioscience. RNA probes were labeled using fluorescein-UTP or digoxygenin-UTP. To synthesize antisense RNA probes, pBK-CMV-*leftover (kctd12.1)* (Gamse et al., 2003) was linearized with *Eco*RI and transcribed with T7 RNA polymerase; pBK-CMV-*right on (kctd12.1*) (Gamse et al., 2005) with *Bam*HI and T7 RNA polymerase; pBS-*gfi1* (Dufourcq et al., 2004) with *Sac*II and T3 RNA polymerase. pBK-CMV-*cpd2 (cadps2)* (Gamse et al., 2005) with Sal I and T7 RNA polymerase, pCR4-*nrp1a* ((Kuan et al., 2007b) with NotI and T3 RNA polymerase, *cxcr4b* (Chong et al., 2001) with EcoRV and SP6 RNA polymerase, pBS-*otx5* (Gamse et al., 2002) with Not1 and T7 RNA polymerase, *mtnr1aa* with XhoI and SP6 RNA polymerase, *mtnr1bb* with EcoRI and SP6 RNA polymerase, and *mtnr1a-like* and *mtnr1ba* with EcoRV and SP6 RNA polymerase. Embryos were incubated at 70°C with probe and hybridization solution containing 50% formamide. Hybridized probes were detected using alkaline phosphatase-conjugated antibodies and visualized by 4-nitro blue tetrazolium (NBT) and 5-bromo-4-chloro-3-indolyl-phosphate (BCIP) staining for single labeling, or NBT/BCIP followed by iodonitrotetrazolium (INT) and BCIP staining for double labeling. All in situ data was collected on a Leica DM6000B microscope with a 10x or 20x objective.

Melatonin ELISA

Melatonin was isolated from zebrafish embryos as previously described (Kazimi and Cahill, 1999) with the following modifications: Methylene chloride was evaporated under vac-
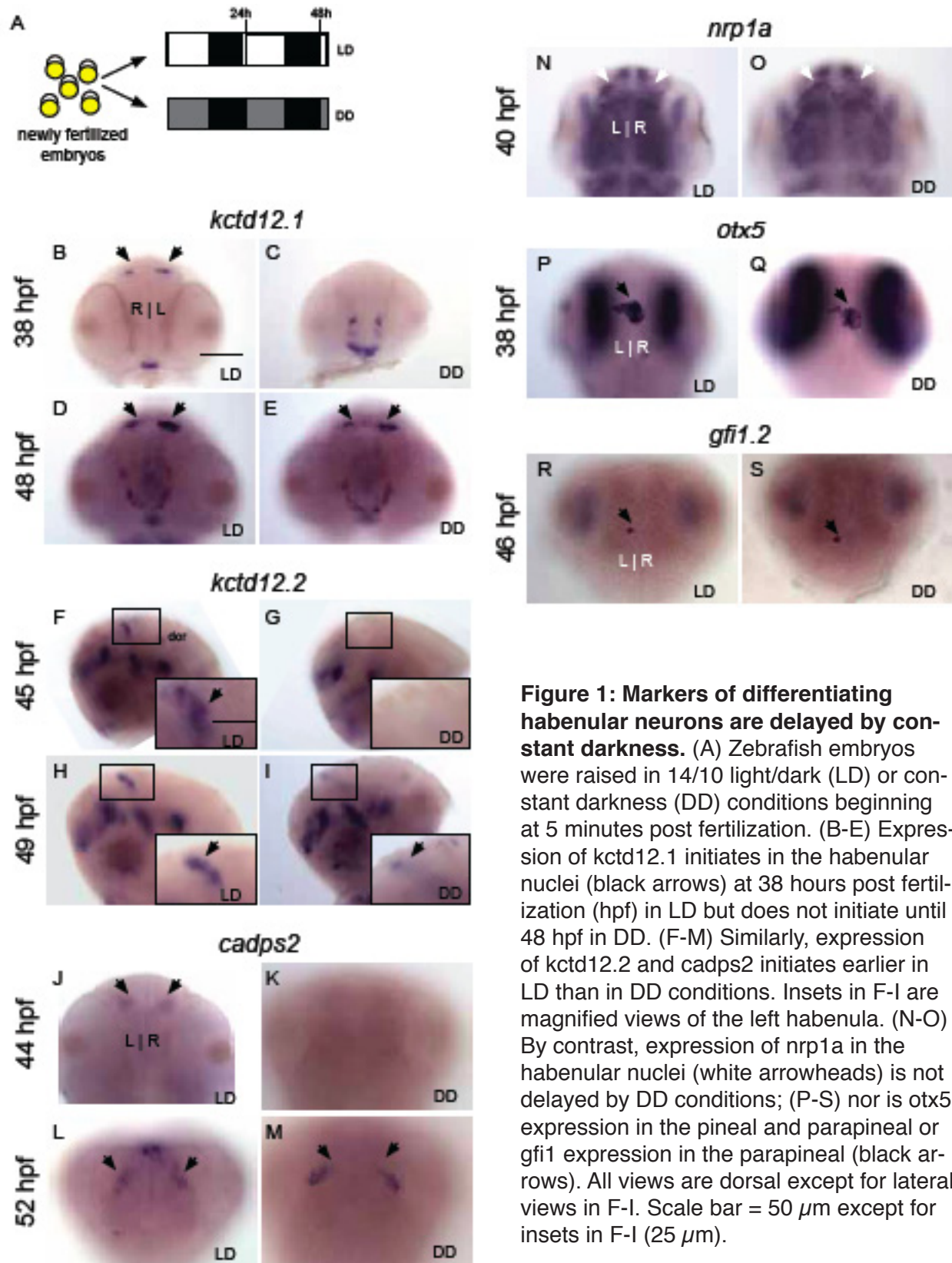
Figure 1: Markers of differentiating habenular neurons are delayed by constant darkness. (A) Zebrafish embryos were raised in 14/10 light/dark (LD) or constant darkness (DD) conditions beginning at 5 minutes post fertilization. (B-E) Expression of kctd12.1 initiates in the habenular nuclei (black arrows) at 38 hours post fertilization (hpf) in LD but does not initiate until 48 hpf in DD. (F-M) Similarly, expression of kctd12.2 and cadps2 initiates earlier in LD than in DD conditions. Insets in F-I are magnified views of the left habenula. (N-O) By contrast, expression of nrp1a in the habenular nuclei (white arrowheads) is not delayed by DD conditions; (P-S) nor is otx5 expression in the pineal and parapineal or gfi1 expression in the parapineal (black arrows). All views are dorsal except for lateral views in F-I. Scale bar = 50 μm except for insets in F-I (25 μm).

LD **DD**
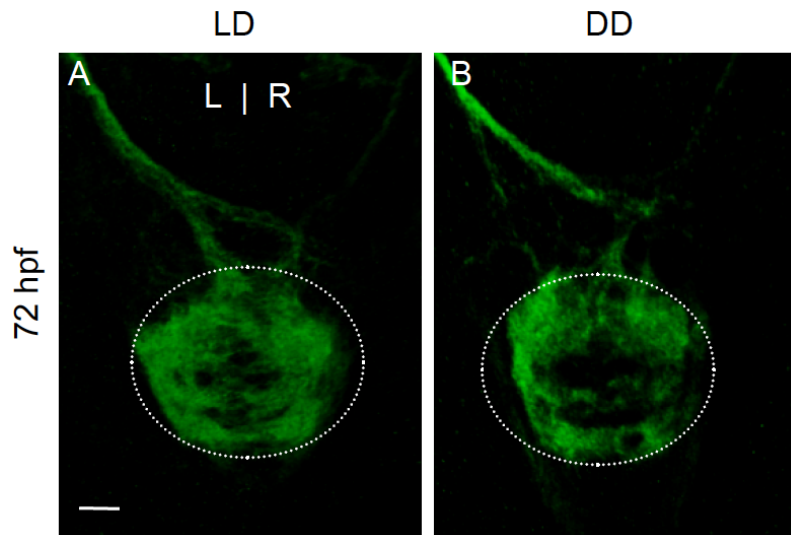
Supplemental Figure 1: Axonal targeting to the midbrain is unaffected by DD conditions. (A-B) Targeting of kctd12.1-expressing axons from the habenular nuclei to the interpeduncular nucleus of the midbrain (white circle) is similar in LD and DD larvae. Dorsal views. Scale bar = 20 μm.

uum using a rotary evaporator with the collection vial semi-submerged in a room-temperature water bath. Dried extracts were eluted in 0.2 mL 0.1% porcine gelatin (type a) in PBS. This volume was used in full to generate duplicate samples that were subsequently analyzed using a Direct Saliva Melatonin ELISA (Alpco) following manufacturer's instructions, beginning with acid/base pretreatment. In order to validate the use of the ELISA assay for detecting melatonin from zebrafish embryos, we quantified the amount of melatonin in 43 hpf embryos raised in LD conditions, with a sample of 5 versus 15 embryos. The amount of melatonin that was reported by the ELISA increased by 2.7 times when the number of embryos was increased 3-fold, indicating that the assay is valid.

Immunofluorescence

For whole-mount immunohistochemistry with rabbit or mouse-derived antibodies, larvae were fixed overnight in 4% paraformaldehyde or Prefer fixative (Anatech). Paraformaldehyde-fixed samples were permeabilized by treatment with 10 μg/ml Proteinase K (Roche Applied Bioscience) and refixed in 4% paraformaldehyde. Prefer-fixed samples were not permeabilized. All samples were blocked in PBS with 0.1%TritonX100, 10% sheep serum, 1% DMSO, and 1% BSA (PBSTrS). For antibody labeling, rabbit anti-Lov (Kctd12.1) or rabbit anti-Ron (Kctd12.2)
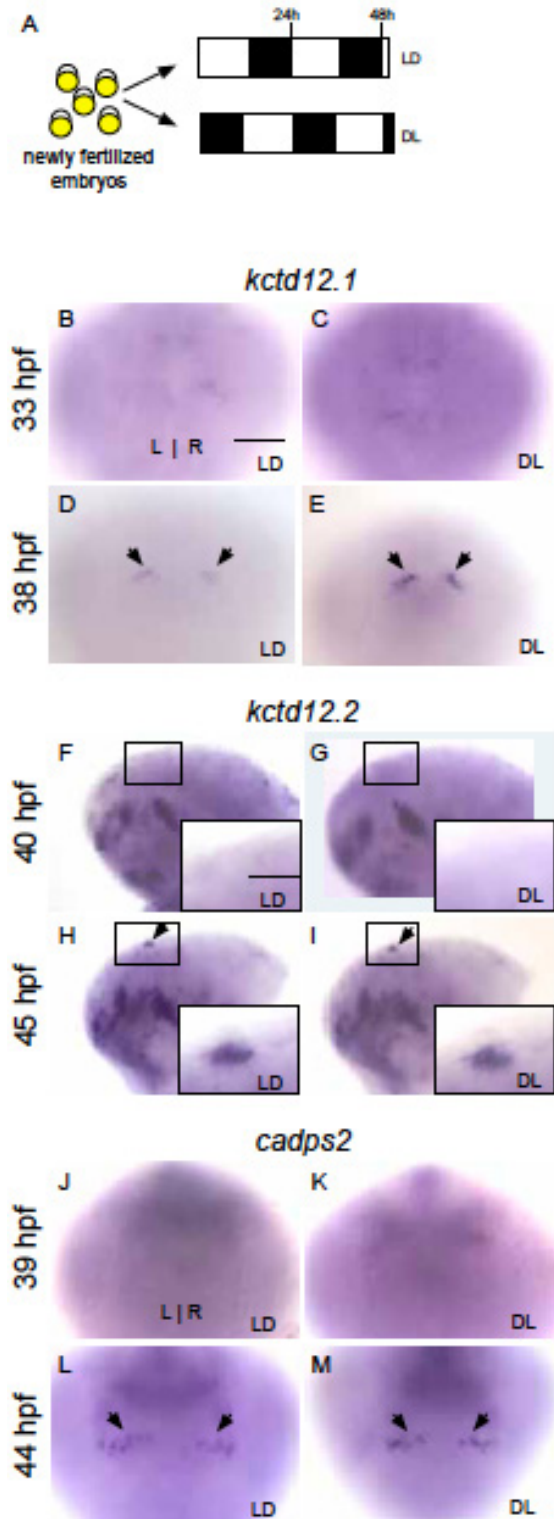
Figure 2: Reversal of the photoperiod phase does not significantly advance the timing of gene expression in the habenular nuclei. (A) Zebrafish embryos were raised in 14/10 light/ dark (LD) or 10/14 dark/light (DL) conditions beginning at 5 minutes post fertilization. (B-E) Expression of kctd12.1 is absent at 33 hpf in the habenular nuclei and initiates at 38 hours post fertilization (hpf) in LD (black arrows). Expression is higher in DL than in LD embryos. (F-M) Similarly, expression of kctd12.2 and cadps2 initiates at the same time in LD and DL conditions. Insets in F-I are magnified views of the left habenula. All views are dorsal except for lateral views in F-I. Scale bar = 50 μm except for insets in F-I (25 μm).

(1:500; Gamse et al, 2005), rabbit anti-GFP (1:1000, Torrey Pines Biolabs), HuC-D (1:200, Invitrogen), SV2 (1:500, Developmental Studies Hybridoma Bank), acetylated alpha-tubulin (1:1000, Sigma) were used. Larvae were incubated overnight in primary antibody diluted in PBSTrS. Primary antibody was detected using goat-anti-rabbit or goat-anti-mouse secondary antibodies conjugated to the Alexa 568 or Alexa 488 fluorophores (1:350, Invitrogen). Samples were counterstained with TOPRO3 (1:10,000, Invitrogen).

For quantitation of neuropil, confocal data was imported into Volocity (Improvision), and the lasso tool was used to select all anti-acetylated tubulin fluorescence within the left or right habenular nucleus, excluding the habenular commissure. The volume of this region was calculated using Quantitation module of Volocity.

We recorded the volume of the largest contiguous labeled region as the volume of neuropil in the habenulae (in order to exclude the large amount of small speckle artifacts).

All immunofluorescence data were collected on a Zeiss LSM510 confocal microscope with a 40x oil-immersion objective and analyzed with Volocity software (Improvision).

RESULTS

Constant darkness causes delayed gene expression in the habenular nuclei

To test the effects of photoperiod on neuronal differentiation, we examined the development of the habenular nuclei under different light/dark conditions (Figure 1A). In a 14 hour light:10 hour dark (LD) photoperiod, habenular neurons express the potassium-channel-tetramerization-domain (KCTD) containing genes *kctd12.1* and *kctd12.2*. *Kctd12.1* is expressed in the lateral sub-nucleus, which is larger in the left habenula, while
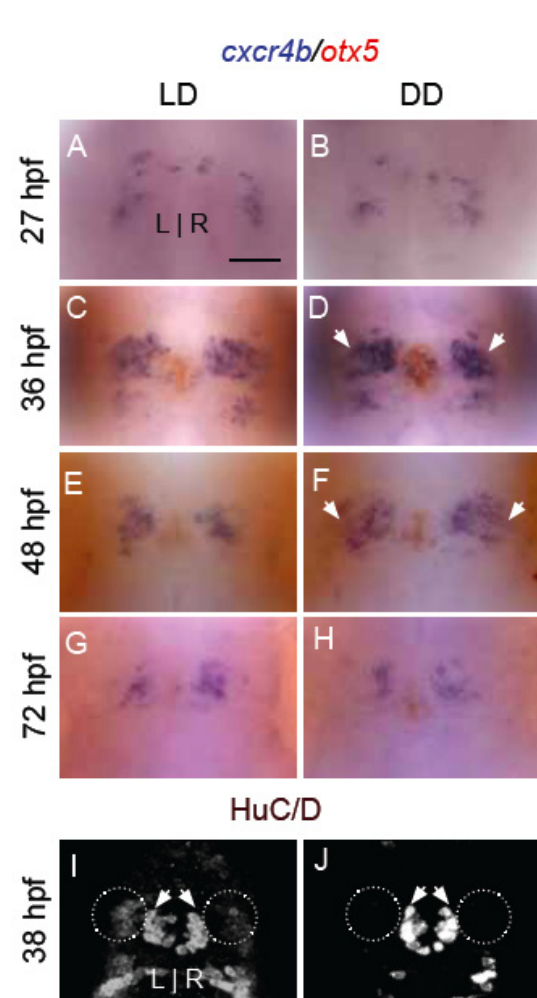
Figure 3: Habenular progenitor cells accumulate in an undifferentiated state in constant darkness. (A-B) A similar number of cxcr4b-positive habenular progenitor cells are specified at 27 hpf in LD and DD. (C-F) However, at 36 and 48 hpf, many more progenitor cells accumulate in DD conditions than in LD. (G-H) By 72 hpf, only a few progenitor cells are detected in LD or DD. (I-J) At 38 hpf, fewer HuC/D-positive post-mitotic precursor cells are detected in the habenular nuclei (white ovals), consistent with the retention of habenular cells in a progenitor state. HuC/D-positive projection neurons in the pineal complex (white arrowheads), meanwhile, are unaffected by DD conditions (average of 22 cells in LD versus 21 cells in DD, p>0.42 in two-tailed T-test). Image in J is intentionally overexposed to confirm the absence of HuC/D signal in the habenular nuclei. All views are dorsal. Scale bar = 50 μm.
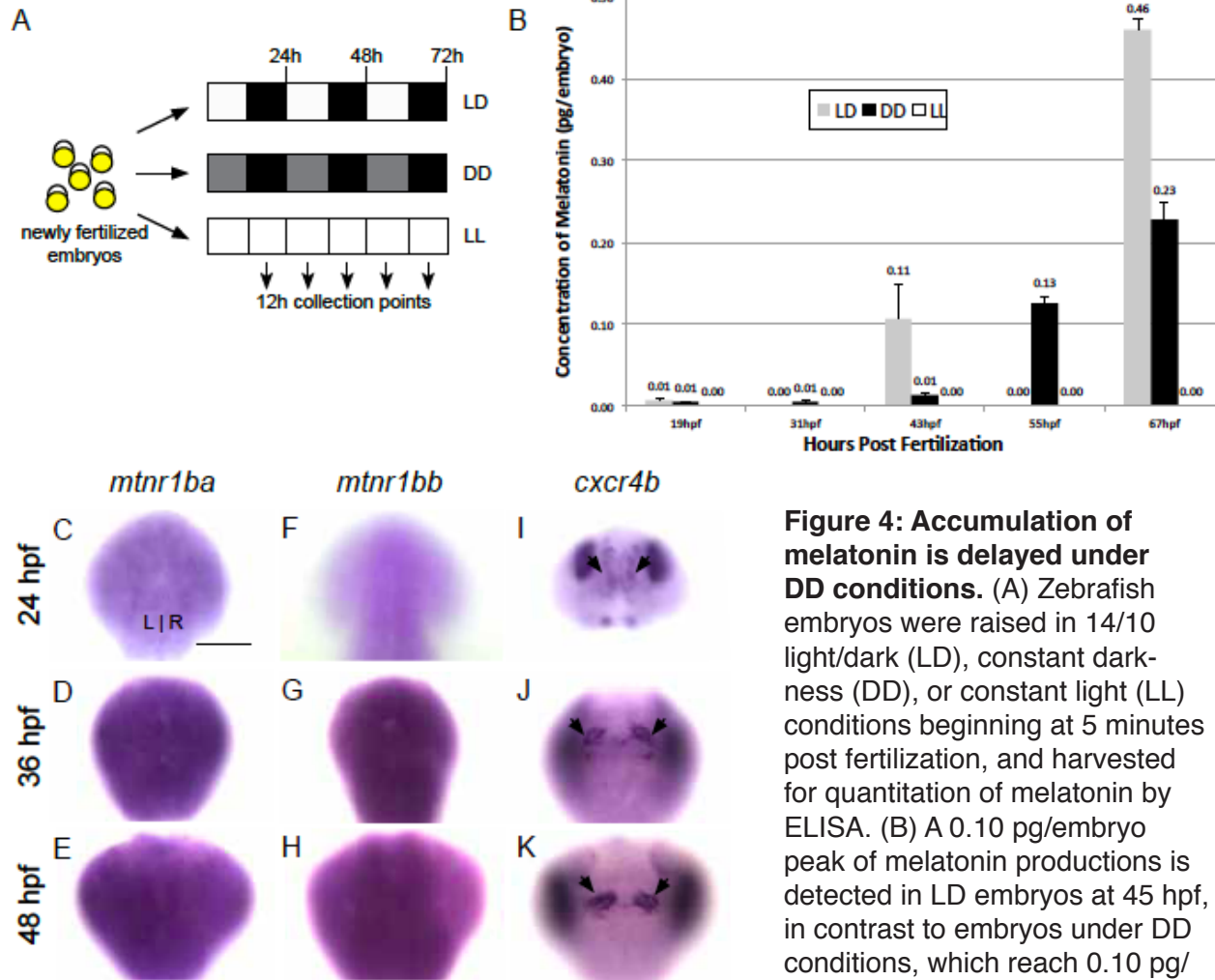
Figure 4: Accumulation of melatonin is delayed under DD conditions. (A) Zebrafish embryos were raised in 14/10 light/dark (LD), constant darkness (DD), or constant light (LL) conditions beginning at 5 minutes post fertilization, and harvested for quantitation of melatonin by ELISA. (B) A 0.10 pg/embryo peak of melatonin productions is detected in LD embryos at 45 hpf, in contrast to embryos under DD conditions, which reach 0.10 pg/embryo 10 hours later. No significant amount of melatonin is detected in LL embryos. Graph shows the average of 3 independent experiments. (C-E) In situ hybridization for melatonin receptor 1ba (mtnr 1ba) and (F-H) melatonin receptor 1bb (mtnr1bb). Expression of mtnr1ba and mtnr1bb is found throughout the brain from 24 to 48 hpf. (I-K) In situ hybridization for cxcr4b reveals that habenular cells (black arrows) are present in the developing brain when mtnr1ba and mtnr1bb are expressed. Samples are siblings of the embryos in (C-H), photographed at the same focal plane. All views are dorsal. Scale bar = 50 μm.

kctd12.2 is expressed in the medial subnucleus, which is larger in the right habenula (Gamse et al., 2005). Neurons of both subnuclei express the synaptic vesicle priming protein *calcium dependent activator protein for secretion 2 (cadps2)* (Gamse et al., 2005). Under LD conditions, transcription of *kctd12.1, kctd12.2* and *cadps2* transcription is first detectable at 38, 45, and 44 hpf respectively in the habenular nuclei (Figure 1B, F, J). However, when embryos are exposed to constant darkness (DD) conditions, neuronal development is significantly postponed. Expres-

sion of *kctd12.1*, *kctd12.2,* and *cpd2* is delayed until 48, 49, and 52 hpf (delay of 10, 4, and 8 hours) respectively (Figure 1C-E, G-I, K-M).

The effect of DD conditions on neuronal differentiation in the epithalamus is not a generalized delay of brain development. Expression of *neuropilin 1a (nrp1a)*, a semaphorin receptor required for habenular axon targeting (Kuan et al., 2007b), is unaffected by DD treatment (Figure
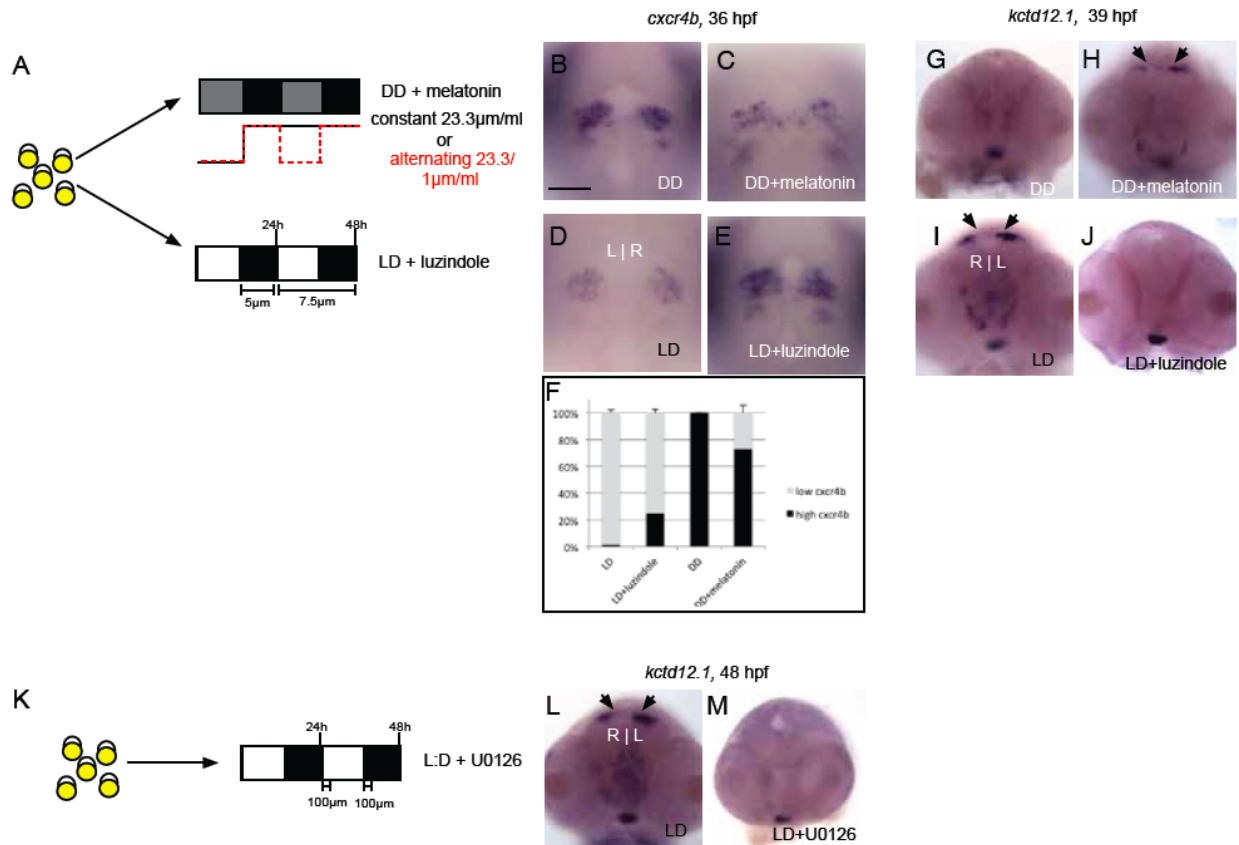
Figure 5: Melatonin signaling is required for the timely differentiation of habenular neurons in constant darkness. (A) Embryos were either placed in DD and treated with melatonin or placed in LD and treated with the melatonin receptor antagonist luzindole. (B-C) Melatonin treatment under DD conditions phenocopies LD embryos: no excess precursors and (G-H) timely appearance of kctd12.1-positive neurons. (D-E) Conversely, antagonism of melatonin receptors under LD conditions results in a phenotype similar to DD embryos: accumulation of excess cxcr4b-positive precursors and (I-J) delayed appearance of kctd12.1-positive neurons. (F) Quantitation of data represented in panels B-E. (K) Embryos in LD conditions were treated with the ERK1/2 phosphorylation inhibitor U0126. (L-M) A delay in the appearance of kctd12.1 neurons, similar to that seen in DD conditions, is observed. All views are frontal except A-D (dorsal views). Scale bar = 50 *μ*m.
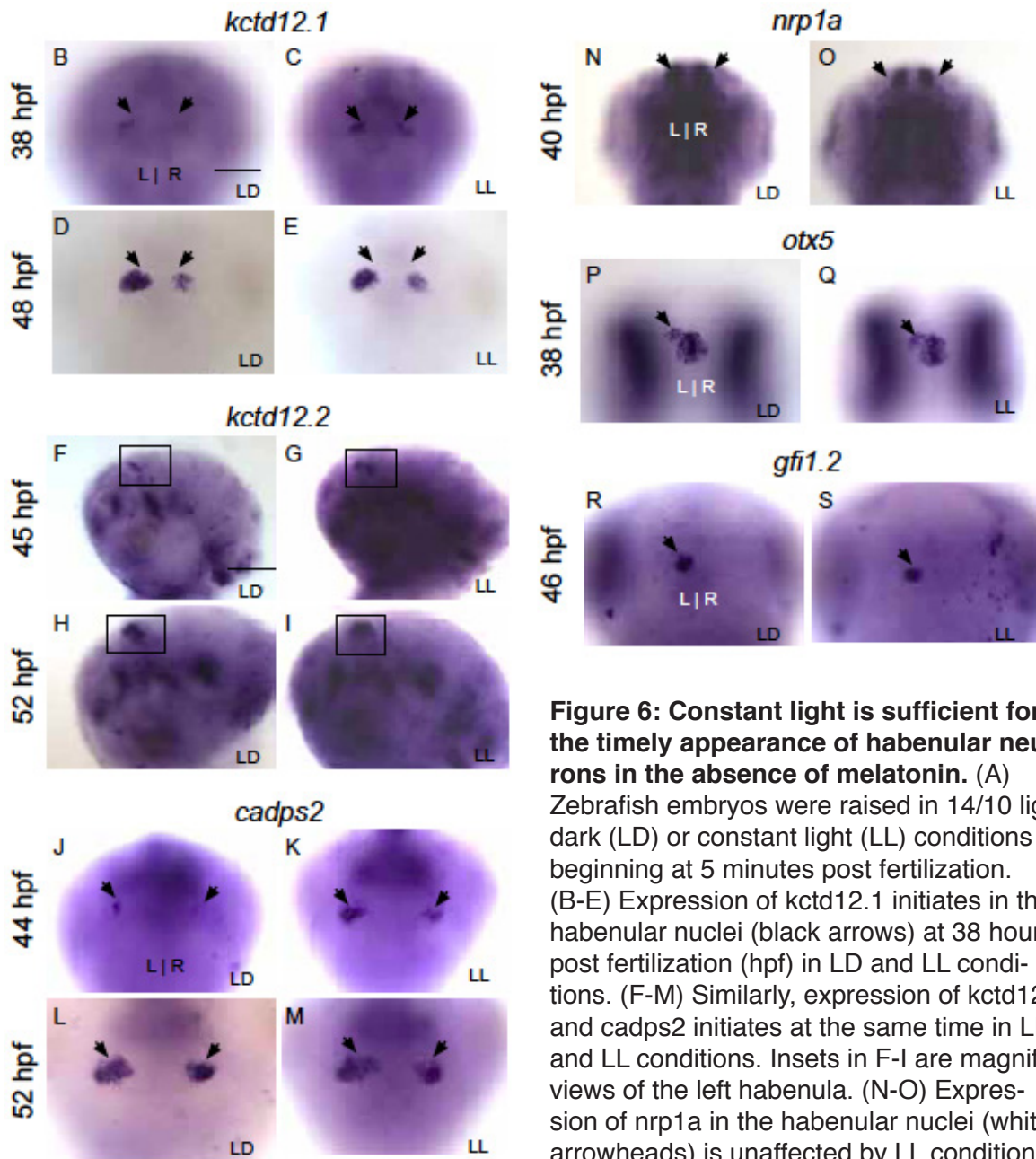
Figure 6: Constant light is sufficient for the timely appearance of habenular neurons in the absence of melatonin. (A) Zebrafish embryos were raised in 14/10 light/dark (LD) or constant light (LL) conditions beginning at 5 minutes post fertilization. (B-E) Expression of kctd12.1 initiates in the habenular nuclei (black arrows) at 38 hours post fertilization (hpf) in LD and LL conditions. (F-M) Similarly, expression of kctd12.2 and cadps2 initiates at the same time in LD and LL conditions. Insets in F-I are magnified views of the left habenula. (N-O) Expression of nrp1a in the habenular nuclei (white arrowheads) is unaffected by LL conditions; (P-S) nor is otx5 expression in the pineal and parapineal or gfi1 expression in the parapineal (black arrows). All views are dorsal except for lateral views in F-I. Scale bar = 50 μm except for insets in F-I (25 μm).

1N&O). Accordingly, habenular axons innervate their appropriate targets in the interpeduncular nucleus of the midbrain (Supplemental Figure 1A&B). Furthermore, the formation of the pineal complex occurs on time, marked by expression of the genes *otx5* (Gamse et al., 2002) and *gfi-1* (Dufourcq et al., 2004) (Figure 1P-S) and by HuC/D in projection neurons (Figure 2I&J, white

arrowheads). In addition, *kctd12.1* expression in the pituitary and *kctd12.2* expression throughout other regions of the brain is unchanged (Figure 1B-I).

Reversal of the photoperiod phase does not significantly advance gene expression in the habenular nuclei

The initial expression of *kctd12.1* at 38 hpf in the habenular nuclei coincides with the start of the second dark phase of the photoperiod, while *kctd12.2* and *cadps2* initiates in the

Figure 7: Neuropil formation in the habenular nuclei is promoted by melatonin. (A-C) At 48 hpf, the amount of dense neuropil in the left habenular nucleus is reduced by 28.5% in DD conditions, relative to LD controls. (D-F) At 72 hpf, total neuropil in both habenular nuclei is reduced by 21% in DD conditions, relative to LD controls. (G-I) Treatment with luzindole under LD conditions causes a reduction in neuropil similar to DD conditions (2 examples are shown). (J-L) Conversely, treatment with melatonin under DD conditions rescues neuropil density to be similar to LD (2 examples are shown). Dashed white lines outline the entire habenular nucleus. Neuropil quantitation includes the volume of all labeled fibers in the habenular nucleus, excluding the habenular commissure. All views are dorsal. The ends of the red rectangle in C, F, I, L are the 25th and 75th quartiles (encompassing the interquartile range); the line across the middle represents the median value, and the error bars represent 1.5 times the interquartile range. ** = $p < 0.02$; *** = $p < 0.002$ by two-tailed T test. Scale bar = 25 μm.

30
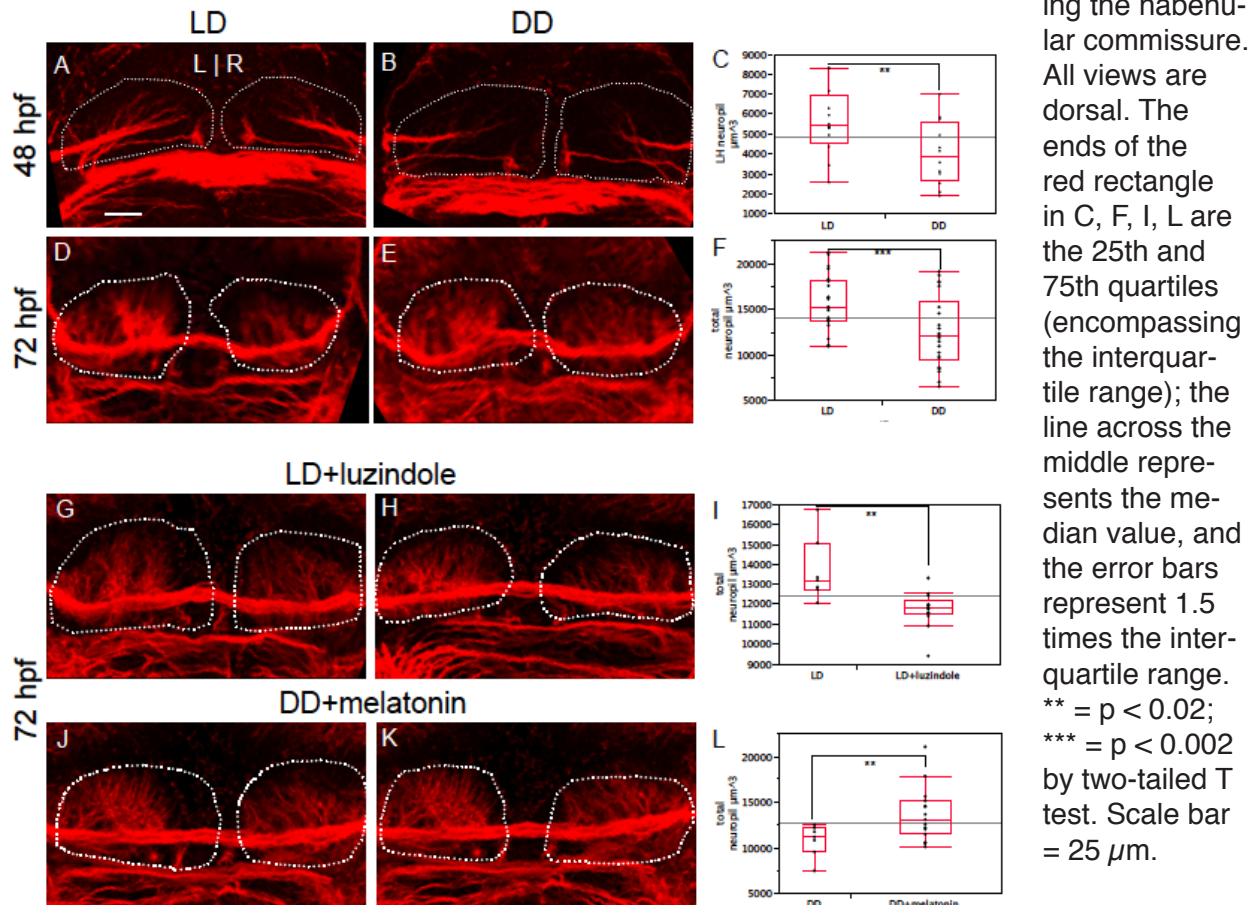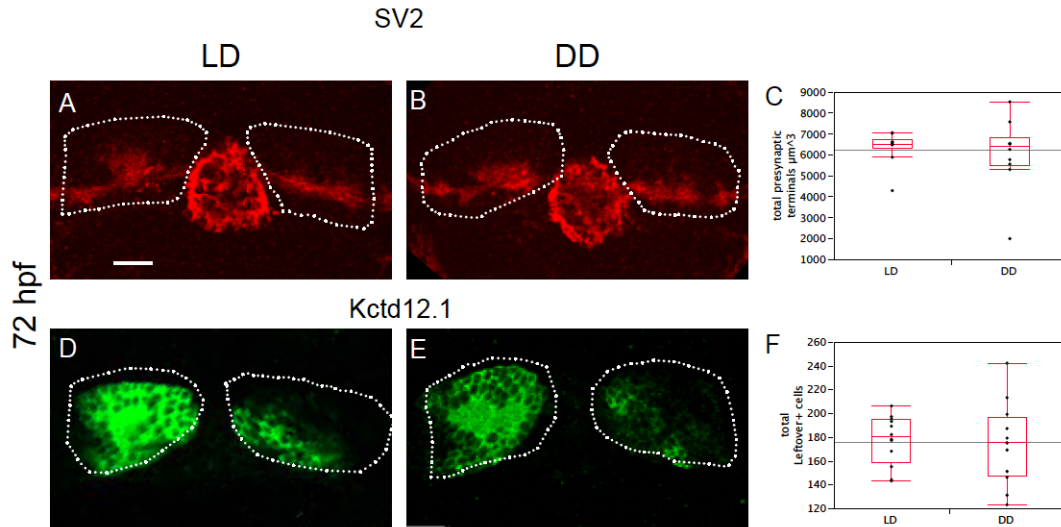
Supplementary Figure 2: Presynaptic densities and kctd12.1-positive cell number in the habenular nuclei is unaffected by DD conditions. (A-C) At 72 hpf, the volume of SV2 signal, representing presynaptic vesicles in axons synapsing on the habenula, is similar in LD and DD larvae. (D-F) The total number of kctd12.1-expressing cells in the habenular nuclei is similar in LD and DD larvae.

middle of the second dark phase. By reversing the phase of the photoperiod to dark-light (DL), the second dark phase would occur 14 hours earlier (Figure 2A). To determine if expression of genes in the habenular nuclei is correlated with the second dark phase, we incubated embryos in DL conditions, and examined whether gene expression was advanced by 5 hours. We harvested LD and DL embryos 5 hours and 0 hours before the first time point that we can detect expression in LD embryos (33 and 38 hpf for *kctd12.1*, 40 and 45 hpf for *kctd12.2*, 39 and 44 hpf for *cadps2,* respectively). Expression of *kctd12.1*, *kctd12.2,* and *cadps2* was absent in DL embryos at the earlier time point, and present at the later time point, similar to LD control embryos (Figure 2B-M). Therefore, gene expression is not advanced by 5 hours in DL embryos relative to LD controls. However, a slight advance in the timing of *kctd12.1* expression may be present. Expression of *kctd12.1* at its onset is low, and increases gradually over time (compare Figure 1B to 1D). In the habenular nuclei, the number of embryos with high expression of *kctd12.1* was greater in DL than in LD embryos at 38 hpf (compare Figure 2D to E; 100% of LD embryos (n=30) had expression equal or less than the example shown in Figure 2D, whereas 83% of DL embryos (n=18) had expression equal or greater to the example shown in Figure 2E, and the remainder

31

resembled ure 2D). We find evidence for slightly premature *kctd12.1* expression in the habenular nuclei of DL embryos compared to LD siblings, and no change in the timing of expression for *kctd12.2* and *cadps2*.

In constant darkness, habenular cells remain in a progenitor state for an extended time

The late development of habenular neurons could result from delayed specification of progenitor cells, or delayed differentiation of progenitors into post-mitotic habenular neurons. We examined expression of *cxcr4b*, a marker of habenular progenitor cells and newly born neurons (Roussigne et al., 2009). Initially, similar numbers of *cxcr4b*$^+$ cells are detected in the epithalamus of LD and DD embryos, but as development progresses, excess *cxcr4b*$^+$ cells accumulate in DD embryos relative to LD embryos (Figure 3A-F). Similar to Roussigne et al, we note a left-biased initial appearance of *cxcr4b*$^+$ cells in both LD and DD conditions. By 72 hpf, the number of *cxcr4b*$^+$cells in DD embryos is similar to LD embryos (Figure 3G&H). The RNA binding proteins HuC/D are expressed in post-mitotic habenular neurons (Kim et al., 1996; Roussigne et al., 2009). Under DD conditions, many fewer HuC/D-expressing precursors are detected in the habenular nuclei at 38 hpf relative to LD siblings (average of 31 total HuC/D-expressing cells for LD versus 9 for DD, $p<0.001$ in two-tailed T-test; Figure 3I&J). Therefore, it appears that in constant darkness, an appropriate number of habenular progenitor cells are specified, but they exit the progenitor state late.

Constant darkness delays the production of high melatonin concentrations

We hypothesized that delayed melatonin production by the pineal organ may be responsible for the delay in habenular neurogenesis, so we examined melatonin production in DD embryos. A previous report demonstrated that raising zebrafish embryos in continuous darkness beginning at 14 hpf resulted in near-basal production of melatonin until 55 hpf (Kazimi and

Cahill, 1999). We confirmed these results by beginning the dark period within 5 minutes post fertilization, and harvesting embryos at 12-hour intervals for analysis by ELISA (Figure 4A). We find that in LD embryos, melatonin is first detectable at 43 hpf, at a concentration of 0.10 pg/embryo (Figure 4B). By contrast, DD embryos do not produce a similar concentration of melatonin until 55 hpf. The 12 hour delay in melatonin synthesis is similar to the 10-hour delay in *kctd12.1* gene expression, the earliest marker of habenular neuron differentiation that we have tested.

We examined the expression of melatonin receptors in the embryonic zebrafish. A previous report had shown that the melatonin receptors *mtnr1aa* (previously Z1.7), *mtnr1ba* (previously Mel1b) and *mtnr1bb* (previously Z2.6-4), are expressed in zebrafish embryos between 18 and 36 hpf (Danilova et al., 2004). To examine which of these receptors is expressed in habenular precursor cells, we performed in situ hybridization at 24, 36, and 48 hpf. We find that *mtnr1ba* and *mtnr1bb* are expressed throughout the central nervous system at all time points examined (Figure 4C-H), including in habenular precursor cells, which is marked by expression of *cxcr4b* (Roussigne et al., 2009) (Figure 4I-K). Expression of *mtnr1aa* was found in the ventral hindbrain but was not detected in habenular precursor cells (data not shown).

Melatonin is sufficient for the timely differentiation of habenular neurons in constant darkness

Next we tested the role of melatonin signaling in timely development of the habenular nuclei. To demonstrate that the delay in neuronal development in constant darkness conditions is due to reduced melatonin levels, we first tested the ability of melatonin to rescue habenular development in DD conditions. DD embryos were treated with exogenous melatonin, either in imitation of circadian rhythm (14 hours (h) low melatonin:10 h high, to simulate levels in LD conditions) or continuously (24 h high melatonin) (Figure 5A), starting at 14 hpf. Either treatment rescues habenular development in DD embryos to resemble LD embryos (Figure 5B, C, F, G, H). Next, we tested if blocking melatonin receptor activity in LD embryos could replicate the

delayed differentiation phenotype of DD embryos. We found that treatment of embryos in LD conditions with the transmembrane melatonin receptor MT1/2 antagonist luzindole (Dubocovich, 1988) can delay habenular development similar to DD conditions (Figure 5D, E, F, I, J). Therefore, melatonin signaling is necessary to promote timely differentiation of habenular neurons.

The MT1/2 melatonin receptors are 7-pass G-protein coupled proteins that can signal intracellularly via a number of pathways, including the MEK/ERK MAP kinase cascade (Jockers et al., 2008). We treated LD embryos with 2x 1-hour pulses of the MEK–specific inhibitor U0126, at 24 and 36 hpf (Figure 5K). Following this treatment, habenular development was delayed similar to DD or luzindole treatment (Figure 5L&M).

Constant light is sufficient for the timely differentiation of habenular neurons in the absence of melatonin

Adult fish or pineal organs kept in constant light (LL) conditions exhibit constitutively low levels of melatonin production (Bolliet et al 1995, Oliveira et al 2007, Amano et al 2006). We find a similar result in zebrafish embryos incubated under LL conditions (Figure 4B). The concentration of melatonin in LL embryos remains below levels detectable by ELISA at all time points assayed.

Since addition of exogenous melatonin to embryos in DD conditions was sufficient to rescue the timely appearance of gene expression in the habenular nuclei, and because pharmacological inhibition of melatonin receptors was sufficient to inhibit timely gene expression in LD embryos, we examined LL embryos to determine if melatonin was necessary for the timing of gene expression. Surprisingly, we detected no delay in gene expression in the habenular nuclei of LL embryos (Figure 6 B-M). In fact, a slight advance in the timing of gene expression may be present in the expression of *kctd12.1* and *cadps2*. Expression of both of these genes at the onset is low, and increases gradually over time (compare Figure 6B to D, Figure 6J to M). In the habenular nuclei of LL embryos, 63% of embryos exhibited moderate to high expression

of *kctd12.1* at 38 hpf (moderate expression is shown in Figure 6C), while 66% of LD embryos exhibited low or no expression of *kctd12.1* at 38 hpf (low expression is shown in figure 6B). A similar although less striking increase in expression is detected for *cadps2* (LL: 35% with moderate expression [Figure 6K], 63% with low expression, n=42. LD: 0% with high expression, 61% with low expression [Figure 6J], 39% with no expression, n=44). By 48 and 52 hpf , the number of embryos with moderate or high expression of *kctd12.1* and *cadps2* is nearly equal for LL and LD embryos (LL: 78% for *kctd12.1,* n=83; 98% for *cadps2,* n=48. LD: 70% for *kctd12.1*, n=70; 98% for *cadps2,* n=51. Expression is low for both genes in the remainder of embryos).

Delayed habenular neurogenesis results in reduced neuropil formation

In addition to delaying neurogenesis, raising embryos in DD conditions resulted in reduced neuropil in the habenular nuclei. This neuropil consists of defasciculated axons from the forebrain and dendrites from habenular neurons (Concha et al., 2000; Hendricks and Jesuthasan, 2007; Moutsaki et al., 2003). We used confocal imaging and volumetric analysis of neuropil to assay changes in LD versus DD larvae. At 48 hpf, DD embryos form an average of 28.5% less neuropil volume in the left habenula than LD siblings (Figure 7 A-C). By 72 hpf, a 21% average reduction in total neuropil volume is seen (Figure 7 D-F). We find that decreased neuropil under DD conditions is due to reduced melatonin receptor signaling. Treatment of LD embryos with luzindole causes decreased neuropil relative to untreated LD embryos (Figure 7 G-I). Conversely, DD embryos treated with melatonin exhibit an increase in neuropil relative to DD alone (Figure 7 J-L).

In DD embryos, the volume of presynaptic densities in forebrain axons terminating on habenular dendrites was unchanged relative to LD (Supplemental Figure 2A-C). In addition, at 72 hpf the number of cells in the L/R asymmetric lateral subnucleus was unaffected by LD versus DD (Supplemental Figure 2D-F). Because cell number and inputs appear unchanged, the reduced neuropil is best explained as decreased dendritogenesis by habenular neurons.

DISCUSSION

Light plays a crucial role in starting the circadian oscillator in the pineal organ as well as synchronizing the oscillations of individual cells so as to generate nighttime peaks of melatonin output (Dekens and Whitmore, 2008; Kazimi and Cahill, 1999; Tamai et al., 2007; Vuilleumier et al., 2006; Whitmore et al., 2000; Ziv et al., 2005). We find that both light and melatonin are important for the timing of neuronal differentiation in the habenular nuclei and ultimately for the appropriate elaboration of dendrites from these neurons.

We were able to rescue habenular neuron differentiation in 100% of DD embryos with melatonin, and recapitulate delayed differentiation in 100% of LD embryos with the melatonin receptor inhibitor luzindole. However, we noted changes in the size of the precursor pool (*cx-cr4b*-expressing cells) in only a fraction (~30%) of the melatonin- or luzindole-treated embryos. In addition, LL embryos receiving a constant light signal produce no detectable melatonin, yet they also showed no delay of habenular differentiation, and may exhibit a modest advancement in the timing of some genes' expression in the habenular nuclei. Therefore, although melatonin is sufficient to promote the differentiation of habenular neurons under DD conditions, it is not necessary under LL conditions. One explanation for the sufficiency but not necessity of melatonin is that light may act in a parallel pathway independent of melatonin to stimulate differentiation of habenular neurons. Many tissues of the zebrafish have been demonstrated to be light responsive (Cahill, 1996; Dekens et al., 2003; Tamai et al., 2005; Whitmore et al., 2000), express photosensitive pigments including cryptochromes and teleost multiple tissue (tmt) opsin (Moutsaki et al., 2003; Tamai et al., 2007) and photosensitive enzymes such as acetyl-CoA oxidases (Hirayama et al., 2007; Hockberger et al., 1999; Thisse and Thisse, 2004). Light and melatonin could act on precursors additively in order to initiate differentiation by integrating the duration and intensity of downstream signal transduction Once the total light-mediated and melatonin-mediated signaling reaches a threshold amount, habenular progenitors differentiate. Under LD conditions, light signaling during the day plus melatonin signaling during the night would exceed this threshold

at 38 hpf for activation of kctd12.1 expression, 45 hpf for *kctd12.1* expression, and so on. Under DD conditions, in the absence of light input, the threshold would not be reached until 5-10 hours later, when melatonin production had become great enough for a long enough period of time. Conversely, under LL conditions, constant signaling by light input could reach the threshold more quickly, even in the absence of melatonin, since the amount of time that the embryos are exposed to light is almost doubled. Knocking down each of the photoreceptive proteins in the context of melatonin receptor inhibition should reveal if habenular precursor cells integrate light and melatonin signals in order to time their differentiation.

Integration of light and melatonin signaling might occur via a shared signal transduction cassette, the ERK MAP kinase pathway. Oxidative species, such as those generated by light-sensitive flavin-containing oxidases, induce gene expression via the ERK MAP kinase pathway (Hirayama et al., 2007). Melatonin receptors can also activate ERK MAP kinase signaling (Daulat et al., 2007; Witt-Enderby et al., 2000). We find that inhibition of ERK MAP kinase signaling by U0126 is capable of delaying *kctd12.1* expression in the habenular nuclei. More targeted manipulation of the ERK MAP kinase pathway, such as inactivation of individual downstream targets such as *pea3* and *erm,* will be necessary to test this hypothesis.

Decreased avoidance of a simulated predator is reported for zebrafish larvae raised in constant darkness (Budaev and Andrew, 2009). Budaev and Andrew have hypothesized that light input influences predator response by affecting habenular output (Budaev and Andrew, 2009) via changes in Nrp1a expression and thus axon targeting (Kuan et al., 2007a). However, we do not detect a change in *nrp1a* expression or axonal targeting to the IPN in LD versus DD conditions. We do find that DD conditions result in decreased neuropil density in the habenular nuclei, perhaps because habenular neurons are exposed for a shorter time to intrinsic or extrinsic signals for dendrite formation (Parrish et al., 2007). Habenular neuron function has been recently implicated in zebrafish learning whether it is best to flee or freeze in place in response to a negative stimulus (Agetsuma et al., 2010; Lee et al., 2010), a behavior that is relevant in reacting to predators. It is therefore possible that decreased predator avoidance behavior in DD-raised larvae is a conse-

quence of reduced habenular dendritogenesis.

Conclusions

We show that the timing of neuronal differentiation and subsequently the appropriate outgrowth of dendrites during habenular development are an event that requires light and the hormone melatonin. Intriguingly, alteration of melatonin production is a symptom of some neurological diseases, including autism and Smith-Magenis syndrome (Elsea and Girirajan, 2008; Kulman et al., 2000; Nir, 1995; Tordjman et al., 2005). In addition, mutations of the melatonin biosynthetic enzyme ASMT are linked to increased autism risk (Melke et al., 2008). It has been proposed that altered melatonin during early postnatal development may be causative rather than simply symptomatic of these diseases, by altering formation of brain circuits (Bourgeron, 2007). The zebrafish embryo, with its easily manipulated pathway for melatonin signaling, now provides a platform to explore how melatonin influences brain development.

CHAPTER III

DBX1B DEFINES THE HABENULAR PROGENITOR DOMAIN IN THE ZEBRAFISH DORSAL DIENCEPHALON

In review at: Neural Development

Dean, BJ, Erdogan, B, Gamse, JT, and Wu, S. Dbx1b defines the habenula progenitor domain in the zebrafish dorsal diencephalon. *Neural Developmental*.

INTRODUCTION

The habenular nuclei (habenulae) develop in the dorsal diencephalon of vertebrates. These bilaterally paired nuclei receive inputs from the limbic system and basal ganglia and send outputs to cholinergic, dopaminergic and serotonergic centers. Despite their small size, these nuclei play crucial roles in regulating aversion and reward behaviors (Velasquez et al. 2014). Moreover, the fact that the habenulae are a nexus for monoamine circuits highlights the importance of this brain region for studies of neuromodulation and multi-circuit integration.

Alterations of habenular structure and function have been linked to depression and addiction in human patients (Velasquez et al. 2014). Therapeutically, deep-brain stimulation of the habenulae in treatment-resistant major depression is currently in trials (Kiening & Sartorius 2013). The endophenotypes of decreased reward in addiction and anhedonia in depression have been modeled in monkey, rodent and zebrafish habenulae (Matsumoto & Hikosaka 2007; Jhou et al. 2013; Li et al. 2011; Hong et al. 2013; Okamoto et al. 2012). Beyond translational research, the zebrafish habenulae also serve as an excellent model to study the basic mechanisms underlying the development of left-right brain asymmetry. Though mammalian habenulae are asymmetric, teleost habenulae asymmetry is more dramatic in anatomy, gene expression and functional connectivity (Bianco & Wilson 2009).

Interest in how the habenulae integrate into monoaminergic circuitry has put pressure on researchers to understand habenular development. Genetic markers of habenular neurons have been crucial to the aforementioned work; however, habenular development is poorly understood and currently there are no known markers for habenular progenitors. Indeed, recent work has emphasized the neuronal diversity of the habenulae (DeCarvalho et al. 2014). Therefore, finding marker genes that label habenular progenitors will be fundamental to studying how the diverse set of habenular neurons are generated and integrated into neural circuits underpinning aversive behavior as well as pathological addictive and depressive behaviors.

The *dbx* homeodomain transcription factors play a central role in regulating progenitor status in several brain regions (Gribble et al. 2007). However, the upstream regulatory pathways that regulate *dbx* gene-family expression are not well-understood. Here we report that in zebrafish, *dbx1b* is expressed in the dorsal diencephalon where it marks habenular progenitors, and further, that dorsal diencephalic expression of *dbx1b* is controlled by FGF signaling.

MATERIALS & METHODS

Zebrafish maintenance and strains

Zebrafish were raised at 28.5°C on a 14/10 hour light/dark cycle and staged according to hours post-fertilization. The following fish lines were used: the wild-type strain AB* (Walker 1999), *TgBAC[dbx1b:Cre-mCherry]nns13a* (Koyama et al. 2011) and *Tg[-10actb2:LOXP-mCherry-LOXP-nlsEGFP]pd31* (Kikuchi et al., 2010). All experiments were approved by the Vanderbilt University's Institutional Animal Care and Use Committee (IACUC) and Office of Animal Welfare, and performed according to national regulatory standards.

Whole mount *in situ* hybridization
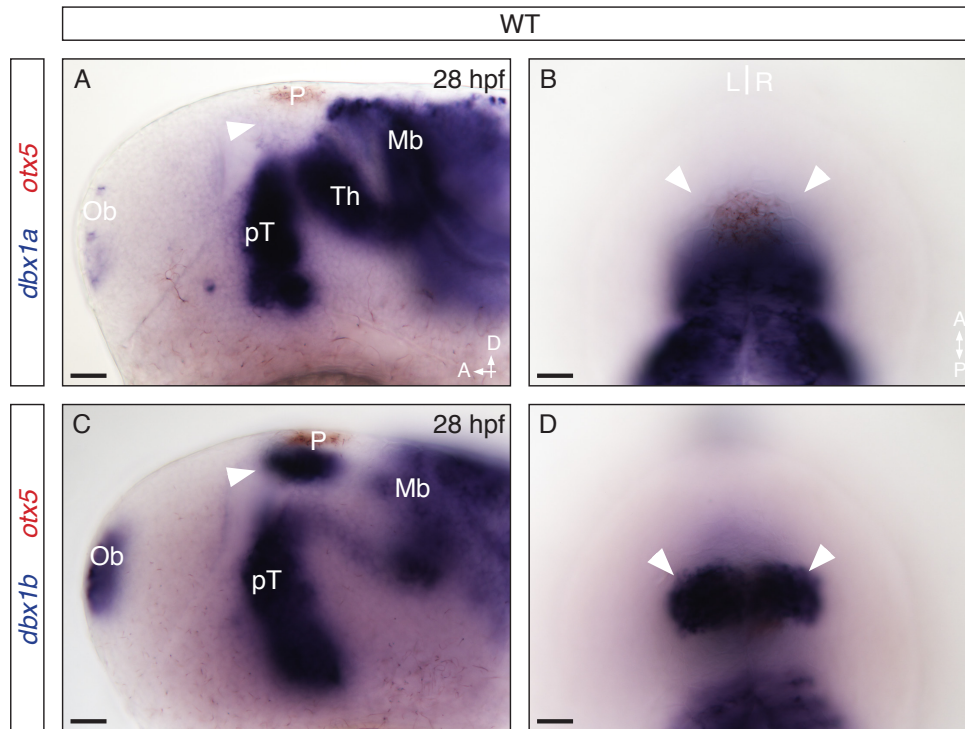
Supplementary Figure 1: *Dbx1b* is expressed in the dorsal diencephalon. Lateral and dorsal views of a 28 hpf wildtype embryo. (A & B) In situ hybridization for *dbx1a* (blue) revealed several expression domains including the olfactory bulb (Ob) prethalamus (pT), thalamus (Th), midbrain (Mb) throughout the brain but no expression in the dorsal diencephalon (arrow heads). (C & D) *dbx1b* transcript (blue) was expressed in a similar pattern but with greatly reduced expression in thalamus and robust expression in the dorsal diencephalon and olfactory bulb. *otx5* (red) marks the pineal complex (P), a component of the dorsal diencephalon. Scale bars are 10um.

Whole-mount RNA *in situ* hybridization was performed as described previously (Gamse 2003), with one change: 5% dextran sulfate was added to the hybridization buffer. Hybridized probes were detected using alkaline phosphatase conjugated antibodies (Roche) and visualized by 4-nitro blue tetrazolium (NBT; Roche) and 5-bromo-4-chloro-3-indolyl-phosphate (BCIP; Roche) staining for single colorometric labeling, or by NBT/BCIP followed by iodonitrotetrazolium (INT) and BCIP staining for double colorometric labeling. *dbx1a* probe (Gribble et al. 2007) was produced from pCRII-*dbx1a* plasmid linearized by EcoRV and transcribed by SP6 RNA polymerase. *dbx1b* probe (Gribble et al. 2007) using pCRII-*dbx1b,* BamHI and T7 RNA polymerase, and *otx5* (Gamse et al. 2002) using pBS-*otx5,* Not1 and T7 RNA polymerase.

Whole mount fluorescent *in situ* hybridization and immunohistochemistry

Whole-mount fluorescent *in situ* hybridization and immunohistochemical co-labeling was
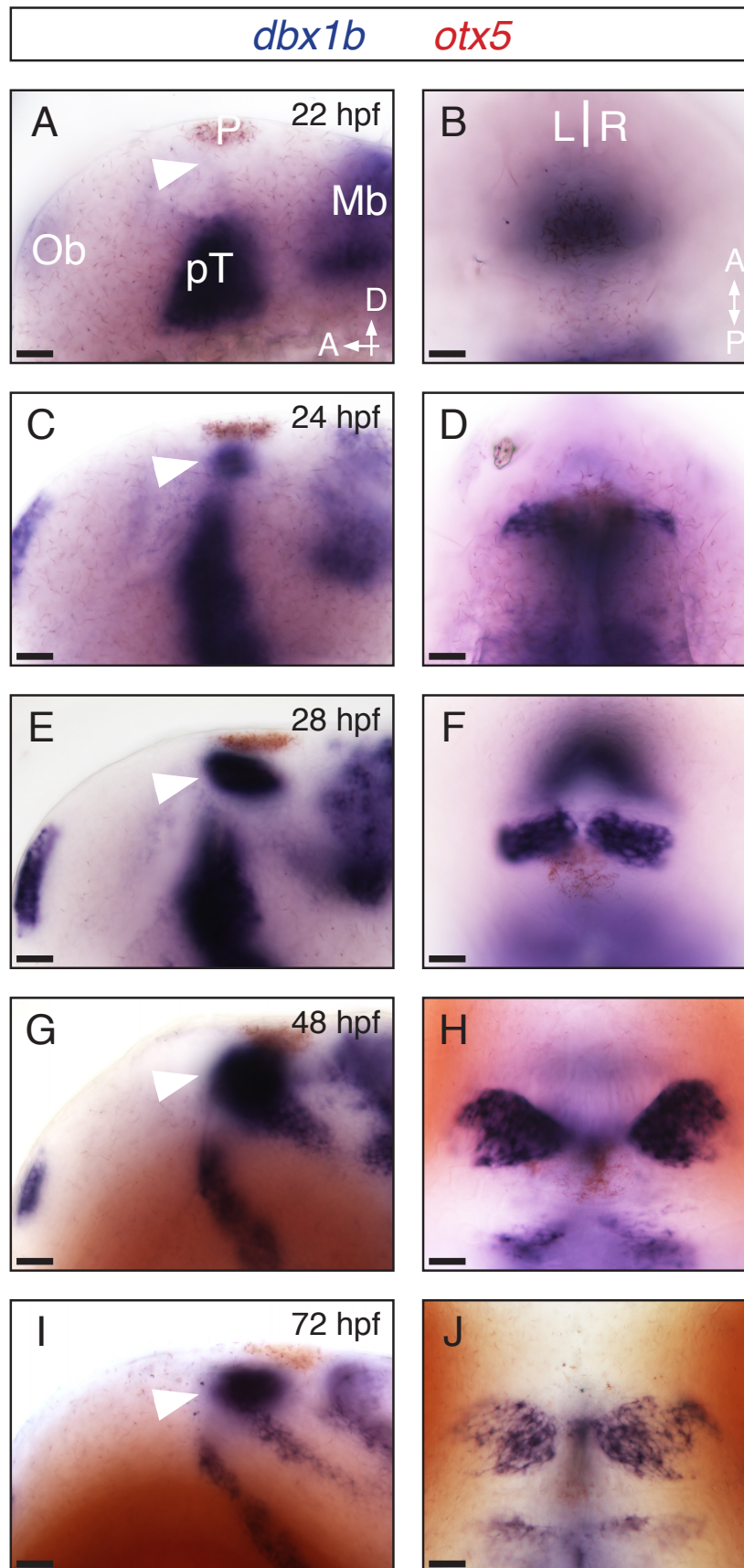
Figure 1: *Dbx1b* is expressed throughout habenular development. (A-J) Lateral and dorsal views of *dbx1b* expression (blue) during early brain development. Dorsal diencephalic expression of *dbx1b* appeared shortly after 22 hpf and continued through 72 hpf (arrowhead). *otx5* (red) marks the pineal complex (P). Ob – olfactory bulb, pT – prethalamus, Mb – midbrain. Scale bars are 10um.

performed as described previously (Doll et al. 2011a), with the following additional reagents: In addition to Fast Red substrate (Sigma, F4648), some experiments used 3 x 5 minutes washes in Fast Blue Buffer (Lauter et al. 2011)mapping of overlapping and abutting regulatory gene expression domains by chromogenic two-color in situ hybridization has helped define molecular subdivisions of the developing vertebrate brain and shed light on its basic organization. Despite the benefits of this technique, visualization of overlapping transcript distributions by dif-
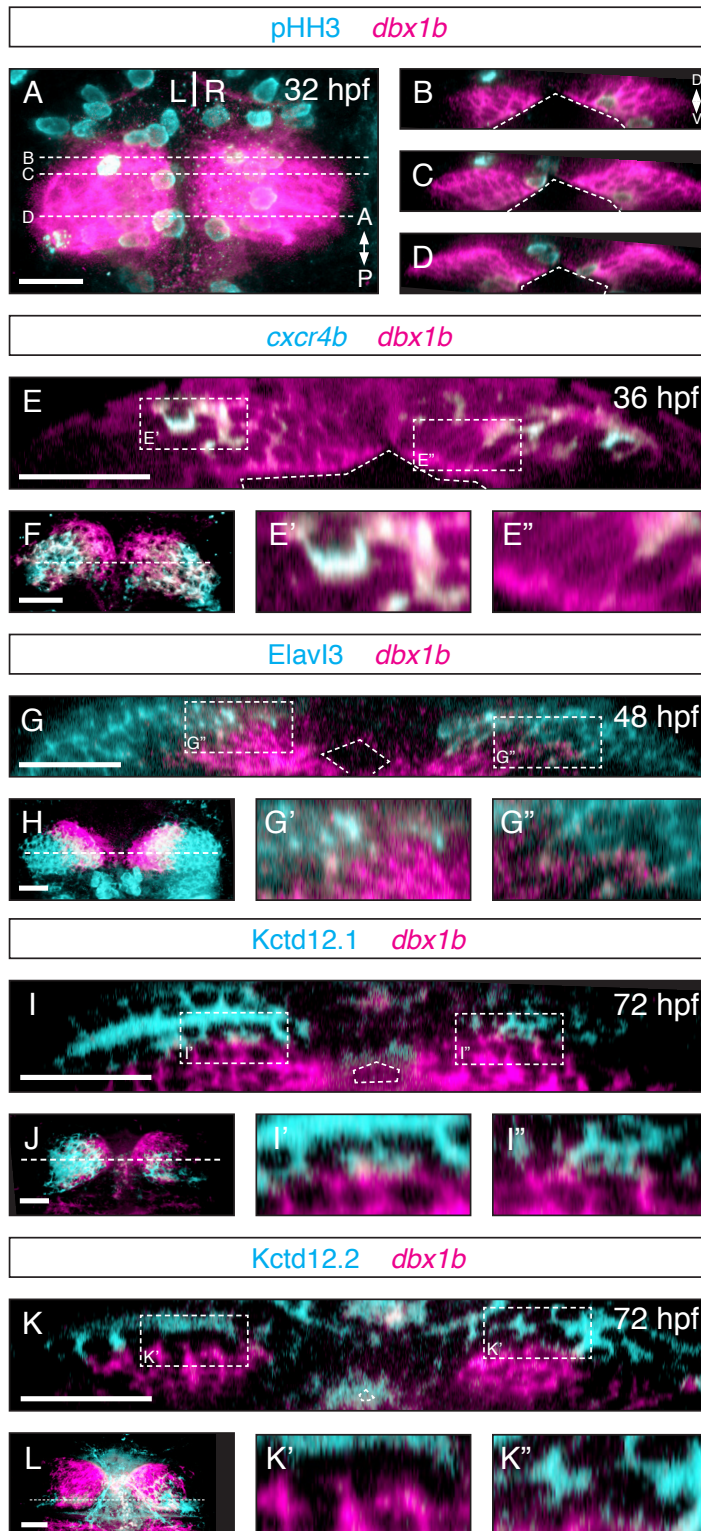
Figure 2: *Dbx1b* marks a proliferative periventricular domain in the dorsal diencephalon. (A) A dorsal view of the epithalamus showed *dbx1b* and phosphohistone H3 (pHH3) expression. (B-D) Coronal optical sections revealed that *dbx1b*-positive cells are pHH3-positive. (E-F) A presumptive habenular precursor marker, *cxcr4b*, showed partial overlaps with *dbx1b*. Significantly, the co-expression domain (E') was more dorsolateral while the *dbx1b*-only domain (E") was along the ventricle. (G-H) *dbx1b* expression showed very little overlap with the neuronal marker Elav3l. (I-L) No co-expression was observed between *dbx1b* and markers of differentiated habenular neurons, Kctd12.1 and Kctd12.2. The ventricle is marked by angled dashed lines. Insets are shown with dashed rectangles. Scale bars are 50uM.

ferently colored precipitates remains difficult because of masking of lighter signals by darker color precipitates and lack of three-dimensional visualization properties. Fluorescent detection of transcript distributions may be able to solve these issues. However, despite the use of signal amplification systems for increasing sensitivity, fluorescent detection in whole-mounts suffers from rapid quenching of peroxidase (POD and were developed in Fast Blue Substrate (0.25mg/mL Fast Blue Substrate and 0.25mg/mL nAMP in Fast Blue Buffer) diluted in Fast Blue Buffer. In addition to the anti-DIG antibody, the primary antibodies used were rabbit anti-pHH3
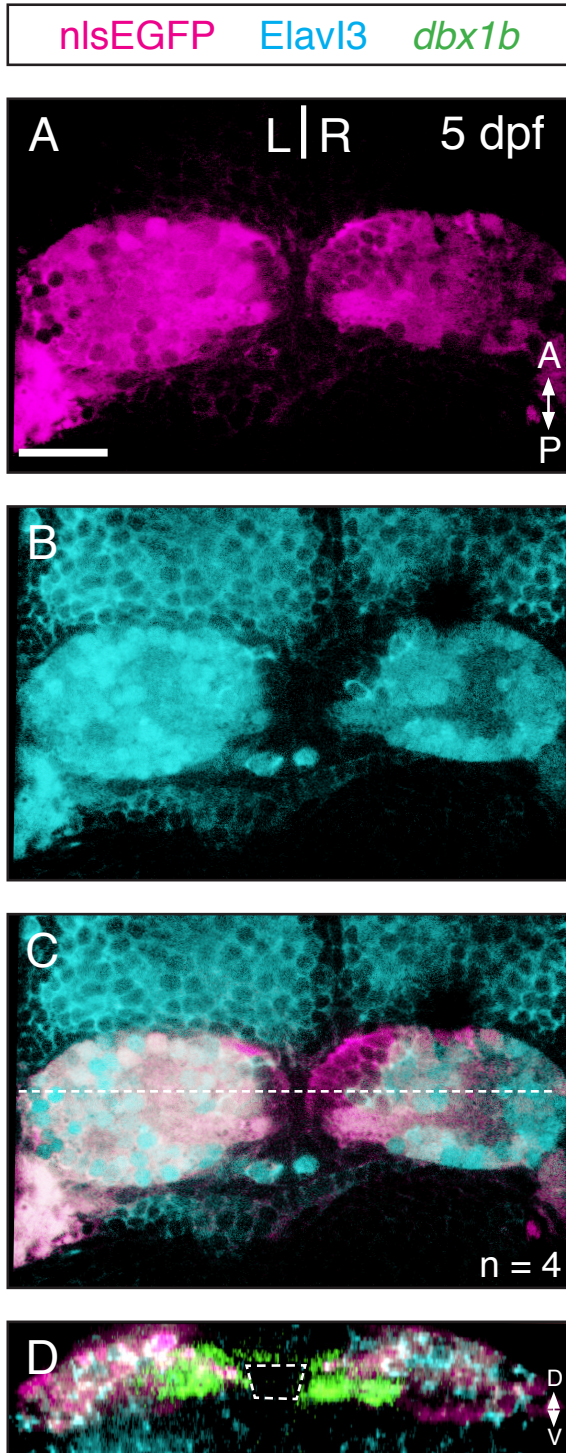
Figure 3: Lineage labeling shows dbx1b-positive cells give rise to dorsal habenular neurons. (A-C) A dbx1b:cre transgene lineage-labeled (magenta) nearly all Elav3l-positive neurons in the habenulae (cyan). See text for details. (D) In a separate lineage-labeling experiment, an Elav3l-negative domain corresponding the habenular progenitor domain, which is labeled by dbx1b expression (green), was clearly discernible as shown by coronal sections. Scale bars are 50uM.

(1:500, Millipore), mouse anti-HuC (1:400, Life Technologies), rabbit anti-GFP (1:500, Torrey Pines Biolab), rabbit anti-Kctd12.1 and rabbit anti-Kctd12.2 (1:300, Gamse et al. 2005)consisting of the pineal complex and flanking dorsal habenular nuclei, provides a valuable model for exploring how left-right differences could arise in the vertebrate brain. The parapineal lies to the left of the pineal and the left habenula is larger, has expanded dense neuropil, and distinct patterns of gene expression from the right habenula. Under the influence of Nodal signaling, positioning of the parapineal sets the direction of habenular asymmetry and thereby determines the left-right origin of habenular projections onto the midbrain target, the interpeduncular nucleus (IPN. Primary antibody was detected using goat-anti-rabbit or goat-anti-mouse antibodies conjugated to Alexa 488, Alexa 568 or Alexa 633 fluorophores (1:300, Molecular Probes).

Double fluorescent in situ hybridization was performed with the following modifications

to the above colorometric *in situ* protocol. After hybridization of DIG and fluorescein labeled

probes, anti-DIG antibody was applied (1:5000, Roche) overnight at 4°C. The following day em-

bryos were washed 4 x 20 min in PBS with Triton (PBSTr) and 3 x 5 min in Fast Blue Buffer and

developed in Fast Blue Substrate diluted in Fast Blue Buffer. After color development, embryos

were washed 2 x 10 min in PBSTr. The alkaline phosphatase was acid inactivated by a 10 min

wash in 0.1M glycine HCl pH2.0. After 2 x 10 min PBSTr washes, embryos were incubated in

Supplementary Figure 2: *Fgf8* mutants show normal overall brain patterning. (A-B) In *fgf8* mutants there were no major anterior-posterior patterning defects observed. *eomes*, *shh* and *wnt1* mark the telencephalon (Tel), ZLI and midbrain (Mb) respectively. *otx5* marks the pineal complex. (C-D) Dorsal-ventral patterning was also unaffected in *fgf8* mutants. *wnt3a* (blue) marks the ZLI and midbrain and *shh* (red) marks the ZLI. Scale bars are 10uM.
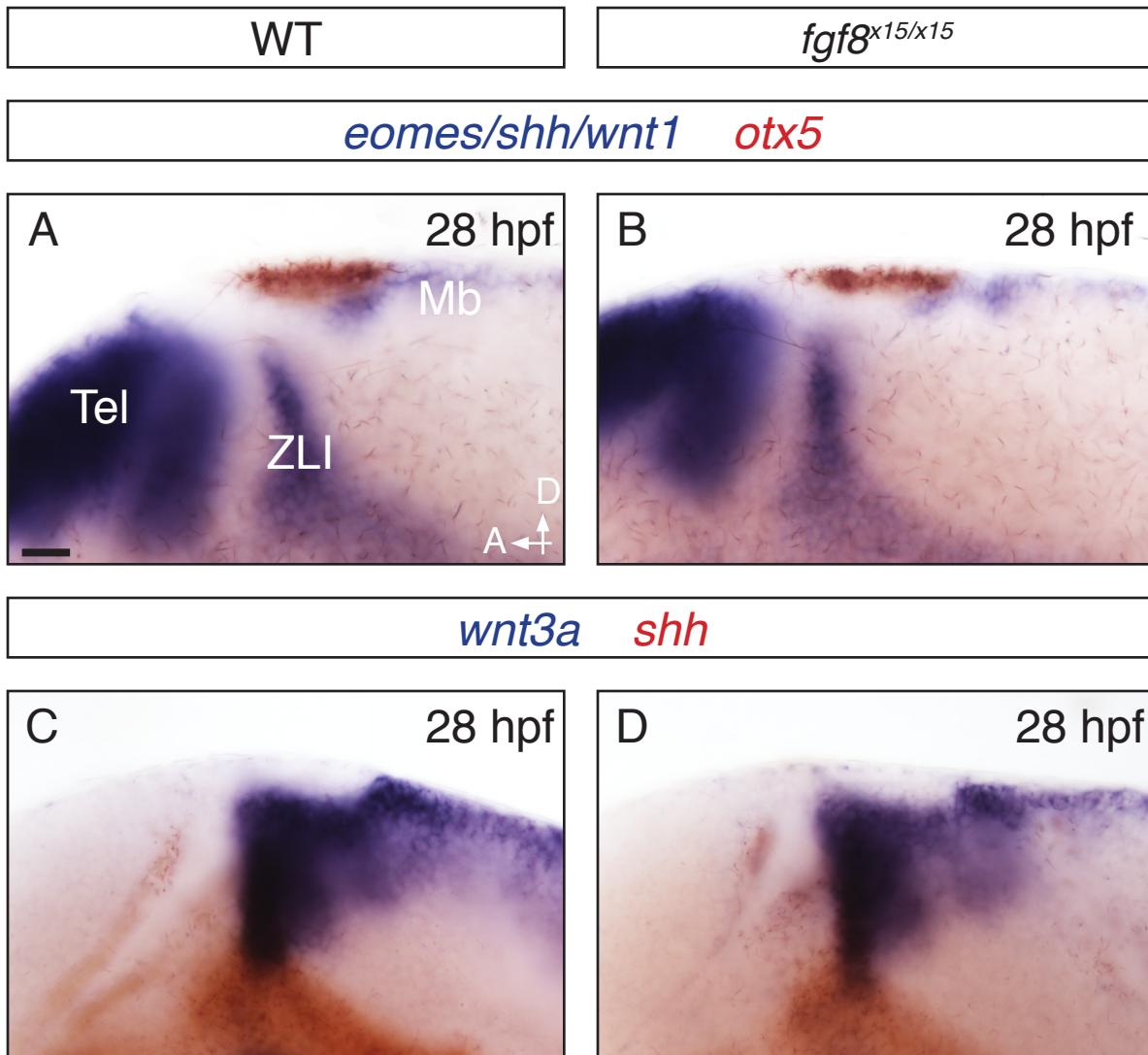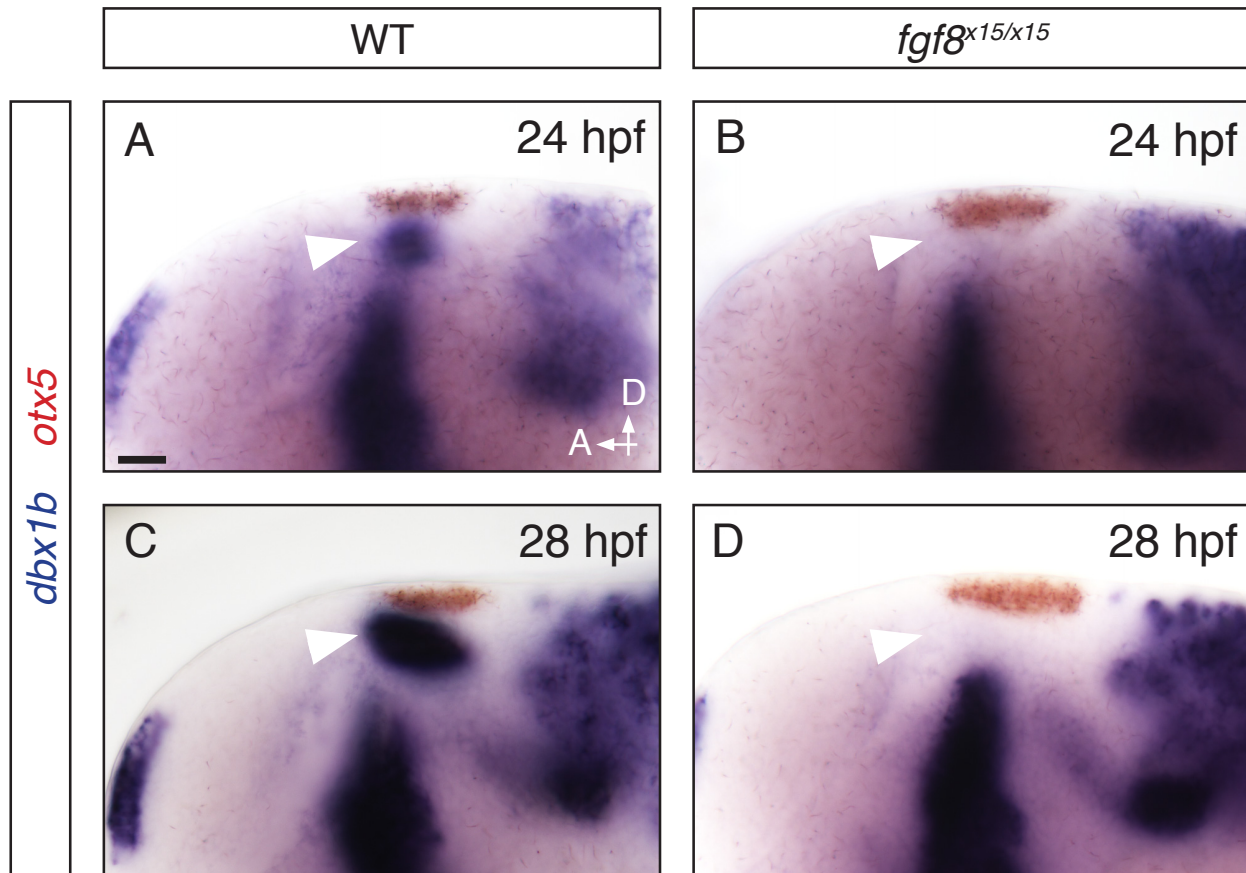
Supplementary Figure 3: *Fgf8* mutants mutants fail to express dbx1b in the epithalamus.
(A-D) In situ hybridization for *dbx1b* (blue) in wildtype and *fgf8* mutant embryos. *otx5* marks the pineal complex. Scale bars are 10uM.

anti-fluorescein antibody (1:1000, Roche) overnight at 4C. The following day, color was developed in Fast Red substrate as in Doll et al. 2011. *cxcr4b* (Chong et al. 2001) probe was generated with EcoRV and SP6 RNA polymerase.

Inhibitor treatments

For whole-mount *in situ* hybridizations and antibody labeling, embryos were incubated in their chorions in 12 uM (for complete receptor inhibition) of SU5402 (Tocris) dissolved in 0.3% dimethyl sulfoxide (DMSO) in egg water supplemented with 0.003% N-phenylthiourea (PTU; Sigma-Aldrich) to prevent melanin formation. Control embryos were treated with 0.3% DMSO in parallel with their SU5402-treated siblings. Embryos were either fixed immediately following
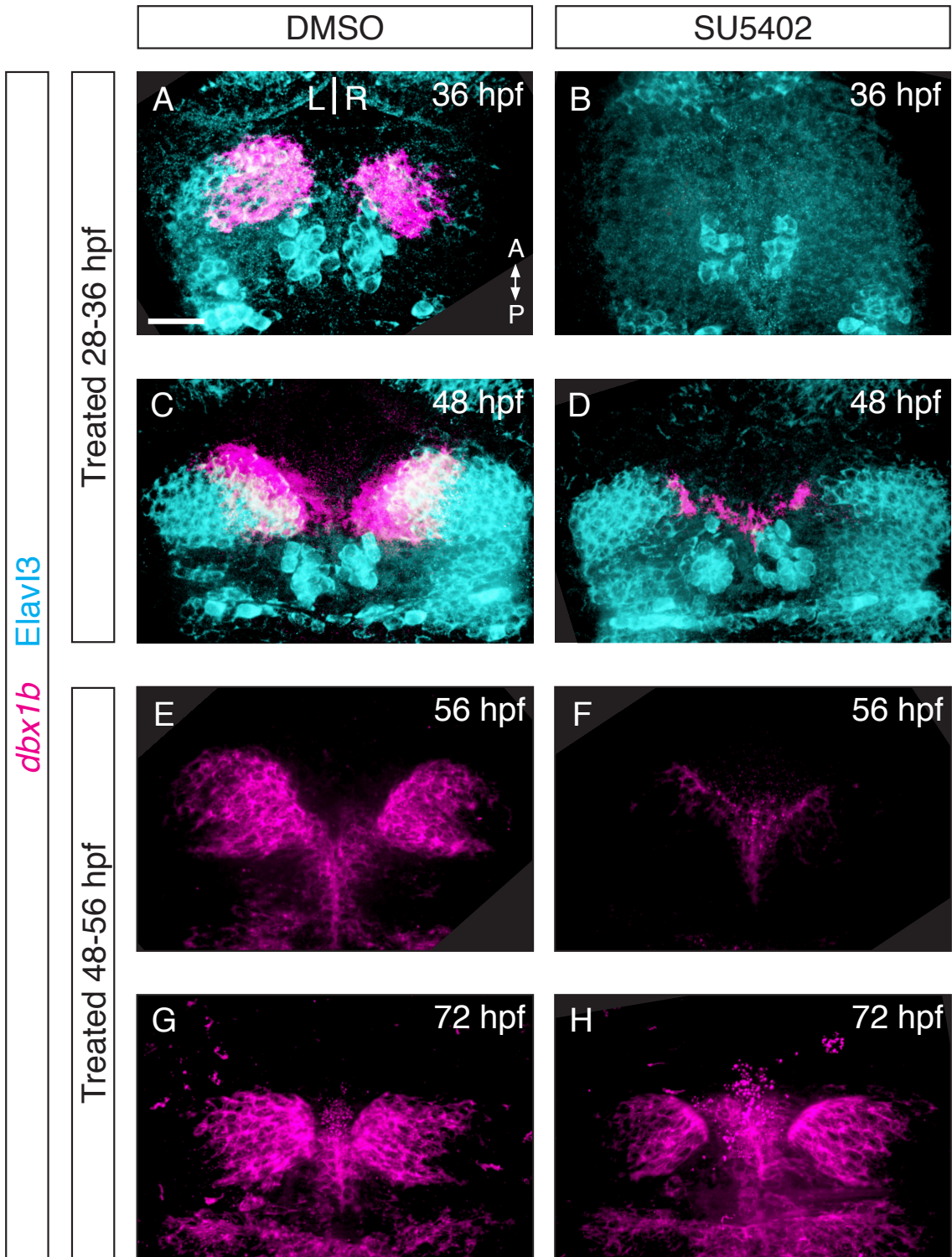
Figure 4: Sustained FGF signaling is required for *dbx1b* expression. (A-D) 8 hour treatment of embryos with the FGF receptor antagonist SU5402 abolished *dbx1b* expression, however expression began to return 12 hours after treatment. (E-H) Similar results were seen when FGF receptor blockade was initiated after *dbx1b* expression began. Generation of Elav3l-positive habenular cells resumed following drug washout at both early and late time points (D, H). Scale bars are 50uM.

treatment or SU5402/DMSO was washed off with 5 x 5 min egg water before being returned to egg water with PTU to develop to the desired stage for fixation.

Imaging

All samples were cleared in a glycerol series (50%, 100%). Colorometric *in situ* images were captured on a Leica DM6000 B compound microscope under a 20X air objective in bright field conditions. Fluorescent images were captured on a Zeiss/Perkin Elmer spinning disk confocal microscope or a Zeiss LSM 510 Meta confocal microscope with a 40X oil-immersion objective and analyzed with Volocity software (Improvision).

RESULTS & DISCUSSION

Dbx1b is expressed in the presumptive habenulae

During our ongoing efforts to characterize transcription factors (TFs) that are expressed in the dorsal diencephalic region between 24 and 48 hours post-fertilization (hpf), we focused on a family of homeodomain-containing TFs encoded by the *dbx* genes. There are three *dbx* genes in the zebrafish genome, and we carefully examined the expression pattern of the two *dbx1* paralogs, *dbx1a* and *dbx1b*. We excluded *dbx2* from our study because its expression has been detailed previously (Seo et al. 1999). At 28 hpf, *dbx1a* and *dbx1b* showed similar yet distinct expression patterns (Supplementary Figure 1). As shown previously (Lauter et al. 2013), *dbx1a* was expressed in sharply restricted domains in the diencephalon with prominent expression in the prethalamus and thalamus (Supplementary Figure 1A). Expression of *dbx1a* and *dbx1b* was similar in the prethalamic region, but in the thalamic region *dbx1b* was expressed at a much lower level than *dbx1a* (Supplementary Figure 1; panel C). A more striking difference between the patterns of these two paralogs was the expression of *dbx1b* in the dorsal diencephalon, where

dbx1a was completely absent (compare arrowheads in Supplementary Figure 1). Expression of *dbx1b* was excluded from the *otx5*-positive pineal complex, the other major structure of the dorsal diencephalon (Supplementary Figure 1C). These data suggested that *dbx1b* could be an early molecular marker for the presumptive habenulae.

Next, we closely examined the expression of *dbx1b* at different developmental stages (Figure 1). At 22 hpf, expression of *dbx1b* was not yet present in the presumptive habenular region, although the prethalamic and midbrain regions showed strong expression (Figure 1A&B). By 24 hpf, habenular *dbx1b* expression appeared (Figure 1C&D) and was maintained through at least 96 hpf (Figure 1E-J and data not shown). Moreover, *dbx1b* expression remained highest adjacent to the 3rd ventricle of the brain, and was absent from regions distal to the ventricle by 48 hpf (ure 1H and 1J; dorsal views). Because neuronal progenitors are often found in regions adjacent to the ventricle in the developing brain, these data led us to speculate that the *dbx1b* expression pattern includes the progenitors of habenular neurons.

Dbx1b labels dorsal habenular progenitors

To support the hypothesis that *dbx1b*-expressing cells represent habenular progenitors, we examined if these cells are proliferative. Indeed, as shown by phospho-histone H3 staining at 32 hpf, the *dbx1b*-positive cells close to the ventricular surface were proliferative, which was consistent with progenitor cell identity (Figure 2A-D). To see if *dbx1b* expression is restricted to progenitors we compared the expression of previously described precursor and neuronal habenular markers. *Cxcr4b* has been proposed as a marker of progenitors as well as post-mitotic habenular precursors (Roussigné et al. 2009). At 36 hpf, a subset of *dbx1b*-expressing cells co-expressed *cxcr4b*. Specifically, *cxcr4b* expression was restricted to the dorsal half of the *dbx1b* expression domain leaving a ventral region of *dbx1b*-only expression along the ventricle (Figure 2E&F). At 48 hpf, Elavl3 (also known as HuC) marks post-mitotic neurons. Expression of Elavl3 and *dbx1b* was more distinct than *cxcr4b* and *dbx1b*, with Elavl3 expressed dorsally and laterally

while *dbx1b* was present medially and ventrally along the ventricle (Figure 2G&H). Kctd12.1 and Kctd12.2 mark different populations of differentiated habenular neurons. At 72 hpf, neither showed any overlap with *dbx1b* expression (Figure 2I-L). Similar results were observed with another habenular differentiation marker, *pou4f1* (or *brn3a*) (data not shown). Together these results indicated that *dbx1b* expression is maintained in a proliferative population of habenular progenitor cells that reside along the ventricle. As habenular progenitors exit cell cycle and mature into post-mitotic, fully differentiated neurons, *dbx1b* is downregulated. Thus, we conclude that *dbx1b* can serve as an early marker to identify habenular progenitors.

To substantiate our conclusion that *dbx1b* is expressed in habenular progenitors, we performed a lineage-tracing experiment using the Cre-lox recombination system. By crossing the *TgBAC[dbx1b:Cre-mCherry]* (Koyama & Kinkhabwala 2011) transgenic line with a reporter line, *Tg[-10actb2:LOXP-mCherry-LOXP-nlsEGFP]* (Kikuchi et al. 2010), almost all Elavl3-expressing habenular neurons were co-labeled with GFP (Figure 3A-C). Indeed, the only domain expressing GFP but not Elavl3 was found along the ventricle, in an area that coincides with *dbx1b* transcription (Figure 3D). These results strongly suggested that most if not all post-mitotic habenular neurons are derived from progenitor cells that express *dbx1b* prior to their differentiation, confirming that *dbx1b* is a marker of early dorsal habenular progenitors.

FGF signaling is required for proper development of the dorsal habenulae

FGF signaling has been shown to play critical roles during the development of the zebrafish dorsal diencephalon, particularly in pineal complex specification and parapineal migration (Regan et al. 2009; Clanton et al. 2013). It has been suggested that the development of both the left and right habenulae requires FGF signaling, as shown by the reduced expression of habenular differentiation markers (Kctd12.1, *pou4f1*) in FGF mutants (Regan et al. 2009). However, how the loss of FGF signaling impacts habenular development remains unclear. We found that in *fgf8a* mutants, in which brain patterning appeared to be normal (Supplementary Figure 2), the

expression of *dbx1b* was completely lost at 24 hpf (Supplementary Figure 3) and this loss of expression persisted at later stages. The latter observation suggested that the loss of FGF-dependent *dbx1b* is not a result of developmental delay. Therefore, FGF signaling is absolutely required for the initiation of *dbx1b* expression.

To explore the regulatory relationship between FGF signaling and *dbx1b* in more detail, we investigated if FGF signaling is continuously required to maintain *dbx1b*-positive habenular progenitors. We took advantage of the FGF receptor antagonist, SU5402, to block FGF signaling in a temporally controlled manner. Since *dbx1b* expression was first detectable at 24 hpf, the embryos were treated with SU5402 for 8 hours, from either 28-36 hpf or 48-56 hpf. The expression of *dbx1b* was analyzed at the end of the treatments as well as after 12 hours of recovery post-treatment. As shown in Figure 4, both treatment regimes abrogated *dbx1b* expression by the end of the treatment window, yet *dbx1b* expression began to return after 12 hours of recovery (Figure 4B, D and 4F, H). This result suggests that FGF signaling is required for not only the initiation, but also the maintenance of *dbx1b* expression. Moreover, at least some neuronal progenitors in the dorsal diencephalon remain FGF-responsive and capable of reactivating *dbx1b* expression upon exposure to FGF signal, even when they were previously deprived of FGF signaling.

CONCLUSIONS

This report describes the expression of *dbx1b*, which we understand is the first reported marker of the neuronal progenitors that give rise to the dorsal habenulae. In addition, we found that FGF signaling controls the expression of *dbx1b* in the dorsal diencephalon. Together with other existing genetic tools, including various *dbx1b* BAC transgenic lines, our discovery of *dbx1b* as a habenular progenitor marker will not only allow for more detailed and nuanced investigation of habenular development, but also provide an exciting way forward to study proliferation, specification and circuit formation of the diverse neuronal populations in the habenular nuclei, and how these processes influence developmental and adult habenula-mediated behaviors.

CHAPTER IV

**FGF ASYMMETRICALLY REGULATES THE TIMING OF HABENULAR NEURO-
GENESIS IN A NODAL-DEPENDENT MANNER**

INTRODUCTION

The generation of the great variety of neuronal subtypes during development is crucial
to vertebrate brain function. Excitatory, inhibitory and neuromodulatory neurons must be gener-
ated in carefully balanced numbers. Indeed errors in neuronal specification are thought to play a
key role in the pathophysiology of many neurodevelopmental disease states including epilepsy,
autism and schizophrenia (Levitt et al. 2004; Rubenstein 2010).

All neurons arise from a pseudostratified neuroepithelium (NE) composed of neural
progenitors (NPs). The NE is 'patterned' by a wide array for secreted factors including effectors
and inhibitors of the BMP, FGF, Wnt, Shh and Retinoic acid families of morphogens. These fac-
tors are secreted from discrete locations – organizers - spread across the NE (Vieira et al. 2010;
Kiecker & Lumsden 2012). How different morphogenic patterning cues are integrated by NPs,
spatially across the NE and temporally throughout development, is an area of intense research
with implications for understanding neurodevelopmental disease and also directing treatment via
stem cell therapy (Southwell et al. 2014; Deidda et al. 2014).

NPs get spatial and temporal information from their dynamic exposure to secreted mor-
phogen and their inhibitors. One or more morphogenic signaling pathways are then integrated
and drive expression of specific sets of homeodomain-containing and basic helix-loop-helix
transcriptions factors (Guillemot 2007). From this combinatorial code NPs become specified
and go on to generate a restricted repertoire of neurons. Patterning by extrinsic factors can vary
over space as well as time due to NP proximity to various organizers, length of exposure and
changes in organizers. As NPs are specified they transition away from purely proliferative divi-

sions (where both daughters retain progenitor status) to neurogenic divisions (where at least one daughter exits the cell cycle and executes a highly specific program of differentiation). The timing and execution of this 'neurogenic switch' and subsequent differentiation are fundamental to generating the proper number and subtype of neuronal daughters (Aizawa et al. 2007; Scholpp et al. 2009).

Most of our understanding of spatiotemporal patterning and neurogenesis has been worked out along the anteroposterior (A/P) and dorsoventral (D/V) axis. For example, motor neuron and interneuron specification along the D/V axis of the spinal cord is a classic example of spatial patterning, where distance away from the floor or roof plate dictates the fate of NP daughters (Kiecker & Lumsden 2012). The generation of excitatory or inhibitory neurons in the thalamus is directed by the temporal progression of a 'neurogenic wave' along the A/P axis (Scholpp et al. 2009). Despite great progress in understanding how spatiotemporal patterning drives neurogenesis along the A/P and D/V body axis, almost nothing is known about how the timing of neurogenesis and its effect on cell fate is regulated across the left-right (L/R) axis.

L/R neuronal asymmetry is highly conserved across vertebrates and is crucial for normal brain function. Thus, spatiotemporal neuronal patterning must be integrated with L/R patterning at some level (Bianco & Wilson 2009). The habenular nuclei are bilaterally paired brain structures in the dorsal diencephalon that connect limbic forebrain components with monoaminergic centers in the midbrain and hindbrain. In many classes across the vertebrate lineage these nuclei are asymmetric (Bianco & Wilson 2009). In the teleost zebrafish, *Danio rerio*, the bilateral habenular nuclei contain two subsets of glutamatergic projection neurons organized into discrete medial and lateral subnuclei. The two habenular neuronal subtypes are represented in asymmetric numbers in the left and right habenula. As well, they have asymmetries in neuropil density and efferent axon projection patterns. It has been previously reported that habenular neurogenesis begins asymmetrically and that this asymmetry is dependent on the left-fate-determining Nodal signaling pathway (Regan et al. 2009). Furthermore, the timing of neurogenesis is tied to the fate of neuronal daughters (Aizawa et al. 2007). Thus, during development, habenular NPs are

instructed to asymmetrically being neurogenesis and the timing of their neurogenic switch is important for the fate of the neuronal daughters. Together, these observations highlight the utility of the zebrafish habenular nuclei as a model to investigate how spatiotemporal and left-right patterning are integrated during neurogenesis to drive proper fate determination.

The FGF signaling pathway plays a crucial role in patterning the vertebrate brain. *Fgf8* is robustly expressed in the dorsal diencephalon (DD) during habenular development. Indeed, loss of *fgf8* signaling leads to a failure to form the habenular nuclei in the mouse and hypomorphic alleles of *fgf8* in the zebrafish lead to defects in habenular development (Martinez-Ferre & Martinez 2009; Regan et al. 2009). FGF signaling and *fgf8* specifically are known to regulate the neurogenic switch in NPs near the midbrain-hindbrain boundary (Saarimäki-Vire et al. 2007; Lahti et al. 2010). Specifically, high levels of FGF signaling maintain proliferative divisions, but reductions in FGF signaling allow neurogenic divisions. These studies support a classical view of FGF as a dose-dependent developmental effector. As a graded signal, high levels promote proliferation, middling levels promotes differentiation and low levels lead to apoptosis (Garcia-Maya et al. 2006). Thus, we hypothesized that the timing of habenular neurogenesis would similarly depend on levels of FGF signaling.

With a suite of small molecules we tuned FGF signaling levels up and down within physiologic ranges. Here we report that FGF regulates the timing of habenular neurogenesis in a dose-dependent manner and further support the idea that timing of habenular neurogenesis impacts neuronal cell fate. FGF acts by regulating a cell-cycle dependent kinase inhibitor (CDKI), *kip2*. Finally, we find that FGF-regulated neurogenesis is rendered asymmetric by Nodal-driven inhibition of FGF signaling activity in the left habenula. To our knowledge this is the first report of Nodal regulating FGF. We propose that FGF signaling serves as the key regulator of asymmetric habenular neurogenesis integrating L/R and neurogenic patterning.

MATERIALS & METHODS

Zebrafish maintenance and strains

Zebrafish were raised at 28.5°C on a 14/10 hour light/dark cycle and staged according to hours post-fertilization. The following fish lines were used: the wild-type strain AB* (Walker 1999), *Tg(-8.4neurog1:GFP)* (Blader et al. 2003), *TgBAC[dbx1b:eGFP]* (Koyama & Kinkhabwala 2011), *TgBAC[dusp6:d2eGFP]* (Molina et al. 2007)also known as Mkp3, *fgf8^{x15}* (Kwon & Riley 2009), *tbx2b^{c144}* (Snelson et al. 2008), *flh^{n1}* (Talbot et al. 1995). All experiments were approved by the Vanderbilt University's Institutional Animal Care and Use Committee (IACUC) and Office of Animal Welfare, and performed according to national regulatory standards.

Whole mount *in situ* hybridization

Whole-mount RNA *in situ* hybridization was performed as described previously (Gamse 2003), with one change: 5% dextran sulfate was added to the hybridization buffer. Hybridized probes were detected using alkaline phosphatase conjugated antibodies (Roche) and visualized by 4-nitro blue tetrazolium (NBT; Roche) and 5-bromo-4-chloro-3-indolyl-phosphate (BCIP; Roche) staining for single colorometric labeling, or by NBT/BCIP followed by iodonitrotetrazolium (INT) and BCIP staining for double colorometric labeling.

Whole mount fluorescent *in situ* hybridization and immunohistochemistry

Whole-mount fluorescent *in situ* hybridization and immunohistochemical co-labeling was performed as described previously (Doll et al. 2011a), with the following additional reagents: 5% dextran sulfate was added to the hybridization buffer. Hybridized probes were detected using anti-DIG alkaline phosphatase conjugated antibodies (Roche). In addition to Fast Red substrate
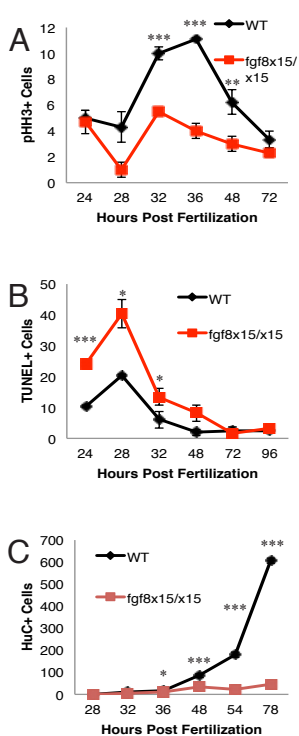
Supplementary Figure 1: *fgf8* mutants show reduced proliferation, increased cell death and failed differentiation. *fgf8* mutants show significantly fewer pHH3+ cells between 32 and 48hpf (A). They also show more TUNEL+ cells between 24 and 32hpf (B). Finally, the remaining cell fail to differentiate into neurons (C). *p<0.05, **p<0.01, ***p<0.005.

(Sigma, F4648), some experiments used 3 x 5 minutes washes in Fast Blue Buffer (Lauter et al. 2011) and were developed in Fast Blue Substrate (0.25mg/mL Fast Blue Substrate and 0.25mg/mL nAMP in Fast Blue Buffer) diluted in Fast Blue Buffer. In addition to the anti-DIG antibody, the primary antibodies used were mouse anti-HuC (1:400, Life Technologies), rabbit anti-GFP (1:500, Torrey Pines Biolab), chicken anti-GFP (1:300, Vanderbilt Antibody and Protein Resource), rabbit anti-Kctd12.1 (1:300, Gamse et al. 2005). Primary antibody was detected using goat-anti-rabbit, goat-anti-mouse or goat-anti-chicken antibodies conjugated to Alexa 488, Alexa 568 or Alexa 633 fluorophores (1:300, Molecular Probes).

Double fluorescent in situ hybridization was performed with the following modifications to the above colorometric *in situ* protocol. After hybridization of DIG and fluorescein labeled probes, anti-DIG antibody was applied (1:5000, Roche) overnight at 4°C. The following day embryos were washed 4 x 20 min in PBS with Triton (PBSTr) and 3 x 5 min in Fast Blue Buffer and developed in Fast Blue Substrate diluted in Fast Blue Buffer. After color development, embryos were washed 2 x 10 min in PBSTr. The alkaline phosphatase was acid inactivated by a 10 min wash in 0.1M glycine HCl pH2.0. After 2 x 10 min PBSTr washes, embryos were incubated in anti-fluorescein antibody (1:1000, Roche) overnight at 4C. The following day, color was developed in Fast Red substrate as in Doll et al. (2011).

dbx1b probe (Gribble et al. 2007) was produced from pCRII-*dbx1b* plasmid linearized by BamHI and transcribed by T7 RNA polymerase. *her6* probe (Scholpp et al. 2009) using pBSSK-*kip2*, NotI and T7 RNA polymerase, *kip2* probe using pBS+-*kip2*, NotI and T7 RNA polymerase and *lefty1* probe using pBSSKII-*lefty1* with NotI and T7 polymerase.
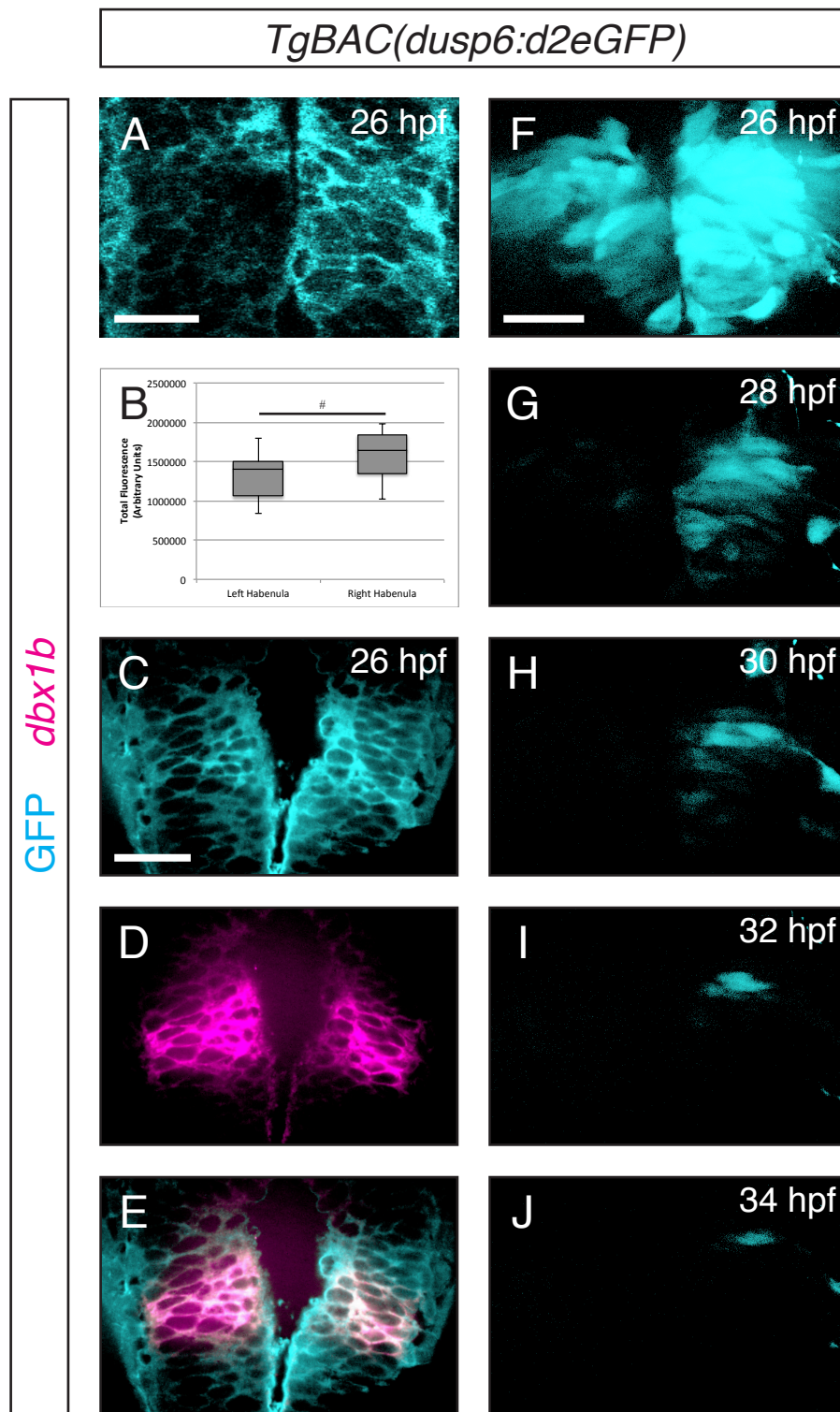
Figure 1: FGF signaling is asymmetric in the early developing habenulae. The FGF reporter *TgBAC(dusp6:d2eGFP)* has higher levels of expression in the right habenula than the left at 26hpf (A-B). This expression pattern coexpresses with the habenulae markers *dbx1b* (C-E). Using in vivo time-lapse confocal microscopy we observed that FGF signaling decreases between 26 and 34hpf falling below detectable levels in the left habenula (28hpf) before loss of signal on the right (34hpf, F-J). #p<1.8 ×10⁻⁶. Scale bars are 50uM.

Inhibitor treatments

For whole-mount *in situ* hybridizations and antibody labeling, embryos were incubated in their chorions in 1uM of SU5402 (Tocris), 10uM, 25uM or 50uM of BCI (Sigma) or 50uM SB505124 dissolved in 0.3% dimethyl sulfoxide (DMSO) in egg water supplemented with 0.003% N-phenylthiourea (PTU; Sigma-Aldrich) to prevent melanin formation. Control embryos were treated with 0.3% DMSO in parallel with their SU5402-treated, BCI-treat-

DMSO

1uM SU5402

Hb asymmetry

Tg(-8.4ngn:GFP)

A L | R 36 hpf

B 36 hpf

C 40 hpf

D 40 hpf

I

40

Left Habenular Neurons

0 10 20 30 40
Right Habenular Neurons

DMSO
1uM

LHb

RHb

E

Number of Neurons (36 hpf)

** DMSO 15
1uM SU5402 23 ***

7
13

30 25 20 15 10 5 0   0 5 10 15 20 25 30

DMSO

25uM BCI

Tg(-8.4ngn:GFP)

F L | R 40 hpf

G 40 hpf

J

40

30

20

10

0

Left Habenular Neurons

0 10 20 30 40
Right Habenular Neurons

DMSO
10uM
25uM
50uM

LHb

RHb

H

Number of Neurons (40 hpf)

DMSO 30
10uM BCI 22
25uM BCI 10
50uM BCI 4

20
17
7
3

*** *** *

*** ***

40 30 20 10 0   0 10 20 30 40

Figure 2: FGF regulates the timing of habenular neurogenesis. Inhibition of FGF signaling by a 1 hour pulse of 1uM SU5402 from 25hpf-26hpf resulted in an increased number of neurons at 36 and 40hpf (A-E). Inhibitor treated embryos retained neurogenic asymmetry (Wilcoxon signed-rank test: for SU5402 p<0.01 for both groups; for BCI p,0.01 for 10uM and p<0.005 for the three remaining groups). *p<0.05, **p<0.01, ***p<0.005. Scale bars are 50uM.

58

ed or SB505124-treated siblings. SU5402 and BCI treatments were all from 25-26 hpf unless otherwise stated. Embryos were either fixed immediately following treatment or SU5402/BCI/ DMSO was washed off with 5 x 5 min egg water before being returned to egg water with PTU to develop to the desired stage for fixation. SB505124 treatments were from 16 hpf until fixation.

Imaging

For fixed tissue, samples were cleared in a glycerol series (50%, 100%). For in-vivo time-lapse microscopy, embryos were anesthetized in 1% Tricaine and mounted in 0.6% agarose containing 0.04% Tricaine and 0.003% N-phenylthiourea (PTU; Sigma-Aldrich) to prevent melanin formation. Time-lapse images were collected every 15 minutes for the hours indicated on a Zeiss/ Perkin Elmer spinning disk confocal microscope. Fixed-tissue fluorescent images were collected on the same Zeiss/Perkin Elmer or a Zeiss LSM 510 Meta confocal microscope. Time-lapse and fixed tissue images were taken with a 40X oil-immersion objective and analyzed with Volocity software (Improvision).

Quantitation & Statistics

Quantitation of wildtype *her6* and *kip2* expression levels took advantage of the *TgBAC(dbx1b:GFP)* transgenic line, which marks the entire habenula. Using Volocity software, the left or right habenula was selected using the GFP channel, and then total fluorescence was recorded from the *kip2* or *her6* channel. Because FGF regulates *dbx1b* this approach was not valid in *fgf8$^{x15/x15}$* mutants. To quantitate relative fluorescence levels of *Tg(dusp6:d2eGFP)* as well as *her6* and *kip2* expression levels in the *fgf8$^{x15/x15}$* background, three optical sections were taken through the habenulae. Using the ventral margin of the pineal gland as an anchor, sections 5um dorsal, 5um ventral and through this anchor were selected allowing for uniformity across samples. Then the fluorescence of the entire left or right diencephalon was measured in each optical
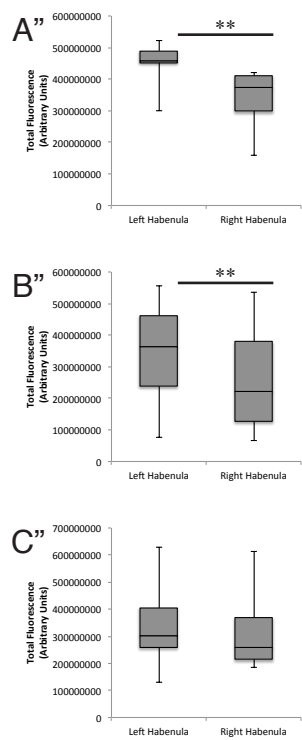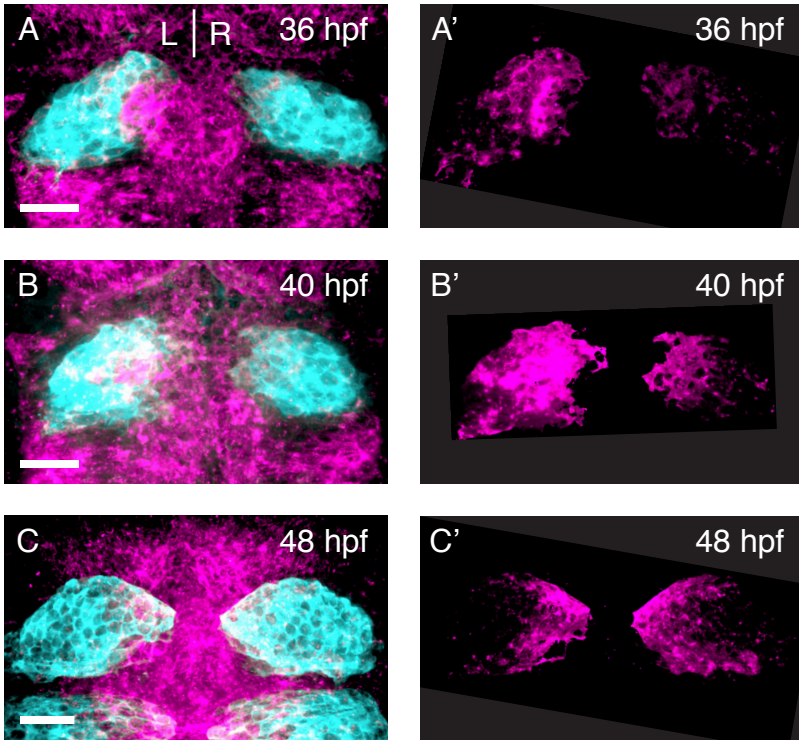
Figure 3: *kip2* appears in asymmetric pulses and is regulated by FGF. *kip2* and a transgene marking the habenula are coexpressed (A, B, C). A pulse of *kip2* expression appears between 36hpf and 48hpf. The pulse peaks on the left at 40hpf and is still increasing on the right by 48hpf (A', B', C'). *kip2* expression is leftward biased at 36hpf and 40hpf (A", B"; Wilcoxon signed-rank test: 36hpf and 40hpf p<0.025). By 48hpf the levels of *kip2* are no longer significantly different (C"). **p<0.01. Scale bars are 50uM.
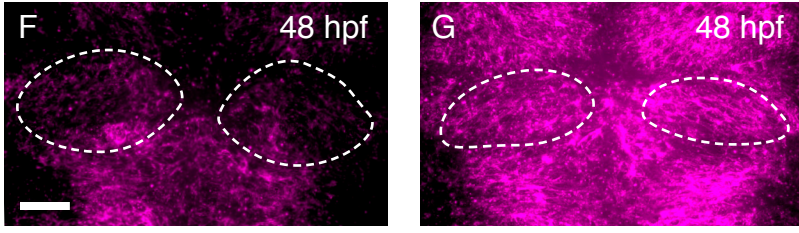
section using Volocity (Improvision). These values were then totaled and taken as representative of the habenular expression. To compare expression levels on the left and right, or to compare the ratio of expression between two groups, Student's T-test was performed. To measure asymmetry of neurogenesis in SU5402 and BCI-treated embryos, we first counted GFP+ or HuC+ neurons and subsequently employed a Wilcoxon signed-rank test (Roussigné et al. 2009).
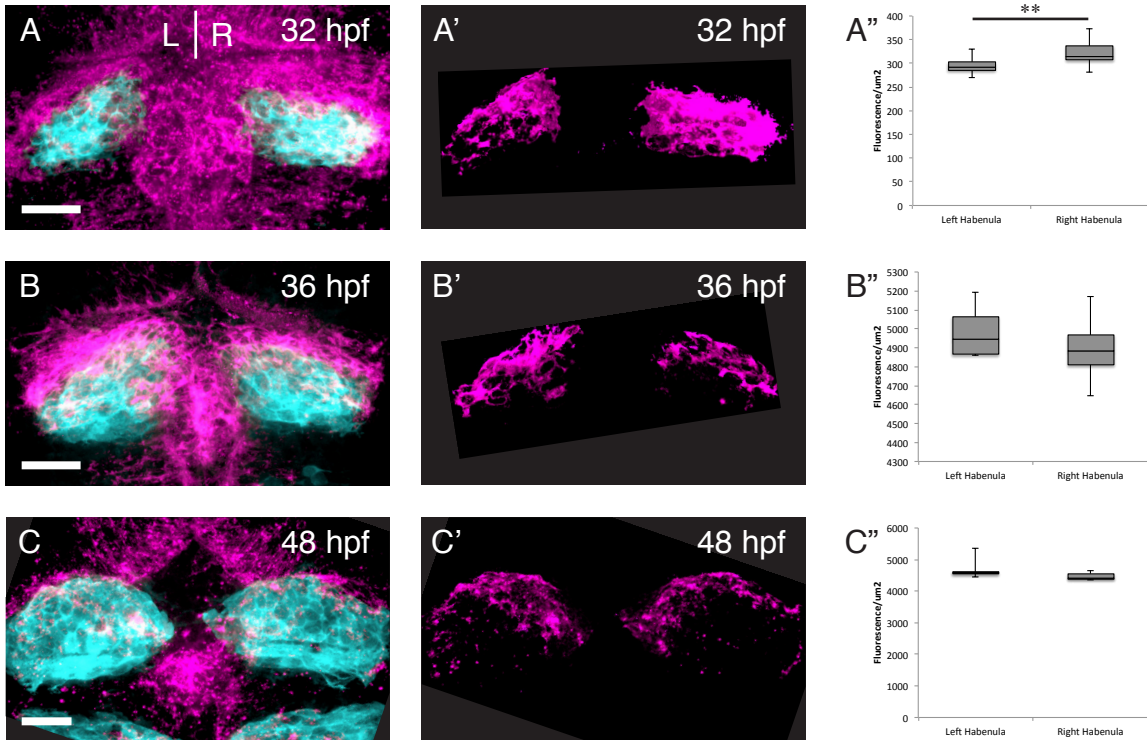
Supplementary Figure 2: *her6* expression is present at high levels on the right early in habenular development. *her6* is expressed at higher levels in the right habenula at 32hpf (A-A"). By 40 and 48hpf expression levels have reduced and become symmetric (B-C"). *p<0.01. Scale bars are 50uM.

RESULTS

FGF signaling is asymmetric during early habenular development

Previous analysis of the DD of zebrafish $fgf8^{ti282/ti282}$ hypomorphs showed a possible role for FGF signaling in habenular development (Regan et al. 2009). Subsequent analysis of $fgf8^{x15/x15}$ null mutants confirmed that FGF signaling is crucial for normal habenular development. In the absence of *fgf8*, the developing habenulae have decreased proliferation, increased apoptosis and the cells that are produced fail to differentiate in neurons (Supplementary Figure 1A-C). Thus, FGF signaling regulates the number of habenular cells, their survival and is required for their proper differentiation. However, the severity of the null mutant makes is hard to separately inves-
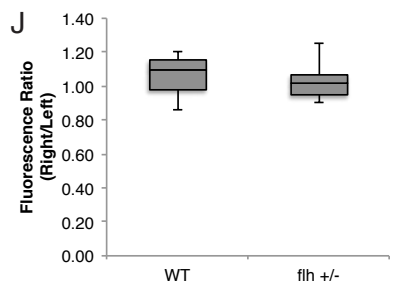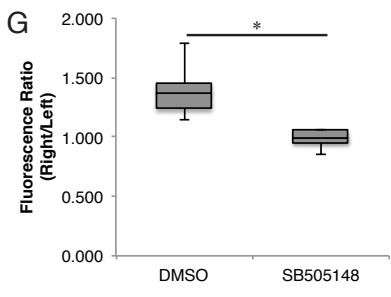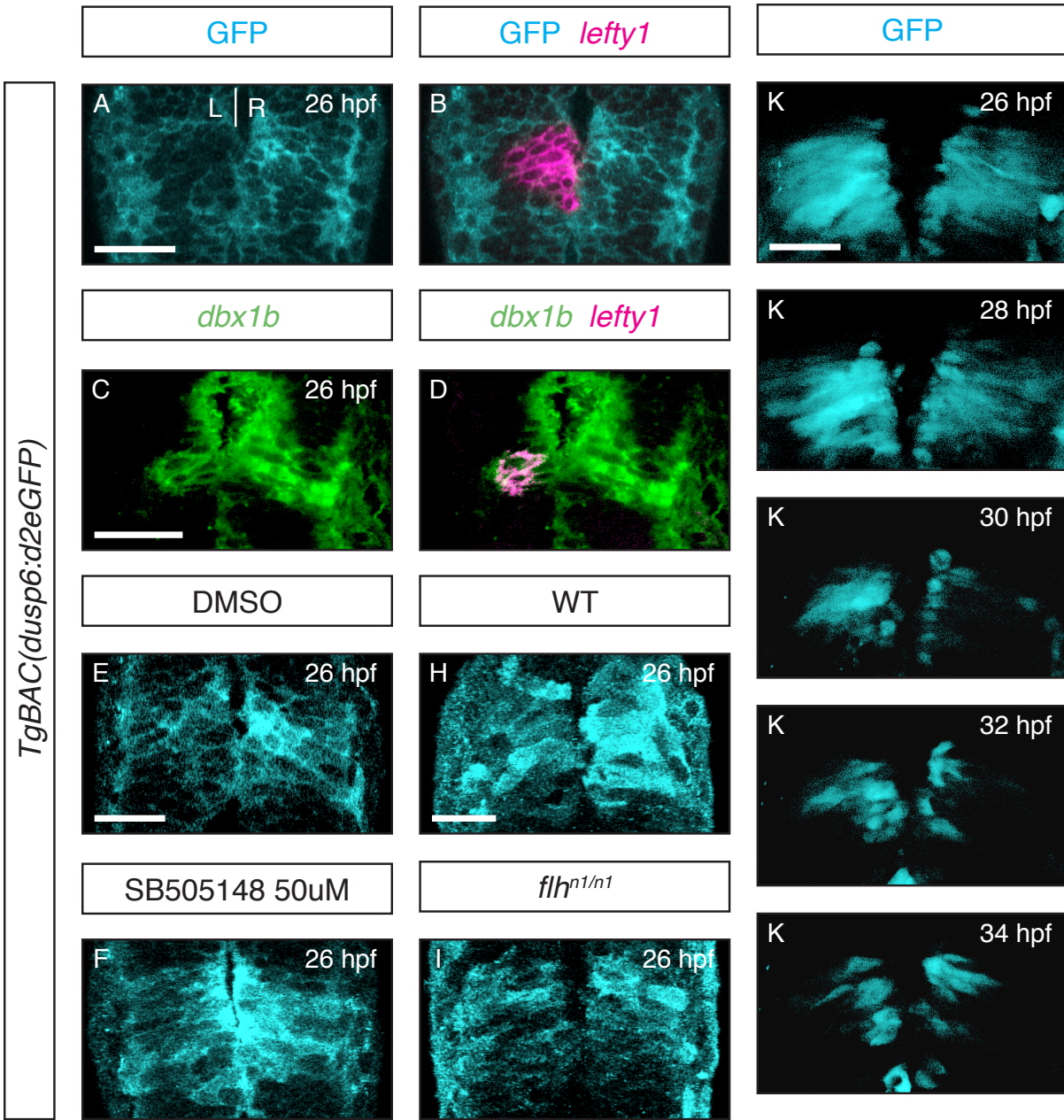
Figure 4: Nodal regulates FGF signaling in the developing habenulae. The Nodal signaling component *lefty1* is expressed in the plane of asymmetric FGF activity (A-B). As well, *lefty1* is co-expressed with the habenular marker *dbx1b* on the left (C-D). Inhibition of Nodal by the small molecule or instantiation of bilateral Nodal in the *flh* mutant led to a symmetrization of FGF signaling activity (E-J). This was significant in the case of SB505124 treatment (G-J, Wilcoxon signed-rank test: for SB505124 p<0.025). As well, in vivo time-lapse imaging show that symmetrization of FGF activity persisted through 34hpf after drug treatment (K-O). *p<0.05, **p<0.01, ***p<0.005. Scale bars are

tigate how FGF signaling regulates neurogenesis versus differentiation.

To investigate habenular FGF signaling more directly, we took advantage of a validated FGF reporter line where a *dusp6* promoter element drives expression of a destabilized enhanced-GFP (Molina et al. 2007)also known as Mkp3. *dusp6* is a member of the dual-specificity phosphatase family of phosphatases and is a feedback inhibitor of the FGF signaling pathway. Thus, this reporter is activated in the presence of robust FGF signaling. The enhanced-GFP used is fused to a PEST sequence leaving the mature protein with only a 2 hour half-life (Li 1998). As a transgenic line, *TgBAC(dusp6:d2eGFP)* allow for analysis of FGF signaling activity in fixed tissue as well as *in vivo* time-lapse confocal microscopy allowing for the acquisition of dynamic changes in FGF signaling activity.

Strikingly, a robust asymmetry in FGF activity was evident at 26 hpf, at the beginning of habenulogenesis (Figure 1A&B). FGF activity was higher in the right habenula and lower in the left habenula (Figure 1B). To confirm that asymmetric FGF activity was in the habenulae, we analyzed the co-expression of our transgene with the recently reported habenular progenitor marker, *dbx1b* (Dean et al., Submitted). Single optical sections reveal that asymmetric FGF signaling is present in the early habenulae (Figure 1C&D).

Taking advantage of the destabilized eGFP in our reporter, we employed in-vivo time-lapse confocal microscopy to study the temporal dynamics of FGF signaling in the habenula. Between 26 hpf and 34 hpf asymmetry in transgene expression persist while overall levels of signaling decline on both sides reaching undetectable levels at 28 hpf and 32 hpf respectively (Figure 1F-J). We concluded that in the early stages of habenular development, FGF signaling is greater in the right habenula. As development proceeds, FGF signaling activity decreases greatly, but in a stabile asymmetric fashion.

Asymmetric habenular neurogenesis is FGF-dependent

It has been previously reported that post-mitotic neurons appear in the habenulae asym-
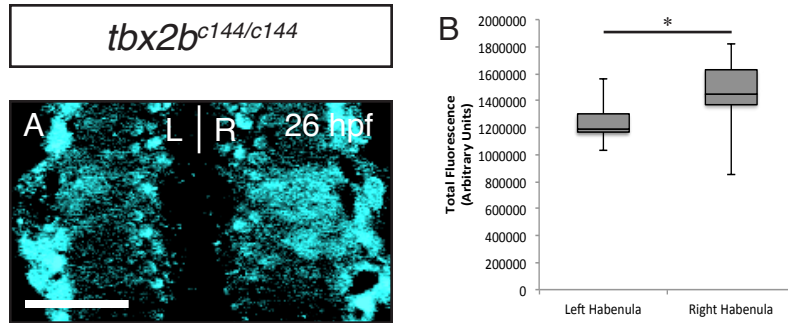
Supplementary Figure 3: Right-biased FGF activity is independant of parapineal development. *tbx2b* mutants retain right-biased FGF activity at 26hpf (A-B). *p<0.05. Scale bar is 50uM.

metrically, with the earliest born neurons appearing in the left habenula about 4 hours before they appear on the right (Roussigné et al. 2009). Neurogenesis begins shortly before 36 hpf and the asymmetric distribution of neurons is apparent through 40 hpf (Figure 2A, C and I).

High levels of FGF signaling have previous been associated with progenitor maintenance (Garcia-Maya et al. 2006; Lahti et al. 2010). Given the asymmetric activity of FGF signaling 10 hours before the appearance of neurons, and its sustained activity on the right where neurogenesis begins later, we hypothesized that FGF signaling in habenular progenitors regulates the timing of neurogenesis.

To track neurogenesis we use both transgenic fish with a *neurogenin1* promoter driving GFP (*Tg(-8.4neurog1:GFP)*) and antibody labeling for HuC (a ribosome binding protein that marks post-mitotic neurons). Knowing that severe attenuation of FGF signaling broadly undermines habenular development, we employed a small molecule approach seeking to reduce FGF signaling activity without stopping habenular development. SU5402 is an FGF receptor antagonist. At doses of 12uM, SU5402 has a maximal effect on habenular development phenocopying the *fgf8* null mutants (Data not shown). Using 1uM doses of SU5402 and a short pulse of treatment (1 hour from 25 hpf-26 hpf), we identified a treatment regimen that had no effect on the number of neurons at 48 hpf (Data not shown). Using this 'sub-maximal' dose of FGF antagonist, we measured the appearance of neurons at 36 hpf and 40 hpf using *Tg(-8.4neurog1:GFP)* zebrafish.

Sub-maximal inhibition of FGF signaling resulted in a premature appearance of neurons at the earliest stages of habenular neurogenesis (Figure 2A-E). Both the left and right habenula
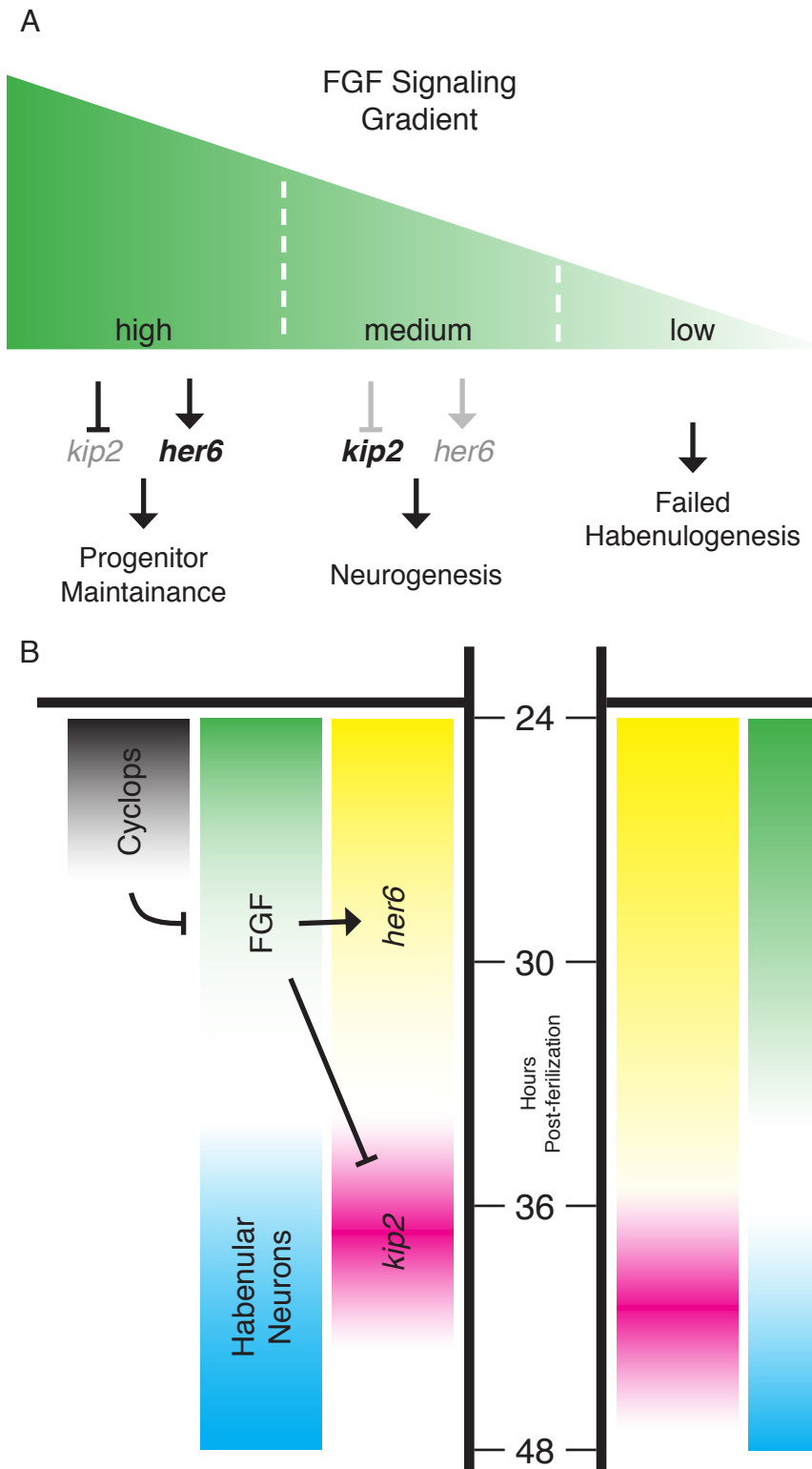
Figure 5: Levels of FGF signaling regulate the timing of neurogenesis in the habenula. Nodal inhibits FGF signaling on the left resulting in earlier neurogenesis. We propose a model where early high levels of FGF inhibit the CDKI *kip2* and promote pro-progenitor factors such as *her6*. This maintains habenula NPs in a pro-genitor state.As levels of FGF signaling drop, kip2 is derepressed and her6 expression decreases. This allows NPs to begin neuro-genic divisions where neuronal daughters exit the cell cycle and turn on pro-neural genes (HuC, ngn1). Drastic reduction of FGF signaling (fgf8x15/x15 null mutant) leads to failed habenulogen-esis sue to decreased proliferation, increased apoptosis and failed differentiation (A). FGF is a key regulator of a neurogenic cassette (along with Notch). Asymmetric habenu-lar neurogenesis is achieved by left-sided Nodal inhibition of FGF signaling. This initiates the decline of FGF signaling earlier on the left (B).

DMSO	1uM SU5402

A · L | R · 54 hpf
B · 54 hpf

Left Hb

C

Left Habenular Kctd12.1-positive Cells

93.2 · 103.5
DMSO · 1uM

Right Hb

D

Right Habenular Kctd12.1-positive Cells

*

66.3 · 84.0
DMSO · 1uM
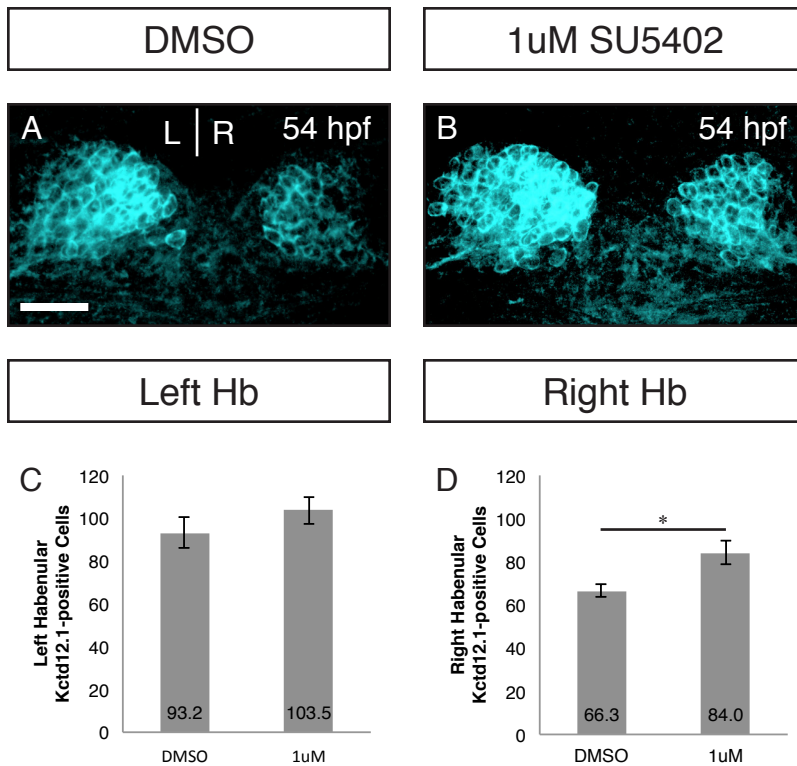
Supplementary Figure 4: Timing of neurogenesis impacts habenular cell fate. SU5402 treatment reults in an increase in Kctd12.1 neruons by 54hpf in the left habenulae and to a significant degree in the right habenula (A-D). *p<0.01. Scale bar is 50uM.

show significant increases in GFP+ cells ($p<0.01$ and $p<0.005$ respectively, Figure 2E). Interestingly, habenular asymmetry is maintained despite premature neurogenesis (Figure 2I, $p<0.01$). Thus, sub-maximal inhibition of the FGF signaling pathway led to premature habenular neurogenesis. This is consistent with a model where the level of FGF signaling acts as neurogenic switch, as FGF signaling levels drop below a certain threshold NPs begin to make neurogenic divisions.

A prediction of this model is that if high levels of FGF activity are sustained, there should be a delay in the onset of neurogenesis. BCI is an allosteric inhibitor of Dusp6, an FGF feedback inhibitor. Dusp6 inhibition leads to increased FGF activity, but the increase will not exceed physiologic levels. Treating embryos from 25 hpf-26 hpf in increasing doses of BCI resulted in a dose-defendant delay in habenular neurogenesis (Figure 2F-H). Again, the temporal shift in neurogenesis had no effect on the asymmetry of neurogenesis (Figure 2J, $p<0.005$). Therefore, tuning FGF signaling up and down is sufficient to regulate the timing of habenular neurogenesis. We conclude that FGF activity acts as a gating mechanism for the timing of habenular neurogenesis.

FGF represses Cyclin-dependent kinase inhibitor, *kip2*, during habenular development

So far we have demonstrated that FGF signaling is asymmetrically deployed to regulate the timing of neurogenesis. But how does FGF regulate the switch from proliferative to neurogenic divisions in NPs? FGF signaling often targets cell cycle regulators and in neural tissues is known to repress Cyclin-dependent kinase inhibitors (CDKIs, Frederick & Wood 2004). This prompted our investigation of the expression of two CDKIs, *kip1/2* in the developing habenula. While *kip1* is not expressed in the habenulae (data not shown), *kip2* shows robust habenular expression from 36 hpf to 48 hpf (Figure 3A, B, C). However, its expression is present at high levels in neighboring domains as well, obscuring the details of its habenular expression. To enhance our analysis we employed the transgenic line, *Tg(dbx1b:GFP)*, which marks the habenulae and not immediately neighboring tissue. Using this marker, we were able to isolate habenular expression for further analysis. Interestingly, *kip2* expression seems to progress through the left and right in offset waves. Expression in the left habenula reaches a peak between 36 hpf and 40 hpf before dropping off by 48 hpf (Figure 3A', B', C'). In the right habenula expression continues to accumulate from 36-48 hpf. At 36 hpf and 40 hpf there is significantly more *kip2* expression in the left habenula (Figure3 A"&B"). These data show that *kip2* is asymmetrically expressed during the onset of habenular neurogenesis and therefore might be target of habenular FGF signaling. Indeed, *kip2* is significantly upregulated in *fgf8$^{x15/x15}$* mutants (Figure 3F&G). Thus we conclude that early high levels of FGF inhibit *kip2* expression allowing NPs to retain their progenitor status, but as FGF levels decline, *kip2* is upregulated and drives progenitor daughters to exit the cell cycle and begin differentiation. This processes happens earlier in the left habenula.

In addition to inhibiting cell cycle exit, FGF signaling is also known to directly promote NP maintenance (Lahti et al. 2010). *Her6* is a member of *hes/her* family of pro-progenitor transcription factors. *Her6* has been shown to regulate the timing of neurogenesis and neuron cell fate in the adjacent thalamus (Scholpp et al. 2009). As well, *her6* expression in the habenulae has been reported to have a right-sided bias (Aizawa et al. 2007). Using the same methods as our

kip2 analysis, we observed a complementary expression pattern. After early, bilaterally high, levels of expression, *her6* expression declines on the left before the right (Supplementary Figure2A, A', B, B'). Expression is significantly lower in the left habenula just before neurogenesis begins (Supplementary Figure 2A"). While *her/hes* transcription factor are canonically downstream of the Notch signaling pathway, there are conflicting reports concerning weather *her6* is or is not regulated in a Notch-independent manner (Scholpp et al. 2009; Aizawa et al. 2007; Hans et al. 2004). This confusion and the correlation of FGF and *her6* asymmetry raise the possibility that FGF may regulate progenitor maintenance via *her6*. Together the *kip2* and *her6* data strongly suggest that FGF gates habenular neurogenesis by inhibiting CDKIs and possibly by maintaining expression of pro-progenitor factors.

Nodal signaling leads to early down regulation of FGF signaling in the left habenula

FGF signaling appears to be the center of neurogenic cassette that is asymmetrically regulated in the developing habenula. What is source of the asymmetric regulation of FGF activity? Nodal signaling, specifically its effector in the zebrafish CNS, *cyclops*, is know to establish the asymmetric timing of habenular neurogenesis (Roussigné et al. 2009). We wanted to determine if left-sided Nodal activity drove the asymmetry in FGF signaling we observed. In optical sections, the Nodal target *lefty1* is expressed in the same plane as the asymmetric FGF signal at 26 hpf (Figure 4A&B). As well, *lefty1* expression colocalizes with the habenular marker *dbx1b* (Figure 4C&D). Thus nodal signaling components are active in the habenulae during asymmetric FGF activity.

To directly test if Nodal downregulates FGF signaling in the left habenula, we treated embryos with a Nodal receptor antagonist SB505124 that targets the ALK3/4 receptors selectively. We treated embryos with 50uM SB505124 from 16-24 hpf, a time range chosen to avoid early requirements for Nodal in lateral plate mesoderm patterning and neural plate induction. SB505124 treatment led to a symmetrization of FGF signaling activity at 26 hpf (Figure 4E-G).

Indeed there is an increase in FGF activity on the left in the absence of Nodal signaling (Figure 4E&F). Due to midline defects, Nodal signaling is activated bilaterally in *floatinghead* mutants. So we tested what effect there might be on FGF activity with bilateral Nodal signaling. In this condition, FGF signaling also becomes symmetric, but with a decrease in FGF activity on the right (Figure 4H-J). Together, these experiments show that asymmetric FGF signaling is established by left-sided Nodal inhibition of FGF activity. To our knowledge this is the first reported regulation of FGF by the Nodal signaling pathway.

Several habenular asymmetries in the zebrafish are established by the leftward migration of the small accessory organ, the parapineal. Asymmetric habenular neurogenesis is known to be parapineal-independent (Roussigné et al. 2009). In *tbx2b^c144/c144* mutants, there is failure to form a left sided parapineal. To determine if asymmetric FGF signaling was parapineal-dependent, we analyzed FGF signaling activity in *tbx2b ^c144/c144* mutants and found no change in asymmetry of FGF signaling (Supplementary Figure 3A&B). Thus, asymmetric FGF activity regulates the asymmetric onset of habenular neurogenesis. This neurogenic gate is rendered asymmetric by left-sided Nodal signaling in a parapineal-independent manner.

DISCUSSION

Here we report an FGF regulatory cassette that determines the timing of neurogenesis in the habenular nuclei (Figure 5A&B). Early in habenular development previously established FGF signaling begins to diminish. This derepresses the cell-cycle dependent kinase inhibitor, *kip2* (and may be the cause of the downregulation of the pro-progenitor transcription factor *her6*). The pulsatile expression of *kip2* helps drive habenular neural progenitors to begin neurogenic divisions leading to the appearance of the first habenular neurons. This neurogenic program proceeds asymmetrically with neurons appearing in the left habenular several hours before they appear in the right. This syncopation of neurogenesis is a result of Nodal signaling acting in the left habenula to attenuate FGF signaling earlier on that side. Thus, FGF serves as a crucial

point of signal integration between L/R patterning driven by Nodal and spatiotemporal patterning defining habenular cell fate.

Several key questions follow from this exciting discovery. The Notch signaling pathway is crucial to habenular neurogenesis and its manipulation can also alter the timing of neurogenesis (Aizawa et al. 2005). However, no clear asymmetries in Notch signaling have been reported. Thus it is unknown how Notch-mediated habenular neurogenesis is rendered asymmetric. How are asymmetric FGF signaling and Notch signaling integrated? Given the contradictory literature on how *her6* is regulated, it may be the case that Notch and FGF signaling converge at *her6*. Aizawa et al. (2005) also demonstrated a correlation between the timing (early vs. late) of habenular neurogenesis and the fate of a neuron. Early-born neurons take a lateral subnucleus fate, while late-born-neurons take a medial subnucleus fate. If FGF regulates the timing of neurogenesis, do perturbations of FGF-mediated neurogenesis have an effect on cell fate? Indeed, preliminary analysis shows that 'sub-maximal' SU5402 treatment (which results in precocious neurogenesis) results in an increase in lateral subnucleus (Kctd12.1+) neurons (Supplementary Figure A-D). It will be exciting to see if BCI-treated embryos show a decrease in this same population and an increase in medial subnucleus neurons.

By studying neurogenesis in simple model systems we have uncovered some exciting new targets and pathways regulating the NP switch to neurogenesis and cell fate decisions as well as validating a small molecule approach to manipulating those targets and pathways. To our knowledge this is the first report of Nodal regulation of FGF signaling – two signaling pathways central to stem cell maintenance and differentiation (Sui et al. 2013). Still, the molecular mechanisms connecting the two pathways are unclear. Transcriptome analysis has shown Nodal to be upstream of *dusp4* in the developing lateral plate mesoderm, a member of dual-specificity phosphatase family capable of down regulating FGF signaling (Brown et al. 2008). However, we found no evidence for asymmetric activation of *dusp4* during habenulogenesis (Data not shown). In addition to the Nodal regulation or FGF activity, our use of small molecules *in vivo* to tune endogenous signaling pathways and regulate neurogenesis contributes to a growing body of work

defining how small molecules can be used to determine cell fate (Lu & Atala 2014).

This is a very exciting milieu of tools and targets to apply to questions of basic neuro-development as well as regenerative medicine. Therapeutic application of neurons is coming closer to a clinical reality. But crucial work still needs to be done to develop stem cell protocols that deliver high yields of specific cell types, and treatments to ensure their survival and successful integration into the nervous system (Southwell et al. 2014; Deidda et al. 2014; Anderson & Vanderhaeghen 2014). Models like the habenular nuclei are just the sorts of models that need to continue to be explored for their very real contribution to the next generation of clinical interventions.

CHAPTER V

CONCLUSIONS AND FUTURE DIRECTIONS

Introduction

Profound insights and powerful experimental systems have led to huge strides in answering the basic questions of molecular and cellular developmental neurobiology: How are early neural tissues patterned? How is neuronal diversity achieved? What mechanisms regulate the when and where of particular neurogenic programs? The field is at an exciting point were are beginning to stich together these once separate questions and ask, how are patterning and neurogenic programs integrated? How are canonical signaling pathways inter-regulated? From a growing foundational understanding of the early steps in brain development, the field is better equipped to understand how different neuronal subtypes form connections with each other (synaptogenesis), how these connection are pruned and adjusted during development (circuit formation) and how these circuits underpin organismal behavior (systems and cognitive neurobiology). Needless to say these other realms of neurobiology are all being actively explored, but it is at the margins of each domain, where these different 'levels' interact, that the deep insights of neuroscience await.

The work described here has focused on how L/R patterning and S/T cell fate determination are integrated to generate CNS asymmetry. Specifically, I have focused my attention on the habenular nuclei of the teleost zebrafish. The discovery of new markers of early habenular development and the role FGF signaling plays in integrating L/R patterning with habenular neurogenesis have enriched the power of this model system. Concomitant with advances in zebrafish circuit and behavioral analysis, the field is poised to transcend a molecular and cellular understanding of patterning and cell fate and begin to investigate how early asymmetric development undergirds asymmetric circuit formation and lateralized behavior.
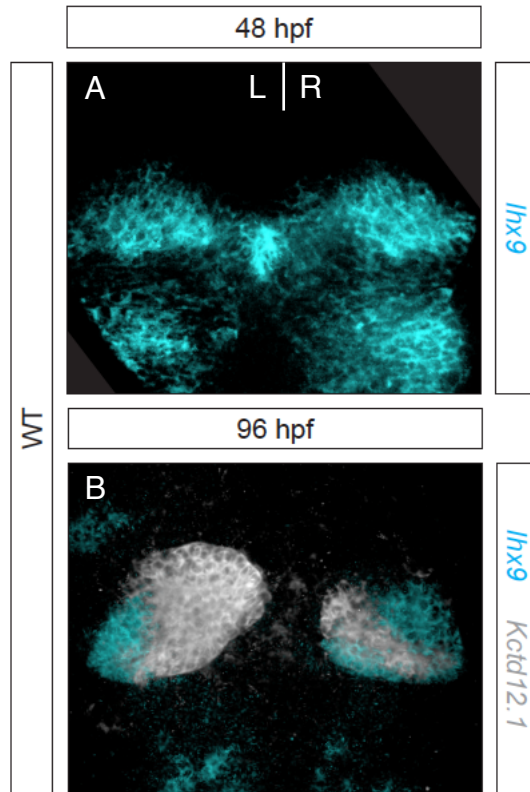
Figure 1: *lhx9* is expressed througout the habenula shortly after neurogenesis, but then restricted to the medial habenula. At 48hpf *lhx9* is expressed symmetrically (A). By 96hpf its expression is restricted to a complementary pattern to Kctd12.1 demonstrating it is now only expressed in the medial habenula (B).

A growing molecular menagerie and fate determination

One limitation of understanding early asymmetric development of the habenulae has been the lack of relevant molecular players. While the above work adds several new genes that function in habenular development, more remain to be discovered or further characterized. As mentioned in the introduction, patterning morphogens activate various combinations of HD-containing TFs, which in turn give rise to expression of pro-neural TFs. What these are and how there are expressed to drive cell fate in the Hb is still unknown. *Lhx9* is an exciting candidate for a fate-specifying habenular transcription factor. *Lhx9* is expressed throughout the habenulae shortly after neurogenesis begins and is subsequently restricted to the medial subnucleus of the habenulae (Figure 1A&B). This raises the tantalizing possibility that this family of TFs plays a role in determining the cell fate of habenular neurons (Guillemot 2007).

Another exciting area for molecular investigation centers on the novel regulation of FGF by the Nodal signaling pathway. Not only are these two classic developmental morphogens, but they also are both central to current efforts in stem cell biology to develop protocols for directed differentiation of embryonic as well as induced pluripotent stem cells (Katoh 2011). But the mechanistic connection between Nodal and FGF signaling pathways is unknown. As has been mentioned, Nodal is known to regulate *dusp4* in the LPM, and the *dusp4* family can regulate FGF, but this connection has yet to be proven in the habenulae.

With a growing list of molecular players in asymmetric habenular development it may also be worthwhile to revisit the uncertain mechanistic unpinning for how light and melatonin play a role in the timing of neurogenesis. These forces were only able to delay neurogenesis and not drive it earlier, while FGF can do both. This perhaps suggests that light and melatonin are upstream of FGF signaling. While tenuous, this may be a fruitful avenue for further research. Additionally, the previous demonstration of Notch signaling as a fundamental component of habenular neurogenesis raises another avenue to investigate signaling pathway crosstalk. Indeed, the implication of *her6* in asymmetric neurogenesis offers an exciting locus for the intersection of FGF and Notch signaling.

Beyond growing our repertoire of molecular players, we are also now in a better position to ask a deep question about how the timing of neurogenesis connects to the binary cell fate choice of lateral versus medial subnuclear neurons. What about being born early or late makes the fate choice for a habenular neuron? In one model, FGF serves as a timing mechanism for when neurogenesis starts. As FGF signaling declines, NPs are released to respond to other extrinsic or intrinsic factors which drive their fate. In another model, FGF may gate the timing of neurogenesis and also instruct cell fate. The highest does of FGF maintain progenitors, the next step down allows neurogenesis and biases NPs to generate one population of daughters, as levels continue to drop, NPs begin to generate the other population.

Another exciting opportunity presented by a growing number of molecular markers is the ability to isolate habenular progenitors at specific developmental time points. These NPs may be studied in culture or be reintroduced in heterochronic studies to illuminate the contribution of extrinsic and intrinsic factors to cell fate determination in the habenulae. *In vitro* experiments have a particular advantage after the validation of FGF small molecules such as SU5402 and BCI as means to manipulate the timing of neurogenesis. This sort of approach has been tremendously helpful in studying cortical and retinal neuronal specification (Belliveau & Cepko 1999; Belliveau et al. 2000; Leone et al. 2008).

From neuronal cell fate to circuits and behavior

Moving beyond cell and molecular neurobiology, the zebrafish dorsal diencephalon is well situated to begin probing how cell fate decisions among neurons effect circuit formation and, beyond that, animal behavior. Similar to asymmetric timing of neurogenesis, another key parapineal-independent asymmetry is found in the morphology of habenular axon terminal in the IPN (Bianco et al. 2008; Roussigne et al. 2012). How differently fated habenular neurons elaborate unique patterns of target innervation is poorly understood, as is how different axonal morphologies impact circuit dynamics in the habenulae and elsewhere. Bianco et al., (2008), took advantage of single-neuron labeling and the amenability of zebrafish to whole mount imaging to analyze axon morphology. With advances in *in vivo* light-sheet microscopy, it is now possible to image entire zebrafish larval brains with cellular resolution (Ahrens et al. 2013). Coupled with refinement of the Cas/CRISPR system for rapid genetic manipulation and the standardization of zebrafish behavioral assays an extraordinary pipeline of experimental discovery emerges (de Souza 2013; Wolman & Granato 2012). Researchers can manipulate genes (Cas/CRISPR) and signaling pathways (small molecules), image the effects on call fate and axon morphology (fixed tissue), image the effects on circuit formation and function (*in vivo* light-sheet-microscopy with calcium indicators) and in the same fish analyze larval and adult lateralized behavior. This platform has the potential to integrate different 'levels' of neurobiology via the simplicity of the zebrafish dorsal diencephalon and create a holistic understanding of the development and function of brain lateralization. I believe this sort of integrative neurobiology will yield incredible insights into brain development and function.

Implications for stem cell biology and regenerative medicine

Nodal and FGF signaling pathways are fundamental pathways in embryonic stem cells and induced pluripotent stem cells. Both pathways are important for maintenance of stem cells as

well as various protocols for driving fate specification (Sui et al. 2013; Katoh 2011). As mentioned, exploration of their regulatory connection will not only deepen our understanding of habenular development but may yield new mediators of stem cell maintenance and differentiation. However, use of protein morphogens in stem cell protocols is often limited by cost and purity. There is great interest in identifying small molecules that can manipulate specific signaling pathways (Lu & Atala 2014). In particular, small molecules that have been tested in *in vivo* contexts show the best promise for use in the clinic. The manipulation of the FGF signaling pathway by SU5402 and BCI – dose-dependently in the case of BCI – had a clear physiological effect on proliferative versus neurogenic stem cell divisions as well as cell fate, both crucial regulatory step in stem cell biology. Along with others, our success in adjusting signaling levels to achieve physiologic outcomes using small molecules should encourage stem cell biologists, especially those with eyes toward the clinic (Southwell et al. 2014; Lu & Atala 2014).

Broader implications for evolution and development of asymmetry in the CNS

Despite the clear role the pP plays in driving some aspects of habenular asymmetry in the zebrafish, the lack of conservation of the pP across vertebrates suggests that deepening out understanding of pP-independent asymmetries may yield more insight into anatomic and functional asymmetries in other vertebrates, including humans. However, very little is known about habenular development in other classes of vertebrates. This work highlights several jumping off points including new molecular mediators of habenular development.

Given the wide conservation of habenular asymmetry it is interesting to consider the evolutionary origins of L/R and S/T pattern integration. At first blush, it seems likely that Nodal-mediated L/R patterning evolved to manipulate an extant program of FGF-mediated habenular neurogenesis. From this point of view, the FGF cassette is present bilaterally, and Nodal acts upstream to modify this in the left habenula. This implies that S/T patterning and neurogenesis of the habenulae evolved first and that the L/R patterning program later coopted it to generate ha-

benular asymmetry. However, secondary organizers, like the FGF signaling center in the DD, are much less conserved than the primary A/P and D/V patterning programs (Kiecker & Lumsden 2012). Indeed many secondary organizers are present in only some ancestral vertebrates (including the FGF signaling center at the midbrain-hindbrain boundary), while L/R patterning is much more deeply conserved (Blum et al. 2014). Thus, it may equally be the case that the evolution of the FGF DD secondary organizer arose later in the vertebrate tree and 'took advantage' of lateralized Nodal activity to drive CNS asymmetry in the habenula.

In closing, I would like the highlight the deep power of model systems to illuminate fundamental questions of evolution, development, disease and therapeutics. With investigation, 'simple' models yield an, initially unappreciated, complexity and beckon us to step further into the mysteries of living organisms.

REFERENCES

Achim, K., Salminen, M. & Partanen, J., 2014. Mechanisms regulating GABAergic neuron development. *Cellular and molecular life sciences : CMLS*, 71(8), pp.1395–415.

Agetsuma, M., Aizawa, H., Aoki, T., Nakayama, R., Takahoko, M., Goto, M., Sassa, T., Amo, R., Shiraki, T., Kawakami, K., Hosoya, T., Higashijima, S., Okamoto, H., 2010. The habenula is crucial for experience-dependent modification of fear responses in zebrafish. Nat Neurosci 13, 1354-1356.

Ahrens, M.B. et al., 2013. Whole-brain functional imaging at cellular resolution using light-sheet microscopy. *Nature methods*, 10(5), pp.413–20.

Aizawa, H. et al., 2005. Laterotopic representation of left-right information onto the dorso-ventral axis of a zebrafish midbrain target nucleus. *Current biology : CB*, 15(3), pp.238–43.

Aizawa, H. et al., 2007. Temporally regulated asymmetric neurogenesis causes left-right difference in the zebrafish habenular structures. *Developmental cell*, 12(1), pp.87–98.

Anderson, S. & Vanderhaeghen, P., 2014. Cortical neurogenesis from pluripotent stem cells: complexity emerging from simplicity. *Current opinion in neurobiology*, 27C, pp.151–157.

Andrew, R.J., Savage, H. & Miklosi, A., 1998. Behavioural Lateralisation of the Tetrapod Type in the Zebrafish (Brachydanio rerio). , 63(1), pp.127–135.

Barth, K.A. et al., 2009. fsi Zebrafish Show Concordant Reversal of Laterality of Viscera , Neuroanatomy , and a Subset of Behavioral Responses. , 15(9), pp.844–850.

Belliveau, M.J. & Cepko, C.L., 1999. Extrinsic and intrinsic factors control the genesis of amacrine and cone cells in the rat retina. *Development (Cambridge, England)*, 126(3), pp.555–66.

Belliveau, M.J., Young, T.L. & Cepko, C.L., 2000. Late retinal progenitor cells show intrinsic limitations in the production of cell types and the kinetics of opsin synthesis. *The Journal of neuroscience : the official journal of the Society for Neuroscience*, 20(6), pp.2247–54.

Bellon, A., Ortiz-Lopez, L., Ramirez-Rodriguez, G., Anton-Tay, F., Benitez-King, G., 2007. Melatonin induces neuritogenesis at early stages in N1E-115 cells through actin rearrangements via activation of protein kinase C and Rho-associated kinase. J Pineal Res 42, 214-221.

Bertolucci, C., Foa, A., 2004. Extraocular photoreception and circadian entrainment in nonmammalian vertebrates. Chronobiol Int 21, 501-519.

Bianco, I.H. et al., 2008. Brain asymmetry is encoded at the level of axon terminal morphology. *Neural development*, 3, p.9.

Bianco, I.H. & Wilson, S.W., 2009. The habenular nuclei: a conserved asymmetric relay station

in the vertebrate brain. *Philosophical transactions of the Royal Society of London. Series B, Biological sciences*, 364(1519), pp.1005–20.

De Biasi, M. & Salas, R., 2008. Influence of neuronal nicotinic receptors over nicotine addiction and withdrawal. *Experimental biology and medicine (Maywood, N.J.)*, 233(8), pp.917–29.

Bisazza, a, Rogers, L.J. & Vallortigara, G., 1998. The origins of cerebral asymmetry: a review of evidence of behavioural and brain lateralization in fishes, reptiles and amphibians. *Neuroscience and biobehavioral reviews*, 22(3), pp.411–26.

Blader, P., Plessy, C. & Strähle, U., 2003. Multiple regulatory elements with spatially and temporally distinct activities control neurogenin1 expression in primary neurons of the zebrafish embryo. *Mechanisms of development*, 120, pp.211–218.

Blum, M. et al., 2014. The evolution and conservation of left-right patterning mechanisms. *Development (Cambridge, England)*, 141(8), pp.1603–13.

Bourgeron, T., 2007. The possible interplay of synaptic and clock genes in autism spectrum disorders. Cold Spring Harb Symp Quant Biol 72, 645-654.

Brown, J.L. et al., 2008. Transcriptional profiling of endogenous germ layer precursor cells identifies dusp4 as an essential gene in zebrafish endoderm specification. *Proceedings of the National Academy of Sciences of the United States of America*, 105(34), pp.12337–42.

Budaev, S., Andrew, R.J., 2009. Patterns of early embryonic light exposure determine behavioural asymmetries in zebrafish: a habenular hypothesis. Behav Brain Res 200, 91-94.

Cahill, G.M., 1996. Circadian regulation of melatonin production in cultured zebrafish pineal and retina. Brain Res 708, 177-181.

Carl, M. et al., 2007. Wnt/Axin1/beta-catenin signaling regulates asymmetric nodal activation, elaboration, and concordance of CNS asymmetries. *Neuron*, 55(3), pp.393–405.

Cholfin, J. a & Rubenstein, J.L.R., 2007. Patterning of frontal cortex subdivisions by Fgf17. *Proceedings of the National Academy of Sciences of the United States of America*, 104(18), pp.7652–7.

Chong, S.W. et al., 2001. Expression pattern of two zebrafish genes, cxcr4a and cxcr4b. *Mechanisms of development*, 109(2), pp.347–54.

Clanton, J.A., Hope, K.D. & Gamse, J.T., 2013. Fgf signaling governs cell fate in the zebrafish pineal complex. *Development (Cambridge, England)*, 140(2), pp.323–32.

Claridge, G. et al., 1998. Schizophrenia risk and handedness: a mixed picture. *Laterality*, 3(3), pp.209–20.

Concha, M.L. et al., 2003. Local Tissue Interactions across the Dorsal Midline of the Forebrain Establish CNS Laterality. , 39, pp.423–438.

Concha, M.L. & Wilson, S.W., 2001. Asymmetry in the epithalamus of vertebrates. *Journal of anatomy*, 199(Pt 1-2), pp.63–84.

Concha, M.L., Burdine, R.D., Russell, C., Schier, A.F., Wilson, S.W., 2000. A nodal signaling pathway regulates the laterality of neuroanatomical asymmetries in the zebrafish forebrain. Neuron 28, 399-409.

Corballis, M.C., 2014. Left brain, right brain: facts and fantasies. *PLoS biology*, 12(1), p.e1001767.

Corballis, M.C., 2009. The evolution and genetics of cerebral asymmetry. *Philosophical transactions of the Royal Society of London. Series B, Biological sciences*, 364(1519), pp.867–79.

D'Autilia, S., Broccoli, V., Barsacchi, G., Andreazzoli, M., 2010. Xenopus Bsx links daily cell cycle rhythms and pineal photoreceptor fate. Proc Natl Acad Sci U S A 107, 6352-6357.

Danilova, N., Krupnik, V.E., Sugden, D., Zhdanova, I.V., 2004. Melatonin stimulates cell proliferation in zebrafish embryo and accelerates its development. FASEB J 18, 751-753.

Daulat, A.M., Maurice, P., Froment, C., Guillaume, J.L., Broussard, C., Monsarrat, B., Delagrange, P., Jockers, R., 2007. Purification and identification of G protein-coupled receptor protein complexes under native conditions. Mol Cell Proteomics 6, 835-844.

DeCarvalho, T.N. et al., 2014. Neurotransmitter map of the asymmetric dorsal habenular nuclei of zebrafish. , pp.1–42.

Decembrini, S. et al., 2009. MicroRNAs couple cell fate and developmental timing in retina. *Proceedings of the National Academy of Sciences of the United States of America*, 106(50), pp.21179–84.

Deidda, G., Bozarth, I.F. & Cancedda, L., 2014. Modulation of GABAergic transmission in development and neurodevelopmental disorders: investigating physiology and pathology to gain therapeutic perspectives. *Frontiers in cellular neuroscience*, 8(May), p.119.

Dekens, M.P., Santoriello, C., Vallone, D., Grassi, G., Whitmore, D., Foulkes, N.S., 2003. Light regulates the cell cycle in zebrafish. Curr Biol 13, 2051-2057.

Dekens, M.P., Whitmore, D., 2008. Autonomous onset of the circadian clock in the zebrafish embryo. EMBO J 27, 2757-2765.

Deneris, E.S. & Hobert, O., 2014. Maintenance of postmitotic neuronal cell identity. *Nature neuroscience*.

Doe, C.Q., 2008. Neural stem cells: balancing self-renewal with differentiation. *Development (Cambridge, England)*, 135(9), pp.1575–87.

Doll, C.A. et al., 2011a. Subnuclear development of the zebrafish habenular nuclei requires ER translocon function. *Developmental Biology*, 360(1), pp.44–57.

Doll, C.A. et al., 2011b. Subnuclear development of the zebrafish habenular nuclei requires ER translocon function. *Developmental Biology*, 360(1), pp.44–57.

Dufourcq, P., Rastegar, S., Strahle, U., Blader, P., 2004. Parapineal specific expression of gfi1 in the zebrafish epithalamus. Gene Expr Patterns 4, 53-57.

Dulcis, D., Spitzer, N.C., 2008. Illumination controls differentiation of dopamine neurons regulating behaviour. Nature 456, 195-201.

Elsea, S.H., Girirajan, S., 2008. Smith-Magenis syndrome. Eur J Hum Genet 16, 412-421.

Essner, J.J. et al., 2005. Kupffer's vesicle is a ciliated organ of asymmetry in the zebrafish embryo that initiates left-right development of the brain, heart and gut. *Development (Cambridge, England)*, 132(6), pp.1247–60.

Frederick, T.J. & Wood, T.L., 2004. IGF-I and FGF-2 coordinately enhance cyclin D1 and cyclin E-cdk2 association and activity to promote G1 progression in oligodendrocyte progenitor cells. *Molecular and cellular neurosciences*, 25(3), pp.480–92.

Gamse, J.T. et al., 2005. Directional asymmetry of the zebrafish epithalamus guides dorsoventral innervation of the midbrain target. *Development (Cambridge, England)*, 132(21), pp.4869–81.

Gamse, J.T. et al., 2002. Otx5 regulates genes that show circadian expression in the zebrafish pineal complex. *Nature genetics*, 30(1), pp.117–21.

Gamse, J.T., 2003. The parapineal mediates left-right asymmetry in the zebrafish diencephalon. *Development*, 130(6), pp.1059–1068.

Garcia-Maya, M. et al., 2006. Ligand concentration is a driver of divergent signaling and pleiotropic cellular responses to FGF. *Journal of cellular physiology*, 206(2), pp.386–93.

Garel, S., Huffman, K.J. & Rubenstein, J.L.R., 2003. Molecular regionalization of the neocortex is disrupted in Fgf8 hypomorphic mutants. *Development (Cambridge, England)*, 130(9), pp.1903–14.

Gothilf, Y., Coon, S.L., Toyama, R., Chitnis, A., Namboodiri, M.A., Klein, D.C., 1999. Zebrafish serotonin N-acetyltransferase-2: marker for development of pineal photoreceptors and circadian clock function. Endocrinology 140, 4895-4903.

Gribble, S.L., Nikolaus, O.B. & Dorsky, R.I., 2007. Regulation and function of Dbx genes in the zebrafish spinal cord. *Developmental dynamics : an official publication of the American Association of Anatomists*, 236(12), pp.3472–83.

Guillemot, F., 2007. Spatial and temporal specification of neural fates by transcription factor codes. *Development (Cambridge, England)*, 134(21), pp.3771–80.

Hans, S. et al., 2004. her3, a zebrafish member of the hairy-E(spl) family, is repressed by Notch signalling. *Development (Cambridge, England)*, 131(12), pp.2957–69.

Heldt, S.A. & Ressler, K.J., 2006. Lesions of the habenula produce stress- and dopamine-dependent alterations in prepulse inhibition and locomotion. *Brain research*, 1073-1074, pp.229–39.

Hendricks, M., Jesuthasan, S., 2007. Asymmetric innervation of the habenula in zebrafish. J Comp Neurol 502, 611-619.

Hikosaka, O., 2010. The habenula: from stress evasion to value-based decision-making. Nat Rev Neurosci 11, 503-513.

Hirayama, J., Cho, S., Sassone-Corsi, P., 2007. Circadian control by the reduction/oxidation pathway: catalase represses light-dependent clock gene expression in the zebrafish. Proceedings of the National Academy of Sciences of the United States of America 104, 15747-15752.

Hockberger, P.E., Skimina, T.A., Centonze, V.E., Lavin, C., Chu, S., Dadras, S., Reddy, J.K., White, J.G., 1999. Activation of flavin-containing oxidases underlies light-induced production of H2O2 in mammalian cells. Proceedings of the National Academy of Sciences of the United States of America 96, 6255-6260.

Hong, E. et al., 2013. Cholinergic left-right asymmetry in the habenulo-interpeduncular pathway. *Proceedings of the National Academy of Sciences of the United States of America*, 110(52), pp.21171–6.

Jhou, T.C. et al., 2013. Cocaine drives aversive conditioning via delayed activation of dopamine-responsive habenular and midbrain pathways. *The Journal of neuroscience : the official journal of the Society for Neuroscience*, 33(17), pp.7501–12.

Jockers, R., Maurice, P., Boutin, J.A., Delagrange, P., 2008. Melatonin receptors, heterodimerization, signal transduction and binding sites: what's new? Br J Pharmacol 154, 1182-1195.

Kaneko, M., Hernandez-Borsetti, N., Cahill, G.M., 2006. Diversity of zebrafish peripheral oscillators revealed by luciferase reporting. Proc Natl Acad Sci U S A 103, 14614-14619.

Katoh, M., 2011. Network of WNT and other regulatory signaling cascades in pluripotent stem cells and cancer stem cells. *Current pharmaceutical biotechnology*, 12(2), pp.160–70.

Kazimi, N., Cahill, G.M., 1999. Development of a circadian melatonin rhythm in embryonic zebrafish. Brain Res Dev Brain Res 117, 47-52.

Kemali, M., Guglielmotti, V., Fiorino, L., 1990. The asymmetry of the habenular nuclei of female and male frogs in spring and in winter. Brain Res 517, 251-255.

Kiecker, C. & Lumsden, A., 2004. Hedgehog signaling from the ZLI regulates diencephalic regional identity. *Nature neuroscience*, 7(11), pp.1242–9.

Kiecker, C. & Lumsden, A., 2012. The role of organizers in patterning the nervous system. *Annual review of neuroscience*, 35, pp.347–67.

Kiening, K. & Sartorius, A., 2013. A new translational target for deep brain stimulation to treat depression. *EMBO molecular medicine*, 5(8), pp.1151–3.

Kikuchi, K. et al., 2010. Primary contribution to zebrafish heart regeneration by gata4(+) cardiomyocytes. *Nature*, 464(7288), pp.601–5.

Kim, C.H., Ueshima, E., Muraoka, O., Tanaka, H., Yeo, S.Y., Huh, T.L., Miki, N., 1996. Zebrafish elav/HuC homologue as a very early neuronal marker. Neurosci Lett 216, 109-112.

Klausberger, T. & Somogyi, P., 2008. Neuronal diversity and temporal dynamics: the unity of hippocampal circuit operations. *Science (New York, N.Y.)*, 321(5885), pp.53–7.

Klein, D.C., 1972. Evidence for the placental transfer of 3 H-acetyl-melatonin. Nat New Biol 237, 117-118.

Kohwi, M. & Doe, C.Q., 2013. Temporal fate specification and neural progenitor competence during development. *Nature reviews. Neuroscience*, 14(12), pp.823–38.

Kong, X., Li, X., Cai, Z., Yang, N., Liu, Y., Shu, J., Pan, L., Zuo, P., 2008. Melatonin regulates the viability and differentiation of rat midbrain neural stem cells. Cell Mol Neurobiol 28, 569-579.

Korf, H.W., Oksche, A., Ekstrom, P., Gery, I., Zigler, J.S., Jr., Klein, D.C., 1986. Pinealocyte projections into the mammalian brain revealed with S-antigen antiserum. Science 231, 735-737.

Koyama, M. & Kinkhabwala, A., 2011. Mapping a sensory-motor network onto a structural and functional ground plan in the hindbrain. *Proceedings of the …*, 108(3), pp.1–6.

Kuan, Y.S., Gamse, J.T., Schreiber, A.M., Halpern, M.E., 2007a. Selective asymmetry in a conserved forebrain to midbrain projection. J Exp Zoolog B Mol Dev Evol 308, 669-678.

Kuan, Y.S., Yu, H.H., Moens, C.B., Halpern, M.E., 2007b. Neuropilin asymmetry mediates a left-right difference in habenular connectivity. Development 134, 857-865.

Kulman, G., Lissoni, P., Rovelli, F., Roselli, M.G., Brivio, F., Sequeri, P., 2000. Evidence of pineal endocrine hypofunction in autistic children. Neuro Endocrinol Lett 21, 31-34.

Kwon, H.-J. & Riley, B.B., 2009. Mesendodermal signals required for otic induction: Bmp-antagonists cooperate with Fgf and can facilitate formation of ectopic otic tissue. *Developmental dynamics : an official publication of the American Association of Anatomists*, 238(6), pp.1582–94.

Lahti, L. et al., 2010. FGF signaling gradient maintains symmetrical proliferative divisions of midbrain neuronal progenitors. *Developmental biology*, 349(2), pp.270–282.

Lauter, G., Söll, I. & Hauptmann, G., 2013. Molecular characterization of prosomeric and intra-prosomeric subdivisions of the embryonic zebrafish diencephalon. *The Journal of comparative neurology*, 521(5), pp.1093–118.

Lauter, G., Söll, I. & Hauptmann, G., 2011. Multicolor fluorescent in situ hybridization to define abutting and overlapping gene expression in the embryonic zebrafish brain. *Neural development*, 6(1), p.10.

Lecourtier, L. & Kelly, P.H., 2007. A conductor hidden in the orchestra? Role of the habenular complex in monoamine transmission and cognition. *Neuroscience and biobehavioral reviews*, 31(5), pp.658–72.

Lecourtier, L., Neijt, H.C. & Kelly, P.H., 2004. Habenula lesions cause impaired cognitive performance in rats : implications for schizophrenia. , 19.

Lee, A., Mathuru, A.S., Teh, C., Kibat, C., Korzh, V., Penney, T.B., Jesuthasan, S., 2010. The Habenula Prevents Helpless Behavior in Larval Zebrafish. Curr Biol.

Leone, D.P. et al., 2008. The determination of projection neuron identity in the developing cerebral cortex. *Current opinion in neurobiology*, 18(1), pp.28–35.

Levitt, P., Eagleson, K.L. & Powell, E.M., 2004. Regulation of neocortical interneuron development and the implications for neurodevelopmental disorders. *Trends in neurosciences*, 27(7), pp.400–6.

Li, B. et al., 2011. Synaptic potentiation onto habenula neurons in the learned helplessness model of depression. *Nature*, 470(7335), pp.535–9.

Li, X., 1998. Generation of Destabilized Green Fluorescent Protein as a Transcription Reporter. *Journal of Biological Chemistry*, 273(52), pp.34970–34975.

Lindell, A.K., 2013. Continuities in emotion lateralization in human and non-human primates. *Frontiers in human neuroscience*, 7, p.464.

Lu, B. & Atala, A., 2014. Small molecules and small molecule drugs in regenerative medicine. *Drug discovery today*, 19(6), pp.801–808.

Markram, H. et al., 2004. Interneurons of the neocortical inhibitory system. *Nature reviews. Neuroscience*, 5(10), pp.793–807.

Martinez-Ferre, A. & Martinez, S., 2009. The development of the thalamic motor learning area is regulated by Fgf8 expression. *The Journal of neuroscience : the official journal of the Society for Neuroscience*, 29(42), pp.13389–400.

Masai, I. et al., 1997. floating head and masterblind Regulate Neuronal Patterning in the Roof of the Forebrain. *Neuron*, 18(1), pp.43–57.

Matsumoto, M. & Hikosaka, O., 2007. Lateral habenula as a source of negative reward signals in dopamine neurons. *Nature*, 447(7148), pp.1111–5.

Melke, J., Goubran Botros, H., Chaste, P., Betancur, C., Nygren, G., Anckarsater, H., Rastam, M., Stahlberg, O., Gillberg, I.C., Delorme, R., Chabane, N., Mouren-Simeoni, M.C., Fauchereau, F., Durand, C.M., Chevalier, F., Drouot, X., Collet, C., Launay, J.M., Leboyer, M., Gillberg, C., Bourgeron, T., 2008. Abnormal melatonin synthesis in autism spectrum disorders. Mol Psychiatry 13, 90-98.

Miklosi, A. & Andrew, R.J., 1999. Right eye use associated with decision to bite in zebrafish. , 105, pp.199–205.

Molina, G. a, Watkins, S.C. & Tsang, M., 2007. Generation of FGF reporter transgenic zebrafish and their utility in chemical screens. *BMC developmental biology*, 7, p.62.

Moriya, T., Horie, N., Mitome, M., Shinohara, K., 2007. Melatonin influences the proliferative

and differentiative activity of neural stem cells. J Pineal Res 42, 411-418.

Morris, J.S. et al., 1999. Covariation of Activity in Habenula and Dorsal Raphe´ Nuclei Following Tryptophan Depletion. , 172, pp.163–172.

Moutsaki, P., Whitmore, D., Bellingham, J., Sakamoto, K., David-Gray, Z.K., Foster, R.G., 2003. Teleost multiple tissue (tmt) opsin: a candidate photopigment regulating the peripheral clocks of zebrafish? Brain Res Mol Brain Res 112, 135-145.

Muñoz-Sanjuán, I. & Brivanlou, A.H., 2002. NEURAL INDUCTION, THE DEFAULT MODEL AND EMBRYONIC STEM CELLS. *Nature Reviews Neuroscience*, 3(4), pp.271–280.

Niebauer, C.L., Aselage, J. & Schutte, C., 2002. Hemispheric interaction and consciousness: degree of handedness predicts the intensity of a sensory illusion. *Laterality*, 7(1), pp.85–96.

Nir, I., 1995. Biorhythms and the biological clock involvement of melatonin and the pineal gland in life and disease. Biomed Environ Sci 8, 90-105.

Noctor, S.C. et al., 2004. Cortical neurons arise in symmetric and asymmetric division zones and migrate through specific phases. *Nature neuroscience*, 7(2), pp.136–44.

Nonaka, S. et al., 2002. Determination of left-right patterning of the mouse embryo by artificial nodal flow. *Nature*, 418(6893), pp.96–9.

Nonaka, S. et al., 1998. Randomization of Left – Right Asymmetry due to Loss of Nodal Cilia Generating Leftward Flow of Extraembryonic Fluid in Mice Lacking KIF3B Motor Protein. , 95, pp.829–837.

Okamoto, H., Agetsuma, M. & Aizawa, H., 2012. Genetic dissection of the zebrafish habenula, a possible switching board for selection of behavioral strategy to cope with fear and anxiety. *Developmental neurobiology*, 72(3), pp.386–94.

Pandi-Perumal, S.R., Trakht, I., Srinivasan, V., Spence, D.W., Maestroni, G.J., Zisapel, N., Cardinali, D.P., 2008. Physiological effects of melatonin: role of melatonin receptors and signal transduction pathways. Prog Neurobiol 85, 335-353.

Parrish, J.Z., Emoto, K., Kim, M.D., Jan, Y.N., 2007. Mechanisms that regulate establishment, maintenance, and remodeling of dendritic fields. Annu Rev Neurosci 30, 399-423.

Pizzagalli, D. et al., 2000. Brain electric correlates of strong belief in paranormal phenomena: intracerebral EEG source and regional Omega complexity analyses. *Psychiatry Research: Neuroimaging*, 100(3), pp.139–154.

Quillien, A. et al., 2011. BMP signaling orchestrates photoreceptor specification in the zebrafish pineal gland in collaboration with Notch. *Development (Cambridge, England)*, 138(11), pp.2293–302.

Ramon Y Cajal, S., 1909. *Histology of the Nervous System*,

Regan, J.C. et al., 2009. An Fgf8-dependent bistable cell migratory event establishes CNS asymmetry. *Neuron*, 61(1), pp.27–34.

Reppert, S.M., Klein, D.C., 1978. Transport of maternal[3H]melatonin to suckling rats and the fate of [3H]melatonin in the neonatal rat. Endocrinology 102, 582-588.

Rivkees, S.A., Reppert, S.M., 1991. Appearance of melatonin receptors during embryonic life in Siberian hamsters (Phodopus sungorous). Brain research 568, 345-349.

De Robertis, E.M. & Kuroda, H., 2004. Dorsal-ventral patterning and neural induction in Xenopus embryos. *Annual review of cell and developmental biology*, 20, pp.285–308.

Roeper, J., 2013. Dissecting the diversity of midbrain dopamine neurons. *Trends in neurosciences*, 36(6), pp.336–42.

Ronan, J.L., Wu, W. & Crabtree, G.R., 2013. From neural development to cognition: unexpected roles for chromatin. *Nature reviews. Genetics*, 14(5), pp.347–59.

Roussigné, M. et al., 2009. Nodal signalling imposes left-right asymmetry upon neurogenesis in the habenular nuclei. *Development (Cambridge, England)*, 136(9), pp.1549–57.

Roussigne, M., Blader, P. & Wilson, S.W., 2012. Breaking symmetry: the zebrafish as a model for understanding left-right asymmetry in the developing brain. *Developmental neurobiology*, 72(3), pp.269–81.

Rubenstein, J.L.R., 2010. Development of the cerebral cortex: implications for neurodevelopmental disorders. *Journal of child psychology and psychiatry, and allied disciplines*.

Saarimäki-Vire, J. et al., 2007. Fibroblast growth factor receptors cooperate to regulate neural progenitor properties in the developing midbrain and hindbrain. *The Journal of neuroscience : the official journal of the Society for Neuroscience*, 27(32), pp.8581–92.

Scholpp, S. et al., 2009. Her6 regulates the neurogenetic gradient and neuronal identity in the thalamus. *Proceedings of the National Academy of Sciences of the United States of America*, 106(47), pp.19895–900.

Seo, H.-C., Nilsen, F. & Fjose, A., 1999. Three structurally and functionally conserved Hlx genes in zebrafish. *Biochimica et Biophysica Acta (BBA) - Gene Structure and Expression*, 1489(2-3), pp.323–335.

Seron-Ferre, M., Valenzuela, G.J., Torres-Farfan, C., 2007. Circadian clocks during embryonic and fetal development. Birth Defects Res C Embryo Today 81, 204-214.

Shepard, P.D., Holcomb, H.H. & Gold, J.M., 2006. Schizophrenia in translation: the presence of absence: habenular regulation of dopamine neurons and the encoding of negative outcomes. *Schizophrenia bulletin*, 32(3), pp.417–21.

Smidt, M.P. & van Hooft, J. a, 2013. Subset specification of central serotonergic neurons. *Frontiers in cellular neuroscience*, 7(October), p.200.

Snelson, C.D. et al., 2008. Tbx2b is required for the development of the parapineal organ. *Development (Cambridge, England)*, 135(9), pp.1693–702.

Snelson, C.D. & Gamse, J.T., 2009. Building an asymmetric brain: development of the zebrafish epithalamus. *Seminars in cell & developmental biology*, 20(4), pp.491–7.

Southwell, D.G. et al., 2014. Interneurons from embryonic development to cell-based therapy. *Science (New York, N.Y.)*, 344(6180), p.1240622.

De Souza, N., 2013. Genetics: RNA-guided gene editing. *Nature Methods*, 10(3), pp.189–189.

Stern, C.D., 2006. Neural induction: 10 years on since the "default model". *Current opinion in cell biology*, 18(6), pp.692–7.

Sui, L., Bouwens, L. & Mfopou, J.K., 2013. Signaling pathways during maintenance and definitive endoderm differentiation of embryonic stem cells. *The International journal of developmental biology*, 57(1), pp.1–12.

Sunmonu, N.A. et al., 2011. Gbx2 and Fgf8 are sequentially required for formation of the midbrain-hindbrain compartment boundary. *Development (Cambridge, England)*, 138(4), pp.725–34.

Sutherland, R.J., 1982. The dorsal diencephalic conduction system: a review of the anatomy and functions of the habenular complex. Neurosci Biobehav Rev 6, 1-13.

Takizawa, T. et al., 2001. DNA methylation is a critical cell-intrinsic determinant of astrocyte differentiation in the fetal brain. *Developmental cell*, 1(6), pp.749–58.

Tamai, T.K., Carr, A.J., Whitmore, D., 2005. Zebrafish circadian clocks: cells that see light. Biochem Soc Trans 33, 962-966.

Tamai, T.K., Vardhanabhuti, V., Foulkes, N.S., Whitmore, D., 2004. Early embryonic light detection improves survival. Curr Biol 14, R104-105.

Tamai, T.K., Young, L.C., Whitmore, D., 2007. Light signaling to the zebrafish circadian clock by Cryptochrome 1a. Proc Natl Acad Sci U S A 104, 14712-14717.

Talbot, W. et al., 1995. A homeobox gene essential for zebrafish notochord development. *Nature*.

Technau, U. & Steele, R.E., 2012. Evolutionary crossroads in developmental biology: Cnidaria. *Development*, 139(23), pp.4491–4491.

Thisse, B., Thisse, C., 2004. Fast Release Clones: A High Throughput Expression Analysis.

Tordjman, S., Anderson, G.M., Pichard, N., Charbuy, H., Touitou, Y., 2005. Nocturnal excretion of 6-sulphatoxymelatonin in children and adolescents with autistic disorder. Biol Psychiatry 57, 134-138.

Toyama, R., Chen, X., Jhawar, N., Aamar, E., Epstein, J., Reany, N., Alon, S., Gothilf, Y., Klein, D.C., Dawid, I.B., 2009. Transcriptome analysis of the zebrafish pineal gland. Dev Dyn 238, 1813-1826.

Upadhyay, N. et al., 2004. Hand preference in patients with allergy, juvenile cancer, and schizophrenia. *Laterality*, 9(3), pp.325–37.

Vallone, D., Lahiri, K., Dickmeis, T., Foulkes, N.S., 2007. Start the clock! Circadian rhythms and development. Dev Dyn 236, 142-155.

Vatine, G., Vallone, D., Appelbaum, L., Mracek, P., Ben-Moshe, Z., Lahiri, K., Gothilf, Y., Foulkes, N.S., 2009. Light directs zebrafish period2 expression via conserved D and E boxes. PLoS Biol 7, e1000223.

Velasquez, K.M., Molfese, D.L. & Salas, R., 2014. The role of the habenula in drug addiction. *Frontiers in human neuroscience*, 8(March), p.174.

Vieira, C. et al., 2010. Molecular mechanisms controlling brain development: an overview of neuroepithelial secondary organizers. *The International journal of developmental biology*, 54(1), pp.7–20.

Vuilleumier, R., Besseau, L., Boeuf, G., Piparelli, A., Gothilf, Y., Gehring, W.G., Klein, D.C., Falcon, J., 2006. Starting the zebrafish pineal circadian clock with a single photic transition. Endocrinology 147, 2273-2279.

Walker, C., 1999. Haploid screens and gamma-ray mutagenesis. *Methods in cell biology*, 60, pp.43–70.

Weaver, D.R., Rivkees, S.A., Reppert, S.M., 1989. Localization and characterization of melatonin receptors in rodent brain by in vitro autoradiography. J Neurosci 9, 2581-2590.

Whitmore, D., Foulkes, N.S., Sassone-Corsi, P., 2000. Light acts directly on organs and cells in culture to set the vertebrate circadian clock. Nature 404, 87-91.

Whitmore, D., Foulkes, N.S., Strahle, U., Sassone-Corsi, P., 1998. Zebrafish Clock rhythmic expression reveals independent peripheral circadian oscillators. Nat Neurosci 1, 701-707.

Witt-Enderby, P.A., MacKenzie, R.S., McKeon, R.M., Carroll, E.A., Bordt, S.L., Melan, M.A., 2000. Melatonin induction of filamentous structures in non-neuronal cells that is dependent on expression of the human mt1 melatonin receptor. Cell Motil Cytoskeleton 46, 28-42.

Wolman, M. & Granato, M., 2012. Behavioral genetics in larval zebrafish: learning from the young. *Developmental neurobiology*, 72(3), pp.366–72.

Zhou, J.X. & Huang, S., 2011. Understanding gene circuits at cell-fate branch points for rational cell reprogramming. *Trends in genetics : TIG*, 27(2), pp.55–62.

Zilberman-Peled, B., Appelbaum, L., Vallone, D., Foulkes, N.S., Anava, S., Anzulovich, A., Coon, S.L., Klein, D.C., Falcon, J., Ron, B., Gothilf, Y., 2007. Transcriptional regulation of arylalkylamine-N-acetyltransferase-2 gene in the pineal gland of the gilthead seabream. J Neuroendocrinol 19, 46-53.

Ziv, L., Levkovitz, S., Toyama, R., Falcon, J., Gothilf, Y., 2005. Functional development of the zebrafish pineal gland: light-induced expression of period2 is required for onset of the circadian clock. J Neuroendocrinol 17, 314-320.